

---

**Travail de fin d'études et stage[BR]- Travail de fin d'études : Analysis of the flexibility potential of low temperature heat pumps for the space heating of residential buildings by underfloor heating[BR]- Stage d'insertion professionnelle**

**Auteur :** Jacques, Théo

**Promoteur(s) :** Lemort, Vincent

**Faculté :** Faculté des Sciences appliquées

**Diplôme :** Master en ingénieur civil électromécanicien, à finalité spécialisée en énergétique

**Année académique :** 2020-2021

**URI/URL :** <http://hdl.handle.net/2268.2/11477>

---

*Avertissement à l'attention des usagers :*

*Tous les documents placés en accès ouvert sur le site le site MatheO sont protégés par le droit d'auteur. Conformément aux principes énoncés par la "Budapest Open Access Initiative"(BOAI, 2002), l'utilisateur du site peut lire, télécharger, copier, transmettre, imprimer, chercher ou faire un lien vers le texte intégral de ces documents, les disséquer pour les indexer, s'en servir de données pour un logiciel, ou s'en servir à toute autre fin légale (ou prévue par la réglementation relative au droit d'auteur). Toute utilisation du document à des fins commerciales est strictement interdite.*

*Par ailleurs, l'utilisateur s'engage à respecter les droits moraux de l'auteur, principalement le droit à l'intégrité de l'oeuvre et le droit de paternité et ce dans toute utilisation que l'utilisateur entreprend. Ainsi, à titre d'exemple, lorsqu'il reproduira un document par extrait ou dans son intégralité, l'utilisateur citera de manière complète les sources telles que mentionnées ci-dessus. Toute utilisation non explicitement autorisée ci-avant (telle que par exemple, la modification du document ou son résumé) nécessite l'autorisation préalable et expresse des auteurs ou de leurs ayants droit.*

---



UNIVERSITY OF LIÈGE  
FACULTY OF APPLIED SCIENCES

---

# Analysis of the flexibility potential of low temperature heat pumps for the space heating of residential buildings by underfloor heating

---

Master's Thesis submitted in partial fulfilment of the requirements for the  
degree of Electro-mechanical Engineering

*Author:*  
Théo JACQUES  
ID: S161139

*Jury:*  
V. LEMORT (ULiège)  
C. CRUNELLE (Laborelec)  
S. ATTIA (ULiège)  
M. DOCLO (Laborelec)  
S. GENDEBIEN (ULiège)

June 9, 2021

ACADEMIC YEAR 2020-2021

# Remerciements

Un travail de fin d'étude ne se fait pas seul, et j'ai eu la chance d'être bien entouré et guidé pour mener à bien ce nouveau défi.

Je tiens tout d'abord à remercier mon promoteur, Vincent Lemort, ainsi que les assistants du Laboratoire de Thermodynamique, Frédéric et Samuel, pour leur aide et le temps qu'ils m'ont consacré.

Je tiens aussi à remercier Etienne de Montigny, pour l'opportunité de partenariat industriel avec Daikin dans le cadre de mon travail, et pour toutes les informations qui m'ont été fournies.

Je souhaite exprimer ma plus grande gratitude envers Cathy, Matthijs et Louis, pour mon intégration au sein de l'équipe, leur suivi tout au long de mon travail, leurs conseils, et l'expérience très enrichissante que j'ai vécue au sein d'Engie Laborelec pendant près de 9 mois.

Enfin, je souhaite remercier particulièrement mes parents et mes sœurs de m'avoir soutenu, ainsi que mon copain, Vincent, pour ses encouragements et sa compassion durant cette période.

# Abstract

In 2018, the residential space heating sector represented 16.64% of the European final energy consumption, and 13.8% of the Belgian green house gases emissions in 2019. A way to reduce the consumption and optimise the generation resources is to use heat pumps -that are expected to replace by 2050 in Belgium most of the fossil fuel based heating technologies-, to implement demand side management (DSM) strategies and to decouple the heat and electricity needs using the thermal energy storage (TES) of the building. This work attempts to evaluate the flexibility potential of residential buildings heated by low temperature heat pumps and equipped with floor heating. The aim is to understand the relevance, the advantages and drawbacks of the strategy on different configurations. In order to achieve this goal, a single zone dynamic building model with a heat pump model is developed, and three cases are investigated: the time period of storage/discharge of heat in the building, the possibility to increase self-consumption of a photovoltaic installation and the economic interest thereof in Belgium, and the potential heat load that can be shifted from peak to off-peak hours in a dynamic pricing context. The building investigated is a representative Belgian detached house, within two refurbishing states: a K30 insulation level and yearly heating needs of 89 kWh/(m<sup>2</sup>\*y), and an advanced refurbishment state with yearly heating needs of 43 kWh/(m<sup>2</sup>\*y) and a K25 insulation level. The results show that the flexibility period can vary from 2h up to more than a day, depending on the outside temperature, the setpoint temperatures and the building insulation. The increase of self-consumption in the configuration of the rule based control defined in this work seems not economically interesting, with a total cost increased by 1% for the lower insulation level, and a cost reduction of 1.8% for the low energy state. However, other control strategies could lead to better results. Finally, a complete shift of the heating demand can be achieved for periods from 2h for lower insulation houses and up to 4 hours for low energy buildings, with an average rebound period of 4 hours for both. An important conclusion of the work is that the flexibility potential is larger for very well insulated buildings, and the insulation level is more important than the building's thermal capacity.

# Contents

<b>Acronyms</b>	<b>5</b>
<b>Symbols</b>	<b>6</b>
<b>Subscripts</b>	<b>6</b>
<b>1 Introduction</b>	<b>7</b>
1.1 Context . . . . .	7
1.2 Flexibility and Demand Side Management . . . . .	9
1.3 Heat pump . . . . .	10
1.3.1 Heat pump operation principle . . . . .	10
1.3.2 Heat pump sales and stock in Europe and Belgium . . . . .	13
1.4 Existing literature . . . . .	14
1.4.1 Flexibility estimation . . . . .	15
1.4.2 Building models . . . . .	15
1.4.3 Heat pump models . . . . .	18
1.4.4 Past researches . . . . .	19
1.5 Goal of the work and approach chosen . . . . .	20
<b>2 Methodology</b>	<b>21</b>
2.1 Building data . . . . .	21
2.1.1 From ProCEBaR (2012) . . . . .	21
2.1.2 From IEE projects (2006-2016) . . . . .	21
2.2 Static building model . . . . .	31
2.2.1 Choice of the house to model . . . . .	34
2.2.2 Validation of the model . . . . .	36
2.3 Heat pump model . . . . .	38
2.4 Interface between heat pump and building models . . . . .	44
2.4.1 Floor heating model . . . . .	44
2.4.2 Sizing of the heat pump . . . . .	47
2.4.3 Water law . . . . .	51
2.5 Dynamic model . . . . .	54
2.5.1 Dynamic model definition . . . . .	54
2.5.2 Dynamic model validation . . . . .	59
<b>3 Results</b>	<b>64</b>
3.1 FS A: Time response of setpoint temperatures changes . . . . .	65
3.2 FS B: Improving self-consumption of PV with TES . . . . .	68
3.3 FS C: Shifting consumption from peak to off peak hours . . . . .	72
<b>4 Discussion</b>	<b>78</b>
4.1 Single zone model . . . . .	78
4.2 Building choice . . . . .	78
4.3 Heat pump model at part load . . . . .	79
4.4 Ground insulation of CS2 . . . . .	80
4.5 Comfort . . . . .	80
4.6 Impact of the capacities . . . . .	81

---

4.7	Heat pump control . . . . .	81
4.8	Overheating . . . . .	82
4.9	FS C: flexibility period of 2x3h for CS1 . . . . .	82
<b>5</b>	<b>Conclusion</b>	<b>84</b>
<b>6</b>	<b>Appendix</b>	<b>86</b>
<b>A</b>	<b>Methodology</b>	<b>86</b>
A.1	TABULA calculation sheets . . . . .	86
A.2	Static model results for CS2 . . . . .	90
A.3	Heat pump manufacturer data . . . . .	90
A.4	Double linear interpolation method of the manufacturer data to model the heat pump . . . . .	92
<b>B</b>	<b>Results</b>	<b>92</b>
B.1	Results of 80 kWh envelope capacity . . . . .	92
B.2	Morning flexibility . . . . .	93
	<b>References</b>	<b>94</b>

## Acronyms

A/A	Air to air
A/W	Air to water
BAU	Business as usual
COP	Coefficient of performance
CS	Case study
CS1	Case study 1
CS2	Case study 2
DHW	Domestic hot water
DSM	Demand side management
FH	Flexibility hours
FS	Flexibility study
FSA	Flexibility study A
FSB	Flexibility study B
FSC	Flexibility study C
G/W	Ground to water
HP	Heat pump
HHP	High temperature heat pump
LHP	Low temperature heat pump
MHP	Medium temperature heat pump
nZEB	Near zero emission building
PI	Proportional integrative
RES	Renewable energy sources
SCOP	Seasonal coefficient of performance
SH	Space heating
TES	Thermal energy storage
WI	Within

## Symbols

A	Area	[m <sup>2</sup> ]
C	Capacity	[J/K]
$C_{p,air}$	Volume specific heat capacity of air	[Wh/(m <sup>3</sup> *K)]
F	Flexibility index	[-]
$n_{air,infiltration}$	Air change rate by infiltration	[1/h]
$n_{air,use}$	Air change rate by use of the house	[1/h]
p	price	[€]
$\dot{Q}$	Thermal power	[W]
R	Resistance power	[W]
$R_x$	Thermal resistance	[(m <sup>2</sup> *K)/W]
$r_r$	Ventilation heat recovery rate	[-]
T	Temperature	[°C]
U	Heat transfer coefficient	[W/(m <sup>2</sup> *K)]
$\dot{W}$	Electrical power	[W]
$\theta$	Wall's accessibility	[-]
$\phi$	Proportion of the wall's capacity accessibility	[-]
$\Phi$	Internal specific heat source power	[W/m <sup>2</sup> ]
$\lambda$	Thermal conductivity	[W/(m*K)]

## Subscripts

av	Average
cd	Condenser
cov	Covering
el	Electricity
env	Envelope
ev	Evaporator
ex	Exit
fh	Floor heating
in	Internal
loss	Losses
max	Maximum
min	Minimum
out	Outdoor
ref	Reference
su	Supply
surf	Surface
tot	Total
ventil	Ventilation
w	Water
z	Zone



# 1 Introduction

## 1.1 Context

According to EuroStat (2020), the households represented 26% of the European final energy consumption in 2018, and 64% of this energy was exclusively dedicated to space heating needs. The situation is similar for Belgium, with residential space heating counting for 13.8% of the total green house gases emissions in 2019 (Climat.be, 2019). According to the last governmental report about the Scenarios for a climate neutral Belgium by 2050 (FPS Public Health, 2021), important efforts have to be done to renovate the Belgian residential building stock in order to reduce its energy needs. The renovation rate has to rise from 1% per year to about 2.5 to 3% of deep renovations per year. The electrification will also play a major role to reduce the environmental impact of this sector. Heat pumps are devices that produce heat and can be powered by electricity. Compared to other conventional heating systems such as boilers or electric radiators, their efficiency is much more larger (see Figure 1), making them a renewable way to heat residential buildings. They are seen to replace most of the fossil fuel based technologies for providing space heating and domestic hot water by 2050 (FPS Public Health, 2021).

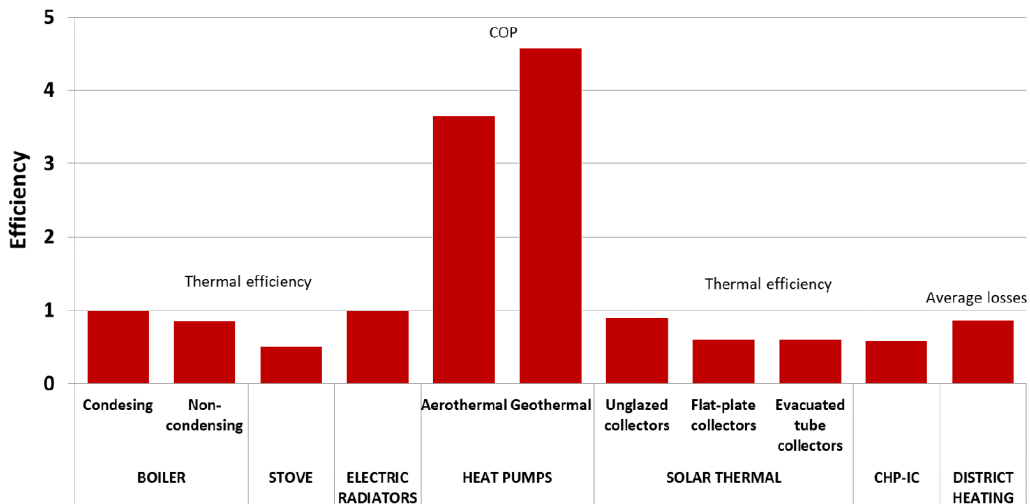


Figure 1: Comparison of the efficiency of the most common heating systems in Europe. Heat pumps are seen as one of the most efficient way to produce heat (Kranzl & TUW, 2019).

Actually, major changes appear on the energy supply sector. It tends to be more decentralised due to the integration of renewable energy sources. Moreover as the grid requires a perfect balance between the supply and demand, strategies have to be investigated in order to take in charge the intermittent nature of the RES. According to Masy, Georges, Verhelst, Lemort, and André (2015), three ways are possible to act on the electrical grid load and help its management: a good prediction of the load associated to the local consumers can be assessed using smart metering devices; shifting the flexible loads from peak to off-peak hours can have a strong impact to reduce the peak load; a real time response can also be preformed for unpredictable mismatches of the supply and demand.

At the European level, new directives are pushing over the decarbonisation of the residential sector and are rethinking its management. The EU targets to reduce greenhouse gas emissions in 2030 to at least 55% compared to 1990 level, to increase the share for renewable energy of 32% and a 32.5% improvement in energy efficiency (European Commission, 2020). Moreover, climate neutrality should be achieved by 2050 according to the European Green Deal plan. The EU initiates supportive policies that target building's energy consumption. One of the most significant is the Energy Performance of Buildings Directive in 2010. It aims to improve energy efficiency and reduce the emissions of buildings by developing national plans to increase the number of near zero emission buildings (nZEB), and states that all new buildings should be built according this standard from 2021. The Eco design Directive in 2010 has set minimum requirements for energy using product's performance to reduce the final energy consumption of buildings. More recently, the Directive 2018/844 on the Energy Performance of Buildings have been published. It highlights the importance of digitalising the building sector, and promotes the implementation of smart grids and smart-ready buildings in order to help the integration of renewable energy sources.

The aim of this work is to investigate and assess the heating flexibility potential of residential buildings equipped by heat pumps and underfloor heating, using smart strategies to promote the market penetration of renewable energy sources, and to help the grid management by reducing peak electricity demand through the shift of the building thermal consumption. The aim of this introduction is to investigate different key subject and answer to the following questions using literature:

- What is the flexibility, and on which energy carrier is the focus ? How can it be achieved for residential buildings ?
- What is a heat pump ? How does it work ? Why is it a smart choice to use heat pumps to heat the building in the scope of the flexibility ? What are the trends for the heat pump market, and the Belgian stock of heat pumps ?
- What is the existing literature in this field ? What models are used in literature for building and heat pump ? What are the main conclusions of these studies ?
- What is the goal of this work and which methodology is used to aim it?

## 1.2 Flexibility and Demand Side Management

The flexibility is defined as the ability to shift the electrical consumption, in order to change the electricity consumption profile (De Coninck & Helsen, 2013). The most common goal is to deviate the consumption from peak to off-peak hours (Masy et al., 2015). The need of a flexible electrical consumption is a key point in terms of grid stability and renewable energy sources (RES) deployment, as well as the optimal use of the generation capacity. The computation of the flexibility is assessed by comparing different cases, and different computations to estimate it are explained in Section 1.4.1.

To assess the electrical flexibility of buildings, a change in the consumer energy demand is required, and can be assessed with different methods. This is called the demand side management (DSM). The aim is to adapt the behaviour of the consumer to help the grid balancing, using different signals and strategies. Two main effects on the energy demand are assessed with DSM strategies: peak shaving and load shifting, illustrated in Figure 2, impacted by the different signals.

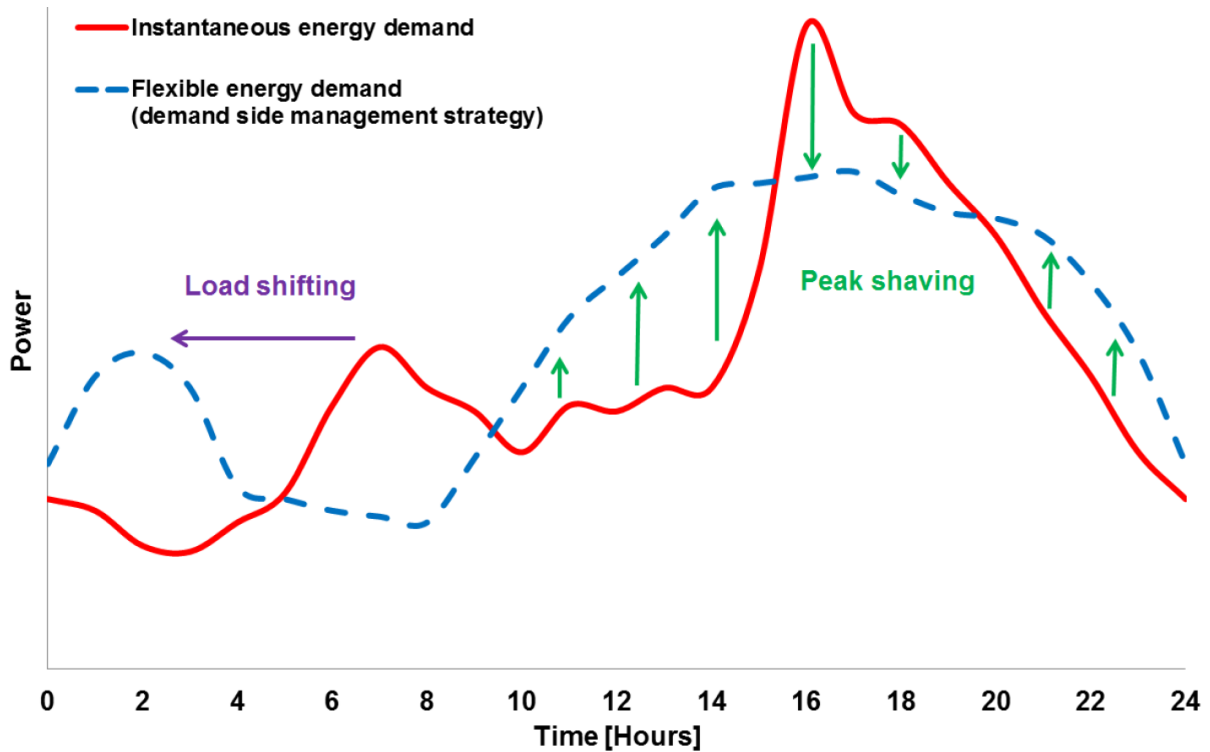


Figure 2: DSM strategies of load shifting and peak shaving (Johra, 2018).

For example, a signal can be the electricity price, as it is strongly related to the asymmetry of the peak and off-peak hours of electricity consumption. A real time pricing of the electricity can lead to a change of consumer behaviour in the consumed electricity schedule: the use of large consuming electrical appliances such as a tumble dryer will be displaced during the off-peak hours, performing load shifting. As explained before, these strategies are being implemented in Europe. The DSM has multiple advantages. Introduced in a smart grid context, it can minimise the cost of installation (with smaller line capacity) and operation of the grid; the grid is more stable in terms of frequency, voltage and transmission capacity; the generation resources are optimally used, reaching

a minimum in costs and  $CO_2$  emissions and facilitating the integration of intermittent RES (Fischer & Madani, 2017).

DSM can act on different energy vectors. The thermal energy storage (TES) of a building is often investigated (Patteeuw et al., 2015), enabling the decoupling in time of the electricity and the heat demand by using the building thermal mass (Georges, 2017). The TES of a building is composed by all the elements of the building that own a thermal capacity and can store thermal energy: the floor, roof, internal or external walls and the internal furniture of the house. The TES can also be increased by adding other elements, such as storage heater, domestic hot water (DHW) tank, or phase change material (Johra, 2018). In the scope of this work, only the activation of flexibility from space heating (SH) using the Building envelope is investigated.

To assess DSM strategies using the TES of buildings, the use of flexibility heating systems is required. This can be done for residential buildings using smart controlled heat pumps or resistance heaters. Heat pumps in smart grid context have been largely investigated. They are seen as really promising for load management (Arteconi, Hewitt, & Polonara, 2013). They can be actively managed in a smart grid context. A lot of protocols already exist, such as Smart Grid Ready. In the recent years, COP of heat pumps have increased thanks to the progress in heat pump development. Simonart (2020) states that thanks to their high share in the electricity consumption, heat pumps are particularly suited for DSM. Therefore, the flexibility of residential building using heat pump is investigated in this work. Vandermeulen, Vandeplas, Patteeuw, Sourbron, and Helsen (2017) explored the case of floor heating coupled with heat pumps and found a lot of advantages: as Johra (2018) and Garsoux (2015) explain, the floor heating have a lower response but will increase the TES of the building compared to conventional radiators, increasing the flexibility potential. Moreover, the need of low temperature leads to an increase in the heat pump performance as the temperature of the evaporator and condenser are closer.

## 1.3 Heat pump

In the frame of this work, the DSM using TES of buildings equipped with heat pumps is investigated. This section provides the information about the heat pump operation principle. A quick overview is provided on the European and Belgian heat pump market and stocks in order to understand which are the most spread types of heat pumps in the considered market.

### 1.3.1 Heat pump operation principle

According to the European Heat Pump Association (EHPA), a heat pump is “a device that can provide heating, cooling and hot water for residential, commercial and industrial applications” (EHPA, 2021). The concept is to transfer thermal energy from an environment to an other, using an additional energy. This driving energy can be electrical or thermal energy. In this work the focus is on electrical heat pumps, typical for residential applications (Fischer & Madani, 2017). Depending on the direction of the transfer, the device will be called a heat pump if it provides heating, or an air conditioning unit if it extracts the heat from the considered environment.

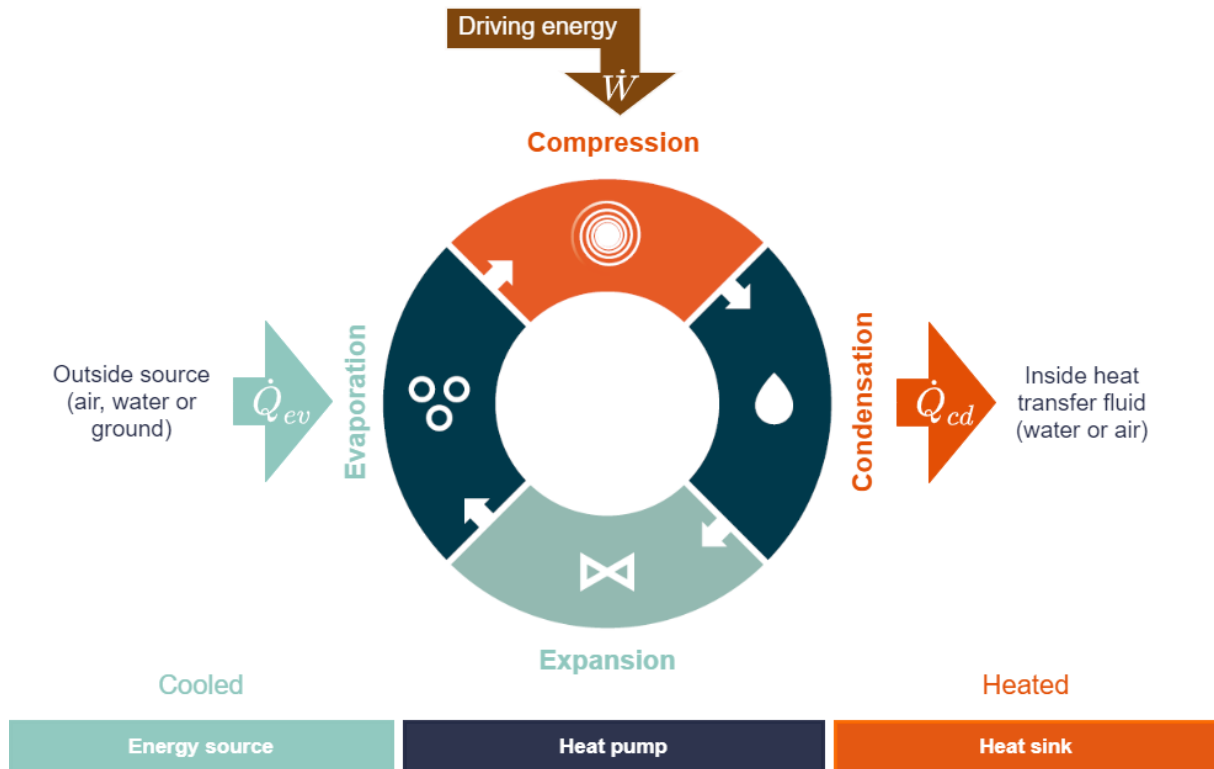


Figure 3: Operation principle of a heat pump, composed of 4 steps acting on the refrigerant state and enthalpy. Inspired by EHPA (2021) and Crunelle and Demeyer (2014).

The most common design and the one that will be considered in this work is the vapour compression heat pump. This cycle is composed of 4 steps according to the state of the *working fluid*, or *refrigerant fluid* (Simonart, 2020), as illustrated in Figure 3 :

1. Compression (gaseous low pressure to high pressure): the driving energy  $\dot{W}$  (electricity) powers the compressor that compresses the working fluid, which increases its pressure and enthalpy.
2. Condensation (gaseous to liquid): the refrigerant is then condensed in an heat exchanger called *condenser*, delivering energy  $\dot{Q}_{cd}$  at high temperature to the inside heat transfer fluid, generally water or air.
3. Expansion (liquid high pressure to low pressure): the expansion valve reduces the refrigerant pressure and enthalpy. Ideally, no energy is lost during this step.
4. Evaporation (liquid to gaseous): finally, the working fluid is evaporated in the *evaporator*, an heat exchanger, absorbing energy at low temperature  $\dot{Q}_{ev}$  from the energy source, that can be ambient air, water or ground.

The process is the same for cooling, but the refrigerant flow is reversed. Heat pumps are characterised by the nature of the energy source and heat sink. They are defined as air to air (A/A), air to water (A/W), ground to water (G/W), etc. The fundamental interest of a heat pump is that the thermal power provided is typically composed by 75% of the energy from the heat source, and 25% of electrical energy. In other words, for 1 kWh of electricity, the device will “pump” 3 kWh from the energy source, providing 4 kWh to the heat sink (Nowak, 2018). Due to the nature of the energy source (ambient air, ground

or water), it is considered as a renewable energy source. Therefore, the efficiency of the heat pump is defined according to the ratio between the electrical work  $\dot{W}$  that has to be provided and the thermal energy provided to the heat sink  $\dot{Q}_{cd}$  (see equation 1). This ratio is called *coefficient of performance* (COP), and should always be greater than one, as the COP of a simple electrical heating resistance is one. The COP is limited by the temperature of the energy source and the heat sink, respectively  $T_{ev}$  and  $T_{cd}$ , expressed by  $COP_{max}$  derived from the Carnot efficiency (equation 2). The smaller is the difference between the two temperatures, the greater is the COP. It will be limited by the performance of the device, e.g. the volumetric efficiency, evaporator and condenser pitch points (i.e. the minimal temperature difference between the hot and cold fluids), etc. The seasonal coefficient of performance (SCOP) is defined as the ratio between the total amount of heat delivered by the heat pump during the heating season  $\dot{Q}_{tot}$ , and the total electricity consumption  $\dot{W}_{tot}$  over the same period of time (equation 3). The renewable nature of the heat pump is also really important to achieve the EU share for renewable energy targets.

$$COP = \frac{\dot{Q}_{cd}}{\dot{W}} \quad (1)$$

$$COP_{max} = \frac{T_{cd}}{T_{cd} - T_{ev}} \quad (2)$$

$$SCOP = \frac{\dot{Q}_{tot}}{\dot{W}_{tot}} \quad (3)$$

The sizing of the heat pump is important and different configurations exist. The heat pump can be sized to cover all the heating needs. However, this causes the heat pump to work at part load during most of the heating season, reducing the efficiency if the part load is too low (see Section 2.3) and unnecessarily increasing the investment costs (see Section 2.4). An other way is to size the heat pump to cover most part of the need, for example 80% (Patteuw, Henze, & Helsen, 2016). The bivalent temperature is defined as the outside temperature at which the building thermal load equals to the heat pump maximum heating capacity. If the temperature is lower than the bivalent temperature, the heat pump needs a backup system to cover the heating needs (Dongellini, Valdiserri, Naldi, & Morini, 2020). This can be done using for example a gas boiler, or more commonly an auxiliary electrical backup heater, a simple resistance that will provide the surplus of energy needed. In this work, the backup system is a resistance, referred to the *backup resistance*. However, since the electrical resistance has a COP of 1, its use leads to large negative impact on the SCOP of the heat pump.

The relative humidity of the air also influences the heat pump performance. If the evaporator temperature is under 0°C and the outside air is humid, frost will take place on the evaporator, generally when the outside air is below 5-7°C (Dott et al., 2013). Since the ice is an insulating material, this added thermal resistance decreases the exchange coefficient between the evaporator and the air. To avoid that, the heat pump should heat the evaporator to melt the frost. This can be done either by using an electrical resistance or reversing the refrigerant rate, to invert the evaporator and condenser position (Gromicko

& Gromicko, 2021). This operation is called the *defrost cycle*.

The heat pumps considered in this work will be A/W heat pumps. This choice is justified along this chapter. Different types of heat pumps exist, according to the configuration of the evaporator and condenser (monobloc or split unit), their level of temperature for the heat sink, the type of compressor (scroll, rolling piston,...), etc (Crunelle & Demeyer, 2014).

The range of operating temperature will rely on the types of heat distribution in the house for space heating (Simonart, 2020). For standard radiators, high temperature heat pumps (HTHP) will be used, with a temperature above 65°C of the supply water  $T_{cd}$ . Medium temperature heat pumps (MTHP), with temperature output between 55°C and 65°C, are well suited for replacement of existing boilers. Low temperature heat pump (LTHP) with supply water around 35°C and up to 55°C when associated to DHW, will be used for convection radiators and underfloor heating.

Finally, some protocols exist in order to have smart grid function implemented on heat pumps. A largely used one is the Smart Grid Ready label (Fischer, Triebel, & Selinger-Lutz, 2018). The heat pump compatible with this label can be remotely controlled. A two digits configuration leads to a four states control (Simonart, 2020):

- Normal operation (state 0.0): the heat pump operates with normal setpoints.
- Forced OFF (state 1.0): the heat pump is switched off until the storage reaches the minimum allowed temperature.
- Recommended ON (state 0.1): the heat pump is switched on and the hysteresis is increased.
- Forced ON (state 1.1): the heat pump is switched on and the storage temperature is increased to the maximum allowed by the heat pump. The choice is possible to use the backup resistance or not.

### 1.3.2 Heat pump sales and stock in Europe and Belgium

By analysing the heat pump market and future trends, a complete understanding on the number of heat pumps installed, their technologies, and the evolution of the market is provided. The European heat pump market is strongly growing. 2018 was the 6<sup>th</sup> year of consecutive growth in sales (Figure 4). France, Italy and Spain are the three biggest markets in Europe, responsible for 50% of all units sold (Nowak, 2018).

In Belgium, the situation is similar (Figure 5, left). From 2007 Belgium started to promote the energy-efficient heating. Since 2014, new residential building in Flanders have to respect a minimum share of renewable sources for the energy demand and the incentives have increased. The incentives and other regulations help the growing share of the heat pumps, especially in Flanders. A strong increase is seen also in 2017. The A/W heat pumps are driving the evolution of the Belgian market (Figure 5, right). According to EHPA the Belgian heat pump stock was counting 91 000 device in 2018. (BRG Building Solutions, 2018) has analysed that the main market for heat pumps remains in the new

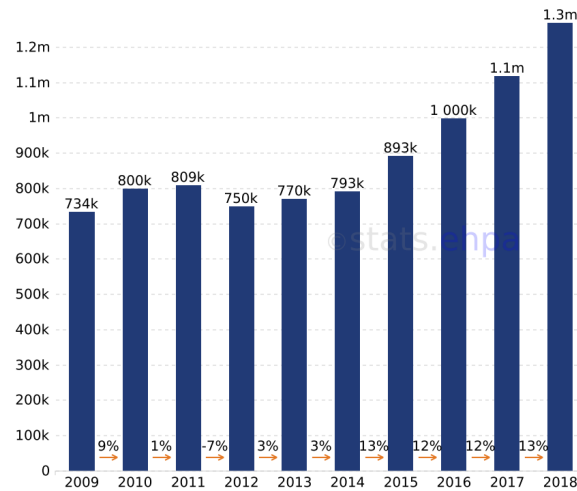


Figure 4: Heat pumps sales in Europe have been steadily increased since 2009 (EHPA, 2019).

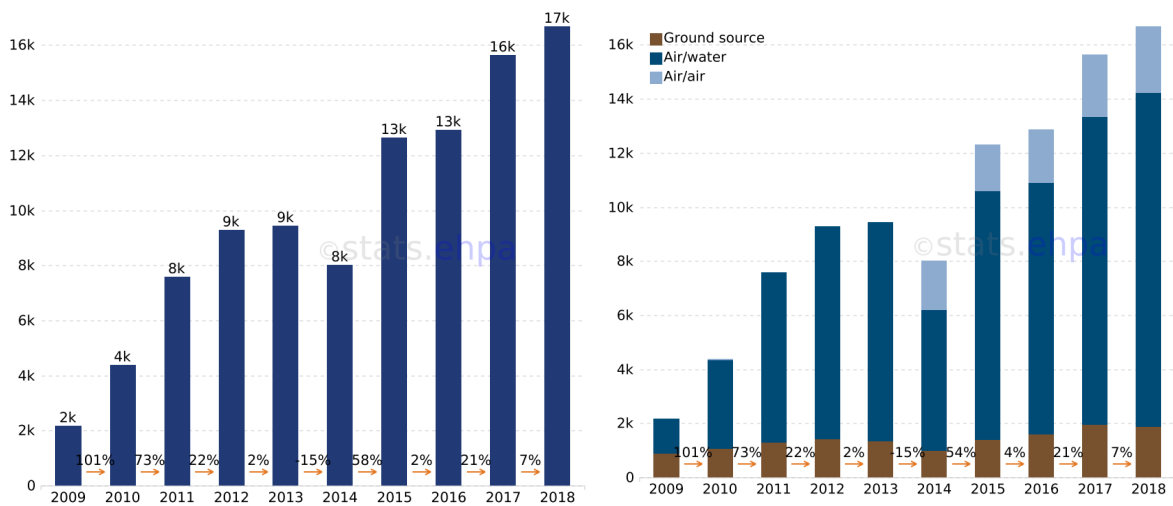


Figure 5: Heat pumps sales in Belgium have increased eight fold since 2009 (left). The majority of these sales are A/W heat pumps (right) (EHPA, 2019).

build segment. The Belgian sales of A/W heat pumps are dominated by Daikin and Mitsubishi covering about 40% of the sales. They also stated that the future trends of the heat pump market are encouraging with a market that will continuously increase in the next years. Finally state policies exist with incentives in order to reduce the purchasing costs of heat pumps in all three regions.

## 1.4 Existing literature

This Section aims to analyse the literature in the field of flexibility analysis, buildings and heat pumps modelling. It is first explained from existing researches how to compute the flexibility. Different approaches to model buildings are presented as well as the ways to model a heat pump. Finally the main results of some researches done on TES and building flexibility through the use of heat pumps are presented as well as some of their assumptions.



### 1.4.1 Flexibility estimation

To compute the flexibility, scenarios have to be compared with a reference scenario of electricity consumption, called the business as usual (BAU) scenario. Many methodologies to assess the flexibility potential exist. Some refer to the amount of hours the operation can be delayed, others on the cost saved by the shift related to the cost of electricity (De Coninck & Helsens, 2013). Johra (2018) defined the flexibility of the building by a *flexibility index*  $F$ , that represents the change in the consumption in high and medium price period, respectively  $\%High$  and  $\%Medium$ , compared to the BAU consumption  $\%High_{ref}$  and  $\%Medium_{ref}$ . The aim is to consume most part of the energy during the low price periods (equation 4). For example, if half of the consumption of the high price periods and half of the consumption from medium price periods are shifted to low price periods, the flexibility index is 50%.

$$F = \left[ \left( 1 - \frac{\%High}{\%High_{ref}} \right) + \left( 1 - \frac{\%Medium}{\%Medium_{ref}} \right) \right] \times \frac{100}{2} \quad (4)$$

$$F = \frac{p_{el,max} - p_{el,av}}{p_{el,max} - p_{el,min}} \quad (5)$$

$$p_{el,av} = \frac{\int_0^t p_{el} * \dot{W}_{el} dt}{\int_0^t \dot{W}_{el} dt}; p_{el,max} = \frac{\int_0^t p_{el,max} * \dot{W}_{el} dt}{\int_0^t \dot{W}_{el} dt}; p_{el,min} = \frac{\int_0^t p_{el,min} * \dot{W}_{el} dt}{\int_0^t \dot{W}_{el} dt} \quad (6)$$

$$Overconsumption = \frac{\dot{W}_{tot} - \dot{W}_{tot,BAU}}{\dot{W}_{tot,BAU}} \quad (7)$$

Masy et al. (2015) defined the flexibility using the average cost of the consumed electricity,  $p_{el,av}$  and the maximum and the minimum electricity price  $p_{el,max}$  and  $p_{el,min}$ , as shown equation 5. The Flexibility is equal to 1 when all the electricity consumed by the heat pump is at the lower price. They also pointed that thermal mass heat storage usually leads to an overconsumption of the total amount of electricity  $\dot{W}_{tot}$ , defined by equation 7.

### 1.4.2 Building models

According to Braun and Chaturvedi (2002), a variety of different approaches to model buildings exist, from the thermal networks, to Fourier series and transfer functions. Two methods can be used to model the residential energy consumption. The *top-down* approach aims to represent the consumption using macroeconomic data and variables. The *bottom-up* approach aims to focus at the building level (Gendebien, Georges, Bertagnolio, & Lemort, 2014). The model order is also fundamental:

- *black-box* model with neural network that are trained require a lot of data and can break the proper physics by introducing high frequency dynamic oscillations that are not real
- *white-box* models can precisely represent the house energy flows and predict the effect when the control strategies are modified, but they need many parameters and really detailed description of the building.
- *grey-box* are an hybrid approach, based on physical parameters constrained to model a simple physical representation of the energy flows in the building.

Two approaches for the grey-box parameters identification exist (Gendebien, Georges, Bertagnolio, & Lemort, 2014): the *typical approach* consists in choosing a reference real building for its characteristics values that represent well the average of the stock represented. The *representative approach* aims to model a fictional building with characteristics computed from average values of the stock it represents. They are also referred as forward and reverse methods.

The general principle of these models is to define a zone, and analyse the heat exchanged by applying an energy balance. A state space model with electrical RC analogy is used. It consists in the use of thermal resistances  $R_x$  and lumped thermal capacities  $C_x$  to represent the elements of the building structure. The parameters required are the typical house geometry and the heat transfer coefficients (U-values, also called thermal admittance) of the different parts of the house envelope. The heat transfer coefficient is the inverse of the thermal resistance of the equivalent resistance circuit and is the proportionality constant between the heat flux and the temperature (GreenSpec (2021a) and GreenSpec (2021b)). Equation 8 shows the general equation of the heat transfer and the different parameters that are needed. The capacity values are used to model the dynamic of the building: they are part of the energy balance to determine the evolution of the temperature in the related zone (equation 9).

$$\dot{Q} = U * A * \Delta T \quad (8)$$

Where:

$U$  is the heat transfer coefficient [ $\frac{W}{m^2 * K}$ ]

$\dot{Q}$  is the heat input or heat lost [W]

$A$  is the heat transfer surface [ $m^2$ ]

$\Delta T$  is the difference in temperature between the solid surfaces [K]

$$C_x * \dot{T}_z = \dot{Q}_{input} - \dot{Q}_{output} \quad (9)$$

The principal differences in the models found in the literature are the number of zones, and the number of elements modelled.

Yang, Pedersen, Larsen, and Thybo (2007) used a two state variables single-zone model, the floor and room temperature, with two heat transfer coefficients: one between the floor and the room, the other between the room and the outside environment. Two capacities are used to represent the floor and the air of the room, forming a 2R2C scheme. Verhelst, Logist, Van Impe, and Helsen (2012) added in the room capacity the capacitance of the

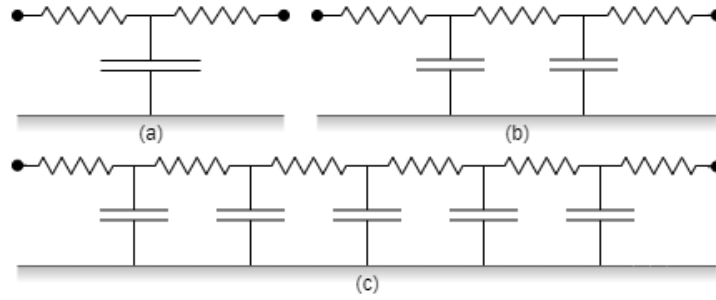


Figure 6: Different walls models found in the literature: (a) 2R1C for external wall (Masy et al., 2015); (b) 2R3C (Braun & Chaturvedi, 2002) and (c) up to 6R5C (Johra, 2018).

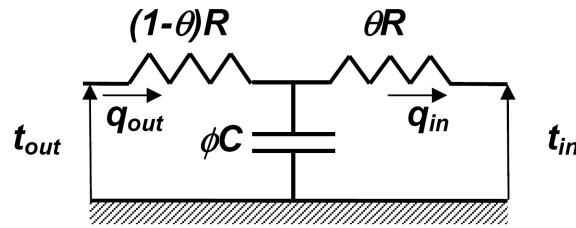


Figure 7: Adjusted 2R1C wall network model provided by Masy (2008) with accessibility parameters.

envelope of the building (the external walls and the roof) and the inside walls. Standard ISO13790 defined a single-zone 5R1C model with 3 states : the temperature of the walls, of the mass-less components (such as the windows and doors) and the room temperature. The internal gains due to the inhabitants and the appliance as well as the solar gains and the ventilation losses are taken into account. Georges (2017) proposed a modification by adding a branch to represent the internal walls. By adding complexity with a multi-zones model, it is possible to model different setpoint temperatures in the rooms, different gains and the heat exchange between the rooms. Masy et al. (2015) modelled a 4 zones building representing the living area, bathroom, sleeping area and staircase, with different levels of occupancy and temperature setpoints, as well as Garsoux (2015), who modelled each zone with a 10R4C scheme representing the external walls, windows, internal walls, ground and air in the zone. Le Dréau and Heiselberg (2016) defined a 8 zones building, with a finite element method to model the walls. Johra (2018) went up to 10 zones for a single building, with the indoor content and furniture represented in each zone capacitance.

The modelling of the gains also differs: they can be neglected as in (Yang et al. (2007) and Verhelst et al. (2012)), or taken into account considering a constant gain coefficient (TABULA Project Team, 2013), or defined using a stochastic-probabilistic model as in (Le Dréau and Heiselberg (2016) and Georges, Gendebien, Bertagnolio, Dechesne, and Lemort (2013)).

Finally, multiple walls model exists, as represented in Figure 6. They can be represented as a single resistance and single capacity at room temperature (Verhelst et al., 2012), 2R1C for external walls (Masy et al., 2015), 2R3C (Braun & Chaturvedi, 2002) or up to 6R5C for internal walls (Johra, 2018). Masy (2008) defined a 2R1C internal wall model

with two dimensionless adjustment parameters  $\theta$  and  $\phi$  (Figure 7).  $\theta$  gives the position of the wall capacity and is called the *accessibility*.  $\phi$  defines the proportion of the capacity that can be accessed.

Finally, Verhelst et al. (2012) states that simplified single-zone model with lumped capacitance are already able to capture the relevant dynamic of the building. Other types of model exists, but they can be limited to a static analysis of the building heating needs. An example is the degree days method. This method is used in HeaSyPac <sup>1</sup>, a tool from Laborelec that compares the performances of different heat pump models for different houses models (from low to high energy demand).

### 1.4.3 Heat pump models

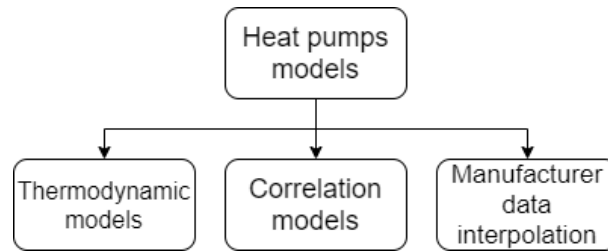


Figure 8: Different heat pumps models exists.

Different types of heat pump models are found in the literature (see Figure 8). A complete model (thermodynamic model) of the heat pump with the refrigerant loop, the heat exchangers, valves and compressor can be performed as Yang et al. (2007) did. Patteeuw and Helsen (2014) presented 3 simplified ways to model heat pumps: direct interpolation of the manufacturer data, constant COP model, or approximation of the COP using correlation functions. An example of these correlation for the electrical consumption and thermal energy provided by a heat pump is given by Verhelst et al. (2012) in equation 10 and 11.  $T_{out}$  is the outside temperature,  $T_{w,su}$  the water supply temperature (leaving the heat pump and supplying the floor), and  $f$  the heat pump frequency. The parameters  $a_x$  and  $b_x$  are fitted from the manufacturer data. A set of assumptions have been also investigated: the part load can be neglected by suppressing the dependency on frequency; the COP can also be defined function of the outside temperature only, or completely constant. In FlexiPac, a heat pump simulation tool which is presented in Section 2.3, Gendebien, Georges, and Lemort (2014) used two quadratic equations to compute the COP and the full load power using the manufacturer data and depending on  $T_{w,su}$  and  $T_{out}$ . The part load is also modelled. Georges (2017) assumed a linear behaviour of the heat pump at part load. Finally in HeaSyPac the manufacturer data have been linearly interpolated.

$$\begin{aligned} \dot{Q}_{hp} = & b_0 + b_1 T_{out} + b_2 T_{w,su} + b_3 f + b_4 T_{out}^2 + b_5 T_{w,su}^2 + b_6 f^2 \\ & + b_7 T_{out} * T_{w,su} + b_8 T_{out} * f + b_9 T_{w,su} * f \end{aligned} \quad (10)$$

$$\begin{aligned} P_{hp} = & a_0 + a_1 T_{out} + a_2 T_{w,su} + a_3 f + a_4 T_{out}^2 + a_5 T_{w,su}^2 + a_6 f^2 \\ & + a_7 T_{out} * T_{w,su} + a_8 T_{out} * f + a_9 T_{w,su} * f \end{aligned} \quad (11)$$

<sup>1</sup>HeaSyPac: Heating System Performance Assessment and Comparison tool

#### 1.4.4 Past researches

In this section, the main results of the researches done on TES and building flexibility through the use of heat pumps are presented.

- Dongellini et al. (2020) investigated the influence of emitters, heat pump size and building thermal inertia on the energy consumption of buildings heated by heat pumps. A/W heat pumps were used in a multi-zone building model. Significant improvements can be achieved, especially with radiant floor heating. An increase up to 10% of the SCOP is reported when the TES of the building is used in order to store the heat when the outside temperature is above the bivalent point to reduce the need of the backup resistance, enabling the use of downsized heat pumps.
- Masy et al. (2015) modelled a multi-zone house equipped with a A/W heat pump. A smart control of the heat pump using TES assessed a shift up to 80% of the electricity consumption to off-peak periods. The higher flexibility potential is assessed by very low energy houses (K30 insulation level) compared to low energy buildings (K45). However, an electricity overconsumption up to 20% has been computed.
- Georges (2017) investigated the flexibility of the heat pump stock in Belgium. The model was a single-zone building equipped with A/W heat pump. It has been found that an amount of 140 MW with 40000 heat pumps can be provided for the winter upward reserve. The rebound effect is 1h15 long. The cost reduction is up to 44%, but will depend of the type of load shifting incentive. High insulation level will have a better flexibility potential. However, this flexibility use will lead to an electricity overconsumption up to 23%. Finally, heat pump smart control can reduce by 10 to 30% the PV surplus electricity production.
- Johra (2018) assessed the flexibility potential of a building composed of 10 zones and equipped with a magnetocaloric heat pump and floor heating. By using the TES of the building to use the heat pump mostly at full load, the SCOP is improved from 1.84 to a range between 2.9 and 3.51. It has been shown that very well-insulated buildings can efficiently store the thermal energy and shift the heating demand over long periods (more than 24 hours). Poorly insulated dwellings can only shift the demand for 1 to 5 hours, but they can move a total energy four times larger than well-insulated building. The benefit of floor heating for the building TES is also stated. Finally, it analyses the use of phase change material for improving TES of light-weight buildings. The flexibility potential using the definition of the flexibility index  $F$  can be improved up to 111% and 87% respectively with phase change material in wallboards or furnishing.
- Le Dréau and Heiselberg (2016) modelled two single family houses: an old one characterised by a yearly heating need of 155 kWh/(m<sup>2</sup>\*year), and a passive one with a need of 14 kWh/(m<sup>2</sup>\*year). Each building has been modelled by height zones, and conduction in the wall has been computed using finite difference method and a time-step of 2 minutes. The main control to assess the flexibility is done by acting on the room setpoint temperature. The house setpoint is fixed at 22°C, and can be increased or decreased by 2°C, depending on the electricity price. Different scenarios are investigated according to the duration of the maximum activation period: 4h, 6h, 12h or 24h. For the old building, it has been found that a large part of the

heat can be shifted for short periods (2 to 5h), but long activation periods lead to uncomfortable conditions for the inhabitants. For low energy buildings, a switch of the need can be assessed for more than 24h, but these types of buildings are sensitive to overheating. Finally, they proved that "the diversity of the building stock can be beneficial to increase the storage potential of the grid and facilitate the transition towards renewable energies".

## 1.5 Goal of the work and approach chosen

This work attempts to evaluate the flexibility potential of residential buildings heated by low temperature heat pumps and floor heating. The aim is to understand the relevance, advantages and drawbacks of the strategy on different building configurations. Three aspects of the flexibility are analysed:

- The time of heat storage/discharge of the building, depending on the house configuration (insulation and energy demand), the outdoor conditions and the setpoint temperatures;
- The potential interest of load shifting strategy to increase the self-consumption when the heating system is coupled to a photovoltaic installation, using a rule based control;
- The potential of heat that can be shifted from peak to off peak hours by changing the setpoint temperature, depending on the setpoint temperature and the shifting time.

In order to achieve it, research on the Belgian housing stock and data available is investigated. Buildings of interest are selected in order to compute a first static model of the selected building. A heat pump modelling is chosen and coupled to the building model, by modelling the floor heating and the heat pump control through a water law. Finally, a dynamic model is derived from the static model, by adding capacities for the floor, the inside air and the building's envelope.

## 2 Methodology

In this chapter, an analysis of the existing researches and databases of the Belgian residential building stock is provided in Section 2.1. The method used to develop the building model is explained and justified, the choice of the building to model is made and a static model is developed in Section 2.2. It is compared to the reference data used. The heat pump choice is justified and its modelling is presented in Section 2.3. The interface necessary to couple the building model and the heat pump model is explained in Section 2.4, as well as the law to control the power needed from the heat pump. Finally, a dynamic model is derived from the static model in Section 2.5 and the static and dynamic model results are compared.

### 2.1 Building data

In the scope of this project, the aim is to analyse the potential of flexibility for a residential building in Belgium. Therefore, some existing researches and databases of the Belgian residential building stock are analysed in this section. Finally, the methodology used in TABULA to assess the computation of the heating needs is explained.

#### 2.1.1 From ProCEBaR (2012)

ProCEBaR <sup>2</sup> is a simulation tool used to analyse the SH, DHW and electrical demand for the aggregated Belgian building stock and developed around 2012 at University of Liège for Electrabel under supervision of Laborelec (Georges et al., 2013). It takes data from existing projects such as the Belgian National Census of 2001, Low Energy Housing Retrofit (Mlecnik et al., 2010), TABULA (Loga et al., 2012a), SuFiQuaD (Sustainability, Financial and Quality evaluation of Dwelling types) (Allacker, 2010) and others.

Four types of buildings are analysed: detached, semi-detached, terraced and apartments, within 5 different periods: before 1945, 1946 - 1970, 1970 - 1990, 1990 - 2006, and after 2007. For each type of building within each period, U-values and capacity values are provided for the walls, windows, roof, floor and door, as well as geometrical characteristics.

#### 2.1.2 From IEE projects (2006-2016)

A second source of information is the different projects initiated by the European programme Intelligent Energy Europe (IEE). Three projects were done consecutively, upgrading and pursuing the work of the previous project to further steps. In these projects is found the TABULA project, one of the main information source of ProCEBaR.

1. DATAMINE project (2006-2008)

The goal of the DATAMINE <sup>3</sup> project was to improve the knowledge about the building stock, using the recently introduced -at that time- Energy Performance

---

<sup>2</sup>ProCEBaR: Profil de Consommation Énergétique des BÂtiments Résidentiels/Profile of residential buildings energy consumption

<sup>3</sup>DATAMINE: collecting DATA from energy certification to Monitor performance Indicators for New and Existing buildings

Certificates (EPC). The project was conducted between 2006 and 2008. A collection of 19.000 datasets from different countries have been analysed and a first classification by size and age of the building stock of the European partners has been achieved (Institut Wohnen und Umwelt GmbH, 2016).

## 2. TABULA project (2009 – 2012)

### (a) European Level

The TABULA<sup>4</sup> project was following the DATAMINE project. During 3 years, 13 European countries (Germany -the project coordinator-, Greece, Slovenia, Italy, France, Ireland, Belgium, Poland, Austria, Bulgaria, Sweden, Czech Republic and Denmark) were working to create a harmonised European building typologies structure. The purpose was to estimate the energy demand of the residential building stock at national scale, in terms of SH and DHW demand to understand the modernisation processes of the building sector in the different countries and the impact of implementation of energy saving strategies (Loga, Stein, & Diefenbach, 2016). Each country, represented by a national partner (a research team), was asked to develop a *national building typology*, according to the TABULA harmonised structure. A national building typology consist of a set of *typical building*, that can be set in three ways, according to the Commission’s guidelines (Ballarini, Corgnati, & Corrado, 2014):

- By selecting real buildings representing the most typical building of a specific category, by means of experience. This approach is used when statistical data are not available. The buildings are then referred as *Real Example Buildings* (ReEX)
- By using statistical analysis on a large number of buildings of the same category, and find a real building having the average characteristics of the sample and including the most common elements. This method is referred as *Real Average Buildings* (ReAv)
- By using statistical data of a building category and defining a virtual building that is then characterised by the mean properties statically detected, referred as *Synthetical Average Building* (SyAv)

Each partner had the choice for the approach, and could use also different approaches to define different typical buildings, depending on the expert information and the statistical data availability. These typical buildings were described: visual appearance, composition of the building structure (elements and composition of the walls, roof, floor, windows and door), geometrical characteristics (volume, area of the different elements of the building structures) and corresponding U-values. The typical buildings are classified according to the construction year and the building type, forming the *building typology matrix* for each country. This main matrix is the central nervous system of TABULA, gathering all the typologies and their corresponding characteristics.

Four types of building have been considered for this matrix: single-family houses, terraced houses, multi-family houses and apartment blocks. Moreover, for each typical buildings, three different states are defined:

---

<sup>4</sup>TABULA: Typology Approach for BUiLding stock energy Assessment



- Existing state: data of the original state based on the construction year standards
- Usual refurbishment: data considering a renovation of the building envelope (of all the elements described before)
- Advanced refurbishment: strong renovation to reach low energy houses standards

The energy demand was then computed using a standard computation common for all the partners, explained later in this section. This approach is based on a simple and transparent calculation of the final energy demand as well as environmental impacts ( $CO_2$  emissions). Finally, a statistic calibration for the models can be done by each participant, using an adaptation factor (Loga et al., 2012a). The tool was then available in the form of an online tool, called *TABULA Tool* in this present report.

(b) Belgian Focus

The Belgian partner of the TABULA project was VITO, the Flemish Institute for Technological Research. As each TABULA partner, three tasks were asked to perform: to develop the national building typology of Belgium, by defining the set of typical buildings and following the harmonised data structure; to compile a national brochure summarising all the typical buildings and energy conclusions; to develop a data base of the Belgian housing stock.

According to VITO, a typical building is “a fictional house that is composed of typical elements for the building envelope and the technical installation. In essence, a typical dwelling must be recognisable and translatable for ordinary citizens”, in order that owners and renters can easily identify their own house from one of the typical building defined for the corresponding Belgian building stock (Cyx, Renders, Van Holm, & Verbeke, 2011). Therefore, the Belgian national typology is built by VITO from typical dwellings closely related to existing buildings, and are chosen for their reference value compared to the examined stock. Average datasets will use to model representative buildings (Diefenbach, Loga, Dascalaki, et al., 2012).

The first step done by VITO to create such database was to analyse the similar researches in neighbouring countries, Netherlands (Senter Novem, 2007) and Germany (Gebäudetypologie, 2005). Then primary data sources of Belgium were used: the General Socio-economic Survey performed in 2001 by the National Institute of Statistics, as ProCEBaR, and the Energy Advice Procedure (EAP) database of 2011, the Energy Performance Certificates (EPC) database, and other researches done about Belgium.

Belgium has been assumed as a single climate zone. VITO first defined the national typology structure as follows (Van Holm, Verbeke, & Stoppie, 2011): 6 types of buildings:

- Detached single family houses
- Semi detached single family houses
- Terraced houses

- Small Multi family houses
- Multi family houses
- Apartments

within 5 different periods:

- Before 1945
- 1946 - 1970
- 1971 - 1990
- 1991 – 2005
- After 2006

The two last types of building are defined since the consumption of a flat will vary a lot according to the surface of the envelope that is exposed to the outdoor environment. The two types represent extreme cases: the multi family house represents an "exposed" flat, and the apartment is a flat completely surrounded by other flats. Real cases are in between of these two extreme cases. For each typical building, the following characteristics had been studied:

- Floor surface area
- Number of storeys of the building
- Number of housing units
- Protected volume
- Transmission loss area of the opaque building envelope components (roof, floor, facades, doors) and the type of bordering (outdoor environment, unheated areas)
- Transmission loss area and orientation (N, S, E, W) of transparent building envelope components (windows, doors)

VITO used different databases to compute these characteristics (Diefenbach, Loga, Corrado, et al., 2012):

- For Flanders, the EPC (Energie Prestatie Certificate, or Energy Performance certificate) database was used. These certificates are mandatory for putting a dwelling on the market since November 2008, and for the rent market since January 2009. In 2011, this database was containing 400.000 certificates.
- For Brussels, the PEB certificate (Performance Energétique des Bâtiments) has been introduced later, in May 2011 for sold building and November 2011 for rented buildings, and was not available during the TABULA project.
- For Wallonia, the PEB certificate has been introduced between June 2010 and June 2011, providing a database of around 1000 certificates.
- The Energy Advice procedure (EAP) database was also used, composed of around 1000 energy audits in Flanders and 10.000 audits in Wallonia.

These databases had provided information to derive the typical geometric characteristics of the representative dwellings, as roof, floor, windows and door surfaces, protected volume, gross floor area, the bordering conditions (outside environment, heated or unheated indoor space), the estimated U-values and insulation thickness, as well as heating and hot water providing systems. For

the two superior insulation levels for each buildings, one was based on the EPBD2010 (European Performance Building Directive) and the second -and more advanced refurbishment- to target low emission level buildings.

Finally, the research showed that the theoretical computation can deviate from the real consumption, especially for old houses. In these types of houses, the consumer behaviour impacts a lot the consumption, by trying to reduce the energy consumption of these uninsulated buildings: unheating some rooms, setting lower ambient temperature, reducing the ventilation. Therefore, the consumption of these houses have been corrected according to real data measured from more than 10 000 dwellings (Loga et al. (2012b) and Van Craenendonck, Lauriks, and Vuye (2016)), by defining an adaptation factor (Van Holm et al., 2011). For example in buildings dated before 1946, the adaptation factor reduces the theoretical energy consumption by the half of its value to represent the real consumption. The adaptation factor is used to compute the Adapted to typical level of measured consumption from the Standard calculation. In the purpose of the building model, the use of the adaptation factor to compute the adapted energy consumption will be discussed in section 2.4.

### 3. Episcope project (2013-2016)

#### (a) European level

The EPISCOPE<sup>5</sup> project followed the TABULA project. 18 countries worked together, from 2013 to 2016. The approach of typical building and national building typology defined in TABULA was further developed. Combined heat and power (CHP) and photovoltaic panels (PV) were implemented. New typologies were developed for the existing countries in the TABULA tool and 6 more countries were added (Cyprus, Spain, Great Britain/England, Hungary, The Netherlands, and Norway). According to EPBD 2010, all the building constructed in EU after 2020 should reach the Near zero emission buildings (nZEB) energy levels (Stein et al., 2014). Therefore, nZEB were largely investigated during this project, and the different definitions for each countries were compared.

During EPISCOPE project, the focus was on data collection and monitoring. Case studies at local, regional and national scale have been analysed (Stein et al., 2016). The TABULA webtool was then updated with this new information, and is available here <sup>6</sup>.

#### (b) Belgian Focus

Three main adjustments were done on the building typology brochure by VITO from TABULA to EPISCOPE projects. First, the nZEB level of refurbishment was added, and the EPB2010 was suppressed, considered non relevant in 2014. Moreover, 5 typical buildings were added, representing the buildings built after 2011. Finally, the prices of the energies were updated.

---

<sup>5</sup>EPISCOPE: Energy Performance Indicator tracking Schemes for the Continuous Optimisation of refurbishment Processes in European housing stocks

<sup>6</sup><https://webtool.building-typology.eu>

In conclusion, 30 buildings represent the Belgian national building typology (Cuypers, Vandeveldel, Van Holm, & Verbeke, 2014): 6 periods (before 1946; 1946-1970; 1971-1990; 1991-2005; 2006-2011; after 2012) and 5 dwelling types (3 types of houses and two types of apartments: detached single family houses; semi detached single family houses; terraced houses; small Multi family houses; multi family houses; apartments). The case study analysed in Belgium in the framework of the EPISCOPE project by VITO was at the local scale, for a housing block in Sint-Amandesberg district of Ghent (Cuypers, Holm, Vandeveldel, & de Vyver, 2016).

The TABULA tool provides for each typology the detailed envelope characteristics described before, the corresponding U-value, as well as the detailed yearly heating needs. The heating need is computed using a standard procedure for the harmonised data structure, that will be referred as the *computation standard methodology of TABULA*. The method implemented is the one defined by standard EN ISO 13790-2008, on the basis of a single-zone building model. It is computed according to the monthly and seasonal method defined in the standard. All the details of the computation method can be found in (TABULA Project Team, 2013) and each building has a corresponding *Calculation sheet* with all the parameters written. This simple method ensures a transparent computation, easily understandable by the different TABULA/EPISCOPE partners, and a fast computation time due to its low complexity.

The computation is based on a number of heating days, defined as the number of days where the mean external temperature is below the heating base temperature, set at 12°C. The average outside temperature during these heating days is computed and referred as the outside reference temperature. The difference of temperature to compute the heating power needed is represented by the difference between the internal setpoint temperature and this average external temperature. A simplified method with monthly average values is presented in Figure 9 to illustrate this method.

The annual heating demand  $\dot{Q}_{h,demand}$  of the house is the difference between the losses and the gains (equation 12) where  $F_{red}$ , the temperature reduction factor represents the non-uniform heating, the unheated space and the heat transfer coefficient by transmission;  $\eta_{h,gn}$  represent the dimensionless gain utilisation factor. They are explained later in this section.

$$\begin{aligned} \dot{Q}_{h,demand} &= Losses - Gains = F_{red} * \dot{Q}_{loss} - \eta_{h,gn} * \dot{Q}_{gain} \\ &= F_{red} * (\dot{Q}_{loss,env} + \dot{Q}_{loss,ventil}) - \eta_{h,gn} * (\dot{Q}_{gain,internal} + \dot{Q}_{gain,solar}) \end{aligned} \quad (12)$$

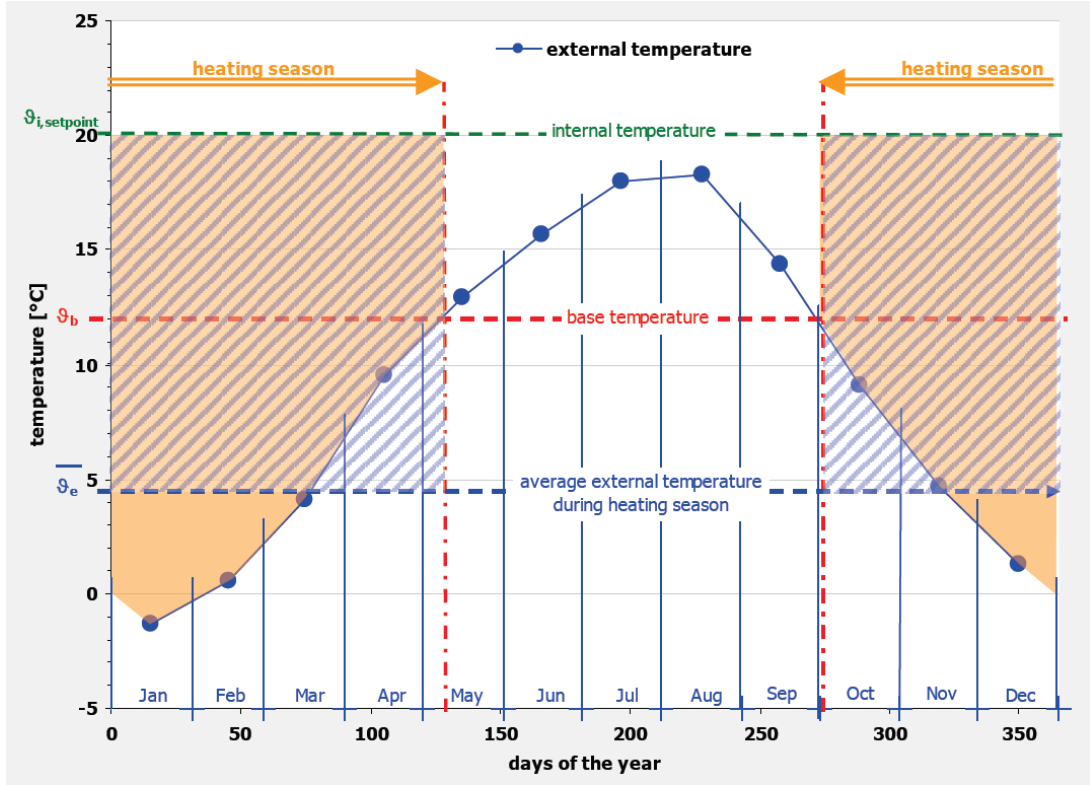


Figure 9: Example determination of the number of heating days on the basis of monthly averages (TABULA Project Team, 2013).

The different terms of the heat balance in equation 12 are explained:

- $\dot{Q}_{loss,env}$  :

The envelope losses represent the conduction losses through the envelope of the building and are computed using the thermal transmittance  $U_x$  [W/(m<sup>2</sup>\*K)] and area  $A_x$  [m<sup>2</sup>] of the walls, roof, floor, windows and door. A soil adjustment factor of 0.5 is added to the floor contribution, representing the fact that the ground has a higher temperature than the external air. Finally, a surcharge  $U_{tb}$  on the envelope losses is added, referring to the thermal bridging (TB). The thermal bridging represents insulation mismatch in the structure, with elements penetrating the insulation and introducing a "by-pass" for the thermal losses. It leads to the overall heat transfer coefficient by transmission  $H_{tr}$  (equation 13), with  $T_{in}$  the internal room's temperature and  $T_{out}$  the outdoor temperature.

The effective U-values are computed by taking into account the state of the environment next to the element (unheated attic under the roof, external air, internal unheated room, cellar,...), according to UNI/TS 11300-1. The heated fraction of the building and the inclination of the roof are also considered (Episcopo Project Team, 2015). The thermal bridging  $U_{tb}$  can have 4 different values, depending on the house considered, defined according to UNI/TS 11300-1 (Table 1).

$$\dot{Q}_{loss,env} = H_{tr} * (T_{in} - T_{out}) = \sum_x (U_x + U_{tb}) * A_x * (T_{in} - T_{out}) \quad (13)$$

Contribution	Description	$U_{tb}$ [ $\frac{W}{m^2 \cdot K}$ ]
Minimal	Envelope non penetrating by elements with high thermal conductivity	0
Low	Thermal bridging only at the junction of cellar and outer walls for buildings with later applied insulation	0.05
Medium	Envelope penetrated by high thermal conductivity elements, inside thermal insulation	0.1
High	Concrete ceilings penetrating the insulation	0.15

Table 1:  $U_{tb}$  value depending on the contribution of TB according to UNI/TS 11300-1.

- $\dot{Q}_{loss,ventil}$  :

The ventilation losses represent the energy lost by recycling of the air and infiltration through the building envelope. They are computed using the volume specific heat capacity of the air  $C_{p,air}$ , multiplied by the volume in the house (reference floor area  $A_{ref}$  multiplied by the height of the rooms  $h_{room}$ ) and by two air change rate factors, representing the air change rate by use of the house (opening of doors, windows, . . .) and by infiltration, respectively  $n_{air,use}$  and  $n_{air,infiltration}$ . This defines  $H_{ve}$ , the overall heat transfer coefficient by ventilation. The losses are expressed by equation 14, with  $C_{p,air} = 0.34$  [Wh/(m<sup>3</sup>\*K)], standard value,  $h_{room} = 2.5$  m and  $n_{air,use} = 0.4$ , two standard values defined for all TABULA dwellings.  $n_{air,infiltration}$  is defined according the insulation level of the house (Table 2). The recuperation rate  $r_r$  represents the recovery of the heat when a heat recovery ventilation system is used in the building.

$$\begin{aligned} \dot{Q}_{loss,ventil} &= H_{ve} * (1 - r_r) * (T_{in} - T_{out}) \\ &= C_{p,air} * A_{ref} * h_{room} * (n_{air,use} + n_{air,infiltration}) * (1 - r_r) * (T_{in} - T_{out}) \end{aligned} \quad (14)$$

Infiltration contribution	Description	$n_{air,infiltration}$ [1/h]
Minimal	Very tight building	0.05
Low	Low air infiltration	0.1
Medium	Medium infiltration	0.2
High	High infiltration	0.4

Table 2: Values of  $n_{air,infiltration}$  according to the building insulation (TABULA Project Team, 2013).

- $\dot{Q}_{gain,internal}$  :

The internal gains are due to occupancy, use of appliances and lighting. Occupants dissipate their metabolic heat when living in the dwelling, produce heat when cooking, washing and use some other appliances like refrigerator or cloth dryer that produce heat. The internal gains depend on the number of people living in the dwelling, but it is assumed in TABULA that the reference area also depends on the number of occupants. The internal gains are computed using an internal heat

source power  $\Phi$  (equation 15), according to UNI/TS 11300-1, and is defined at 3 [W/m<sup>2</sup>] of reference area, a standard value for the TABULA computation method.

$$\dot{Q}_{gain,internal} = \Phi * A_{ref} \quad (15)$$

- $\dot{Q}_{gain,solar}$  :

The solar gains are computed using 3 reduction factors ( $F_{sh}$ ,  $F_F$  and  $F_W$ ), the solar energy transmittance, the area of the windows, and the global solar radiation according to each direction  $j$  (horizontal, east, south, west and north).

$$\dot{Q}_{gain,solar} = F_{sh} * (1 - F_F) * F_W * g_{gl,n} * \sum_j A_{window,j} * I_{sol,j} \quad (16)$$

Equation 16 shows the computation, where:

- $F_{sh}$  is the reduction factor of external shading. It is defined to 0.8 for horizontal surfaces and 0.6 for vertical surfaces.
- $F_F$  is the frame area fraction of the windows, defined to 0.3
- $F_W$  is a reduction factor considering the radiation non perpendicular to the glazing, defined to 0.9
- $g_{gl,n}$  is the total solar energy transmittance for radiation perpendicular to the, defined in ISO 13760
- $A_{window,j}$  is the area of all windows with orientation  $j$  [m<sup>2</sup>]
- $I_{sol,j}$  is the average global irradiation on surface during the heating season for each orientation  $j$  [W/m<sup>2</sup>]

The average global radiation is computed, for each orientation, by the average of the radiation on the heating season for the corresponding orientations.

- $\eta_{h,gn}$  :

The gain utilisation factor for heating represents the fact that, in a steady state model, all the radiations are not included in the heating. In fact, during some periods, the solar radiation will be in excess and will increase the internal temperature inside the house, so this part of the solar gain should not be considered in this static computation, since only a dynamic model can take it in account. The gain utilisation factor reduces the total solar gain as explained in ISO 13790:2008. Equation 17 shows the gain utilisation factor computation, with  $\gamma$  the heat balance ratio defined in equation 18;  $a_H$  defined in equation 19 with  $a_{H,0} = 0.8$  [h] and  $\tau_{H,0} = 30$  [h], constant parameters defined in ISO 13790:2008 for the seasonal method;  $\tau$  the time constant of the building defined in equation 20 where  $C_m$  is the internal heat capacity per square meters and is a standard reference equals to 45 [Wh/(m<sup>2</sup>\*K)] in TABULA, according to the ISO norm.

$$\eta_{h,gn} = \frac{1 - \gamma^{a_H}}{1 - \gamma^{a_H+1}} \quad (17)$$

$$\gamma = \frac{Q_{gain}}{Q_{loss}} \quad (18)$$

$$a_H = a_{H,0} + \frac{\tau}{\tau_{H,0}} \quad (19)$$

$$\tau = \frac{C_m * A_{ref}}{H_{tr} + H_{ve}} \quad (20)$$

- $F_{red}$ :

The temperature reduction factor represents the non-uniform heating. Spaces in the building with lower temperature setpoints, or reduced internal temperature in the house during some weekends, nights or holidays are taken in account. The effect is significant in buildings with poor insulation, but will be small for well insulated buildings, and quasi neglected for nZEB. A simplified linear approach is used, with a linear interpolation between two values of heat transfer by transmission:  $h_a = 1$  [W/(m<sup>2</sup>\*K)] and  $h_b = 4$  [W/(m<sup>2</sup>\*K)], respectively representing high and low thermal quality. Equation 21, 22 and 23 illustrate the approach, with  $H_{tr}$  the surface heat transfer coefficient defined in equation 24.  $F_{red}(h_a)$  and  $F_{red}(h_b)$  are defined for single family house (SFH) and multi family house (MFH) in Table 3.

$$F_{red}(h_{tr}) = F_{red}(h_a) \quad \text{for } h_{tr} \leq h_a \quad (21)$$

$$F_{red}(h_{tr}) = F_{red}(h_a) + (F_{red}(h_b) - F_{red}(h_a)) * \frac{h_{tr} - h_a}{h_b - h_a} \quad \text{for } h_a \leq h_{tr} \leq h_b \quad (22)$$

$$F_{red}(h_{tr}) = F_{red}(h_b) \quad \text{for } h_{tr} \geq h_b \quad (23)$$

$$h_{tr} = \frac{H_{tr}}{A_{ref}} \quad (24)$$

	SFH	MFH
$F_{red}(h_a)$	0.9	0.95
$F_{red}(h_b)$	0.8	0.85

Table 3: Values of  $F_{red}(h_a)$  and  $F_{red}(h_b)$  for single and multi family houses.

- Adaptation method:

The last factor of the computation concerns the adaptation factor  $f_{adapt}$ . In all the steps of the building model (computation of U-values, surfaces, internal gains, ...) assumptions were made. Regarding the number of inhabitants of the dwelling it is easily understandable that, with a rising number of people living in the building, the internal temperature set will decrease and the fresh air demand will increase. The user behaviour is also important as well as the heating system: the internal



temperature with a stove will generally decrease since you have to ignite it and refill it, comparing to central heating, which will be also impacted by fuel price. All these simplifications and assumptions have to be taken into account. Therefore, in TABULA, two types of results are available:

- The Standard calculation, which represents the values obtained by the TABULA methodology explained before.
- The Typical level of measured consumption, where the adaptation factor is applied just at the end of the computation.

This adaptation factor is calibrated using statistical data of a large number of real buildings consumption for the corresponding typical building and for each of them. According to the data available, 3 accuracy levels are defined to understand the way of calibration for each adaptation factor:

- Level A: has been calibrated using the whole building stock or a representative sample.
- Level B: has been calibrated using a large number of example buildings.
- Level C: has been estimated, for example on the basis of a few example buildings.

As explained in the beginning of this section, it has been done for Belgium using a database of 10.000 dwellings (Cuypers et al., 2014).

## 2.2 Static building model

The TABULA tool enables different uses. The typical buildings data can be used to estimate the energy demand and the impact of various saving measures on a specific individual dwelling type (Cyx et al., 2011). Using all the typical buildings types and associating them to a national building stock data, the energy demand and saving potential can then be extended to the whole country housing stock (Loga et al., 2012a). It is the first utilisation, on single buildings, that will be used within the framework of this work. TABULA is also the most recently updated buildings database.

It enables also to have a standardised database for 20 European countries with a lot of typical houses for each of them, and then to reproduce easily this work and the analysis of heat pump flexibility for different types of buildings, in Belgium as well as in the other European countries for a total of 602 typical buildings defined with each 3 different levels of insulation (Loga et al., 2016). Moreover, the choice to use the TABULA computation methodology is that it uses a well-known standard, with a simple method, that will lead to a low computation time, and all parameters are already adapted and well justified inside the TABULA/EPISCOPE projects.

Firstly, a static building model is developed, based on TABULA methodology. This model aims to represent the hourly energy consumption of the house for heating, when TABULA only represents the energy consumption over the heating season. A hourly outside temperature and radiation data is used. A Belgian typical climate data, developed by IRM (national climate institute of Belgium) and ULiège is used (EnergiePlus, 2007) and will

be called the *weather data* in the following sections. Then the equation of the envelope losses, the ventilation losses, the internal gain and the solar gains are implemented, in a relative similar way as in TABULA methodology. The results computed with the model are annually summed and compared to the TABULA results; if the difference is low, the model is assumed accurate and hence validated. Since the TABULA model is already calibrated, any additional resistance will be added to the model as an internal heat convection coefficient or an external one depending on the wind speed for example. The aim of this model is not to choose a real (typical) building and model it precisely, it is to be able to model different types of representative buildings and evaluate the interest of the flexibility for these buildings by taking the TABULA tool information. These two approaches are respectively referred as the *typical* and *representative* approaches (Gendebien, Georges, Bertagnolio, & Lemort, 2014).

The model is designed to be, as the TABULA tool, simple, easily computable, and as general as possible. Moreover, adding complexity will lead to results that derive from the TABULA results and will make the validation process more complex and less accurate, and the possibility to use the model for other typical buildings or other country of TABULA would be lost. The model developed is therefore, as for the TABULA tool, (Georges, 2017), (Yang et al., 2007) and according to standard ISO13790, a single zone model. This assumption is discussed in Section 4.1. The different contributions of the gains and losses are:

- The envelope losses, that are computed with the U-values of the walls, roof, floor, windows and door from TABULA, according to the building simulated, for each hour of the year, using a defined indoor temperature and the outside temperature data, as in equation 13.
- The ventilation losses that are implemented in the same way of the TABULA tool (equation 14), containing the infiltration losses and the air recycling rate by use of the building. The  $n_{air,infiltration}$  factor is taken according to the each building simulated. The recuperation rate is defined from the information found in the TABULA tool: if there is no recovery, the recuperation rate is 0 ; if there is a recovery, VITO defines for Belgium a unique average recovery rate of 80% (for a double flux ventilation with heat recovery and a by-pass) (Cyx et al., 2011), and this is the same value as found in (Masy et al., 2015).

These two components for the losses form together  $\dot{Q}_{loss}$ . In the TABULA methodology, the temperature reduction factor  $F_{red}$  is used to model the non-uniform heating. Since no modification of the single zone model have been done from TABULA to this static model, this factor is kept, and will be defined according to the value in the TABULA tool for each modelled dwelling.

- The internal gains are computed in the same way as the TABULA tool, with  $\Phi$  defined at 3 W/(m<sup>2</sup>\*K) and will be distributed on all the heating hours of the model.
- The solar gains are computed using the same equation as in TABULA methodology (equation 16). However, the solar radiation will be implemented with hourly data, instead of the total radiation over the heating season provided in TABULA. From

the weather data, the global horizontal surface radiation is provided, but no information is provided for the east, south, west and north orientations. The following assumption is made: since VITO has computed for the TABULA tool the radiations of each direction from a daily basis to the seasonal one, the different radiations will be computed from the global horizontal radiation, by adding a multiplication factor derived from the seasonal values of VITO. These factors are defined in the Table 4. Seeing that the east and west radiations have the same values, it might be possible that the assumption was also made by VITO to compute these seasonal values.

Orientation of the surface	Global seasonal radiation of the corresponding orientation [kWh/(m <sup>2</sup> *year)]	Global seasonal radiation on the horizontal surface [kWh/(m <sup>2</sup> *year)]	Correction factor (ratio)
Horizontal	336	336	1
East	202	336	0.601
South	340	336	1.012
West	202	336	0.601
North	110	336	0.327

Table 4: Correction factor of solar gains for the different orientations.

These two last contributions form  $\dot{Q}_{gain}$ . In the TABULA computation methodology, they are multiplied by the gain utilisation factor for heating  $\eta_{h,gn}$ . As explained in Section 2.1 it represents the fact that in a steady state model all the radiation are not used in the heating balance, and the excess solar gain is lost. In this static model, the same situation takes place: when the gains are superior than the heating needs during the heating hours (that are defined at the end of this section), this gain is lost, and is called the *neglected gain*. However, this is reduced directly on the hourly basis. Therefore, any additional reduction factor is needed, and the gain utilisation factor is not considered in the computation of the total gains. Nevertheless, when the excess gain is neglected, it is composed of the internal gains and the solar gains, without the possibility to know the contribution of each. The solar gains and the internal gains of the model results and TABULA results are therefore compared before the excess heat is neglected, and the comparison to validate the final heating demand is computed without the gain utilisation factor for the static model and with the gain utilisation factor for TABULA, to compare and validate this assumption.

To calibrate the model and make it realistic, two assumptions are made. The first one is an heating inactivity during the summer period. Without this condition, the house is heated sporadically for an hour or two in the middle of cold summer nights, which is unrealistic. Indeed, the heating system is usually switched off during the summer period, due to the thermal inertia of the building that is sufficient to cover the needs, and fresh air of colder nights is also useful to refresh the house. This period is chosen when the average day temperature is the highest. Figure 10 shows the average daily temperature throughout the year of the weather data. From the Figure, it is assumed that summer period can be defined between 3500th ( 26th of May) and 6500th hour (28th of September), with a mean value of 5000 (27th of July). This lead to a so-called *summer hours* schedule of 3000 consecutive hours, and reduce the number of heating hours to 5760 hours.

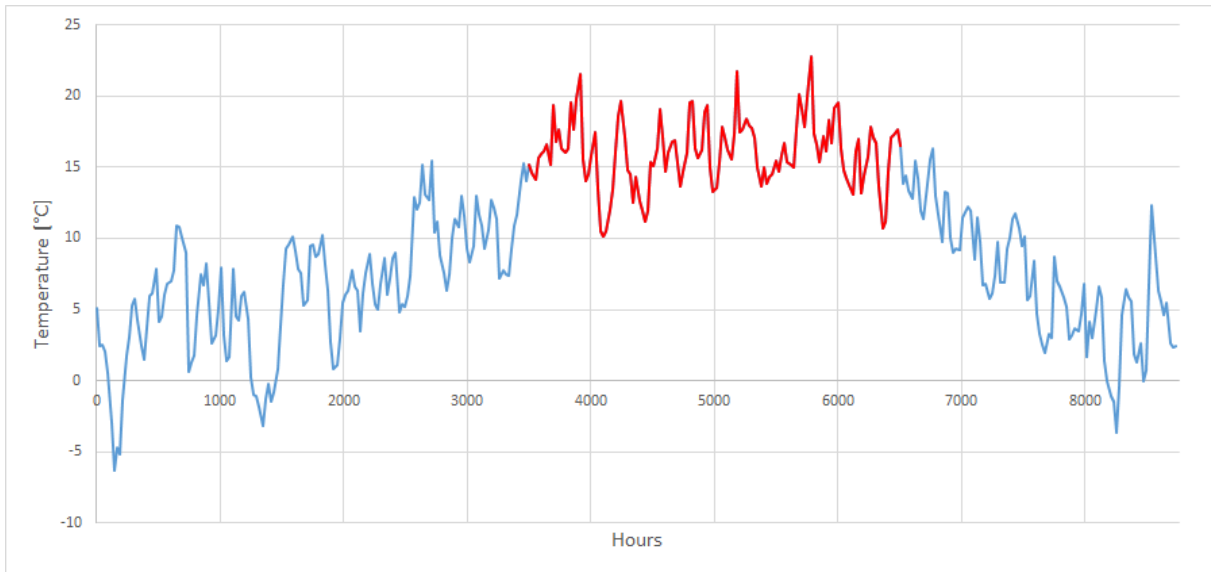


Figure 10: Annual average day temperature from the weather data, with the considered heating season in blue and the unconsidered summer hours in red.

The second assumption is the heating switch off temperature, related to the outdoor temperature. When the outside temperature is above this value, the building is not heated anymore. The purpose of this temperature limit is to avoid chain ON/OFF switching of the heating device around the setpoint that are normally covered by the thermal capacity of the building. Such values are defined in HeaSyPac and taken from Laborelec's internal data and knowledge:

- 11° C for NZE buildings
- 13° C for recent or proper insulated building
- 15° C for old (hardly insulated) building

These two conditions lead to a so-called heating hours schedule. It is composed by 5225 non-consecutive hours of heating.

### 2.2.1 Choice of the house to model

The aim of this work is to investigate the flexibility potential of building equipped with heat pumps. As explained in Section 1.4, the case of a well-insulated building is a interesting choice to analyse the flexibility potential. Indeed, old and poorly insulated buildings do not allow a lot of flexibility of the heating supply in terms of control duration. This choice is discussed in Section 4.2. Secondly, heat pumps are more often installed in peri-urban areas, where you have space and it is allowed to install the outside evaporator block, and in low energy buildings when associated to floor heating.


SFH after 2012	Surfaces [m <sup>2</sup> ]	Elements	U-values [W/(m <sup>2</sup> *K)]	
			CS1	CS2
	$A_{ref}$ : 229.2	Roof <sub>1</sub>	0.21	0.102
	Roof <sub>1</sub> : 107.4	Roof <sub>2</sub>	0.198	0.099
	Roof <sub>2</sub> : 44.895	Walls <sub>1</sub>	0.23	0.23
	Wall <sub>1</sub> : 173.2	Walls <sub>2</sub>	0.22	0.22
	Wall <sub>2</sub> : 28	Floor <sub>1</sub>	0.22	0.22
	Floor <sub>1</sub> : 48	Floor <sub>2</sub>	0.21	0.21
	Floor <sub>2</sub> : 83.9	Windows	1.7	1.5
	Windows: 62.9	Door	1.7	1.5
	Door: 9.5			

Table 5: Principal geometrical characteristics and U-values of the building for the two cases investigated.

Therefore, a recent and detached building of the TABULA stock is chosen: the typical detached Single Family House constructed after 2012 (SFH after 2012). This building will be studied in its existing state, to match also the case of older buildings that have been refurbished, and its advanced refurbishment state, to evaluate the flexibility of low energy buildings (tending to nZEB). These two cases will be referred respectively as *case study 1* (CS1) and *case study 2* (CS2). The Table 5 resumes the principal geometrical characteristics and U-values of the building. However, since the model developed is really flexible, other houses can be very easily investigated by just replacing the inputs values. These inputs values are found in the *Calculation sheet*, provided inside the TABULA tool. The sheet related to the building studied is provided in appendix A.1, where the useful inputs values are highlighted. Table 6 shows the parameters defined in TABULA for CS1 and CS2.  $A_{ref}$  is the conditioned reference area, that includes all zones that are heated directly or indirectly during the heating season (TABULA Project Team, 2013). The subscript 1 or 2 refers to the architectural characteristics of the typical building considered.

Parameters	CS1	CS2
$n_{air,infiltation}$ [1/h]	0.4	0.1
$F_{red}$ [-]	0.89	0.9
$Eta_{h,gn}$	0.92	0.92
$r_r$	0	0.8
Adaptation factor	0.93	1.02

Table 6: Parameters defined for CS1 and CS2 in TABULA.

From the existing state to the advanced refurbishment, extra insulation have been added on the roof, windows and door have been replaced. The level of insulation computed for CS1 is K30, and K25 for CS2, referring to the total transmittance of the house divided by the protected volume. The main differences are that the infiltration rate is lower for CS2, and a heat recovery ventilation is added. The energy needs are respectively 88.92 and 43.22 kWh/(m<sup>2</sup>\*year).

### 2.2.2 Validation of the model

In this section, the yearly simulation is performed to compare the static model and the reference values of TABULA. Considering the climate data, the procedure to compute the heating days of VITO in TABULA is the same for all the Belgian typical dwellings, with a heating season of 210 heating days (5040 hours) and an average external temperature of 6.2° C . The setpoint temperature is 20° C. The same setpoint temperature is therefore chosen for the static model.

The use of the adaptation factor has to be discussed. As explained, this factor is significant for old and not well-insulated houses. It can therefore be really interesting to use it since it is more realistic. However, with the choice of a recent house, where the adaptation factor is 0.93 for CS1 and 1.02 for CS2, it will not be taken in account for this work. For other types of dwelling, it will be up to the user of the tool to choose whether or not he takes this factor into account depending on the aim of the study and the different buildings modelled.

Table 7 provides the results of the computation of the heating needs over the heating season for TABULA and the static model for CS1. Subscript 1 and 2 refer to the geometry of the house defined in TABULA. For CS1 and CS2, the building is divided in two parts, a big one on the left and a small one on the right, with each is own roof, walls and floor U-values.

Parameter	Unit	TABULA	Model	Difference
Number of heating hours	-	5040	5225	3.6 % (7.7 days)
Average external temperature	°C	6.2	5.81	6.71 %
Roof 1	$\frac{\text{kWh}}{\text{m}^2 \cdot \text{year}}$	6.1	6.49	6.39 %
Roof 2		2.4	2.55	6.25 %
Wall 1		10.8	11.4	5 %
Wall 2		1.6	1.77	10.6 %
Floor 1		1.4	1.52	10.8 %
Floor 2		2.3	2.53	10.3 %
Windows		29	30.8	6.2 %
Door		4.4	4.65	5.68 %
Thermal bridging		15.1	16.1	6.62 %
Ventilation losses		42.3	44.9	6.15 %
Internal gain		15.1	15.7	3.97 %
Solar gain		13.9	11.8	17.8 %
Heating losses		115.6	122.7	6.14 %
Gross heating gain		29	27.47	5.57 %
Net heating gain		26.68	26.52	0.6 %
Neglected gain		2.32	0.95	-
Heating need		88.92	96.19	8.18 %

Table 7: Results and comparison of the yearly simulation between TABULA and the static model for CS1.

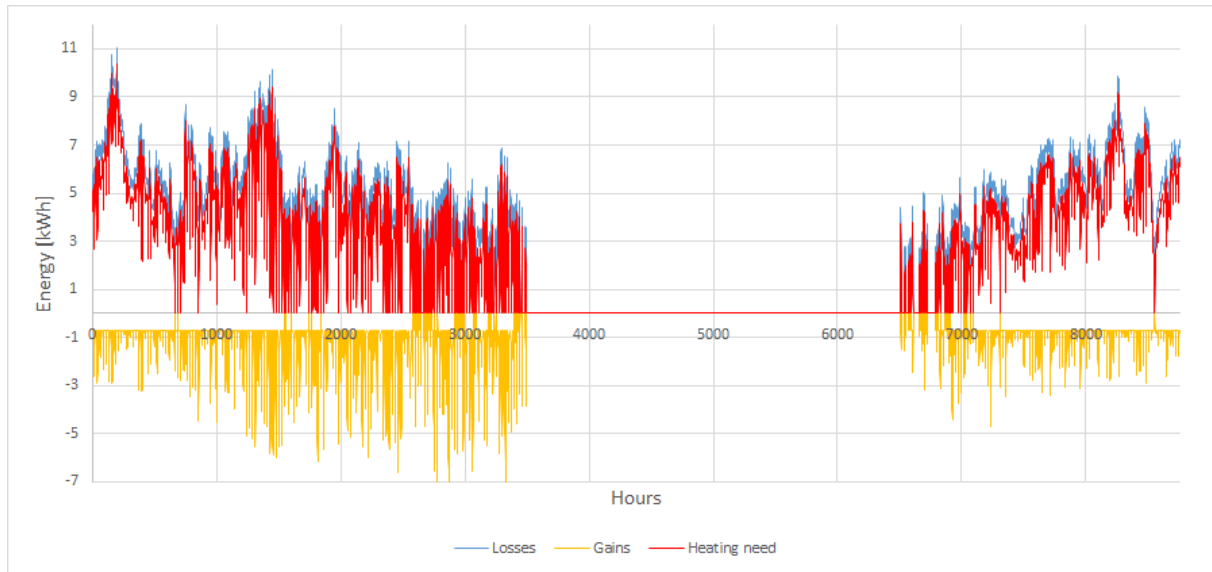


Figure 11: Hourly gains, losses and the final heating needs (sum of the gains and losses) from the static model (CS1) over the heating season.

Firstly, the number of heating hours are slightly higher for the static model. All the losses are also higher for the model but they are relatively close with a final heating need 8.18% higher. A stronger difference can be seen on the solar gains, with a decrease of 17% for the model. However, the input data (outside temperature and solar radiation) are not the same for the two computations. The explanation can be that the typical year used for the model has a slightly stronger winter: the average outside temperature for a larger heating period is lower for the weather data used ( $5.81^{\circ}\text{C}$  versus  $6.2^{\circ}\text{C}$ ), the number of heating hours is larger for the weather data (185 hours more), and a colder and more cloudy winter can also explain the lower solar radiations. The neglected gains show that the difference on this term is quite strong, without considering the gain utilisation factor. However, this method -deleting hour by hour the excess heat- is more logical than using the factor, and since the power considered is very low (2% of the final heating needs), it is considered as a valid assumption. In the dynamic model, the excess gains is not neglected anymore and is taken into consideration by varying the inside temperature of the house, as explained in Section 2.5. To illustrate these results, Figure 11 shows the evolution over the heating season of the hourly heating losses, the net heating gains, and the final heating needs. For CS2, the conclusions are similar, and data and graphs are presented in appendix A.2. In conclusion, the difference of 8% between the proposed model and the data from TABULA is considered small enough to assume it as valid.

A comparison is performed with HeaSyPac to analyse the hourly behaviour and the assumptions. As explained in Section 1.4.2, HeaSyPac is a tool from Laborelec, that compares the performance of different heat pumps by simulating their operation on an hourly basis over a full year, for SH and DHW demand. The building energy need is simulated through the use of the degree day method. The base temperature is fixed to  $15^{\circ}\text{C}$  for old and poorly insulated building,  $13^{\circ}\text{C}$  for recent and insulated buildings, and  $11^{\circ}\text{C}$  for nZEB. These three types of buildings are modelled, but the focus is put on the nZEB that is heated by low temperature floor heating, to compare it to the static model. The data from the building and the heat load is taken from an existing nZEB building in Bruges

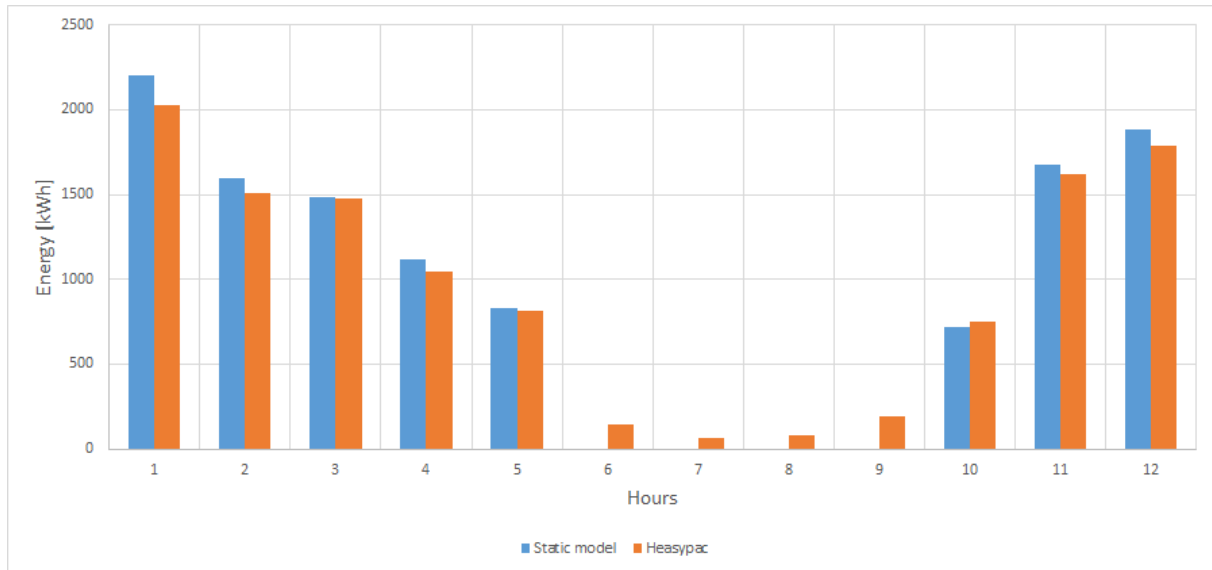


Figure 12: Comparison of the monthly heating needs from the static model (CS2) and HeaSyPac for a same yearly heating needs. It shows that the model is accurate in the monthly computation and validates the assumption of the unconsidered summer hours.

that is monitored.

The same weather data input is provided to both models, the temperature in Bruges for 2019, coming from HeaSyPac. Since HeaSyPac models a nZEB, CS2 is chosen to perform the simulation. The yearly consumption of the static model is computed and equals to 11510.42 kWh/year. This consumption is given as input to HeaSyPac. Figure 12 shows the monthly heating needs. During the summer, it is seen in HeaSyPac that the heating needs are strongly reduced compared to the months of the heating season. It confirms the assumption of 3000 hours of heating inactivity during the summer period of the static model. Since the consumption of both models have been set equals, an overconsumption is seen during the other months for the static model, up to 8.5 % in January. However, this difference stays limited. This will be also confirmed in Section 2.4 by comparing the heat pump consumption to Daikin's real data.

## 2.3 Heat pump model

In Section 1.4, it has been shown that a low temperature A/W heat pump is suitable to assess the flexibility in an insulated building that is equipped of a floor heating in Belgium. From the defined CS1 and CS2, Daikin provided their usual choice for low temperature A/W heat pumps. According to them, the heat pumps from the Daikin Altherma ERGA-EV series are considered as the best candidates to install in these cases. These heat pumps are their standard low temperature split unit heat pump to provide SH and DHW, with a frequency modulated compressor. Three different nominal output powers are available: 4, 6 and 8 kW, respectively referenced as Daikin Altherma ERGA04EV, ERGA06EV and ERGA08EV. They can be equipped without an auxiliary back up resistance, or with a resistance of 3 kW (for ERGA04), 6 kW (ERGA04/06/08) or 9 kW (ERGA06/08). In the scope of this work it has been decided to consider the 6 kW back up resistance for the three nominal powers. These heat pumps are connected heat pumps (with W-LAN



functions, a wireless local network connected to internet) and Smart Grid Ready, making them a clever choice and easy model to implement and to provide flexibility services. The data provided by Daikin is the full load thermal power and electrical consumption, for the outside temperature  $T_{out}$  between  $-20$  and  $20^\circ\text{C}$  and the water condenser temperature  $T_{w,su}$  between  $30$  and  $60^\circ\text{C}$ . However, no data related to the heat pump's part load performances is available. The heating capacity evolution for 3 different exit water temperatures ( $35$ ,  $45$  and  $55^\circ\text{C}$ ) according to the outside temperature for ERGA04EV is illustrated by Daikin in Figure 13. The complete data for the three heat pumps is provided in appendix A.3. The nominal conditions are at  $T_{w,su} = 35^\circ\text{C}$  and  $T_{out} = 7^\circ\text{C}$ . A strong drop can be seen between  $2$  and  $7^\circ\text{C}$ . Daikin confirmed that this is due to the defrost cycles, explained in Section 1.4.

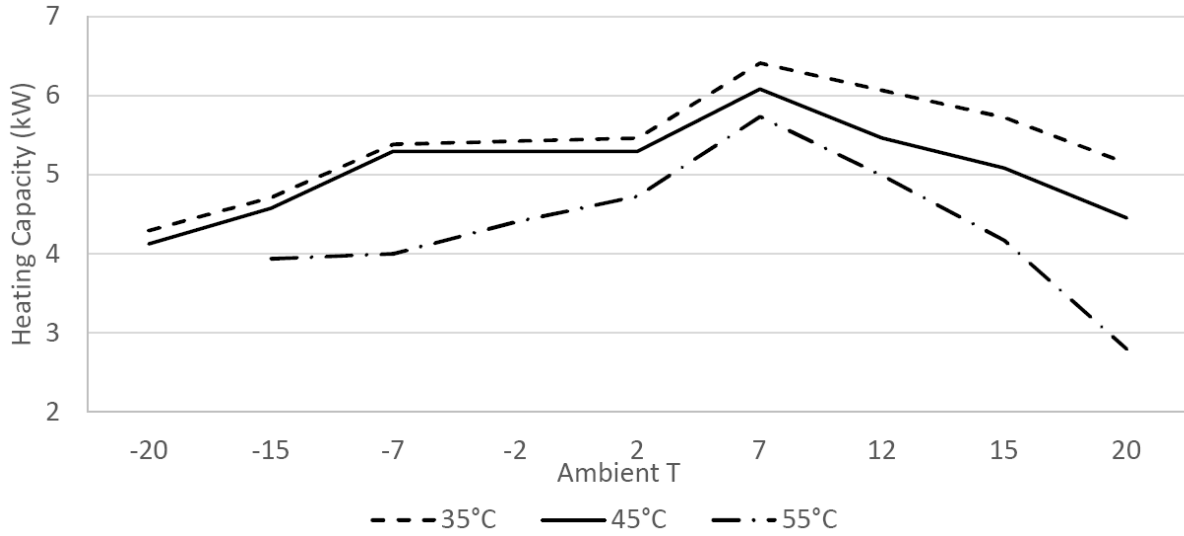


Figure 13: Heating capacity at full load according to of the outside temperature for the ERGA04 heat pump (Daikin Europe N.V., 2020).

In Section 1.4, different heat pumps modelling have been described. It has been decided to start by analysing the FlexiPac model since this model was used in a few past researches analysed in the literature review (Section 1.4) (e.g. (Masy et al., 2015), (Georges et al., 2013), (Georges, 2017) and (Garsoux, 2015)). The aim of this model is to couple it to a building model to analyse the seasonal performance of the heat pump as well as the flexibility for a smart grid integration (Gendebien, Georges, & Lemort, 2014). It models variable frequency heat pumps, and takes as inputs:

- The outside temperature  $T_{out}$  at the evaporator side;
- The temperature of the water leaving the heat pump  $T_{w,su}$ , at the condenser side, called the *supply water temperature*;
- The heating power needed  $\dot{Q}$ .

It gives as output:

- The electrical power consumed;  $\dot{W}$
- The COP.

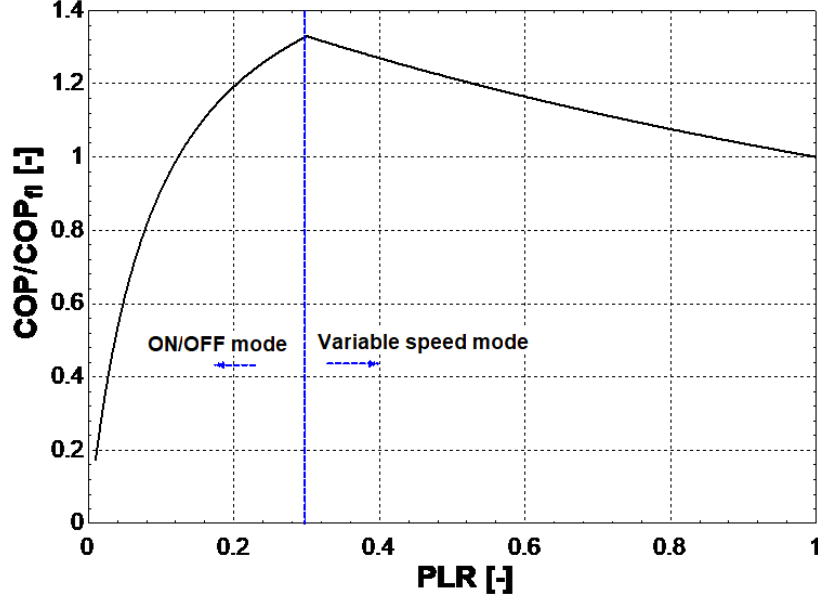


Figure 14: Example of performance at partial load according to the FlexiPac model (Gendebien, Georges, & Lemort, 2014).

The model uses two quadratic equations: one to compute the COP (EIRFT in equation 25 and the other to compute the full load power  $\dot{Q}_{fl}$  (CAPFT, equation 27). EIRFT use the variable  $\Delta T$  expressed in equation 26. These equations use also the provided data of nominal state of the model of heat pump selected ( $\dot{Q}_{nom}$ ,  $\dot{W}_{nom}$  and  $COP_{nom}$ ). A last equation is used to compute the partial load electrical power consumption (EIRFPLR, equation 28) with the variable PLR representing the partial load ratio, defined in equation 29. The  $D_x$ ,  $C_x$  and  $K_x$  parameters are the *calibration parameters* and are interpolated using the manufacturer data. At low PLR, typically under 30 %, the heat pumps stop running at variable speed and run instead in ON/OFF mode. It results in a strong decrease of the COP and this condition has to be avoided during the heat pump operation. Below this critical PLR, the COP is computed using equation 30, with  $a = 0.7701$  and  $b = 0.2299$  from Rivière (2004) and  $PLR_{ON/OFF}$  defined in equation 31. The behaviour of the heat pump at partial load is illustrated in Figure 14.

To model a heat pump using FlexiPac, it is required to have the nominal and full load data of  $\dot{Q}$ ,  $\dot{W}$ , the COP for different values of  $T_{out}$  and  $T_{w,su}$  and different working points at partial load.

$$EIRFT = \frac{COP_{nom}}{COP_{fl}} = C_0 + C_1 * \Delta T + C_2 * \Delta T^2 \quad (25)$$

$$\Delta T = \frac{T_{out}}{T_{w,su}} - \frac{T_{out,nom}}{T_{w,nom}} \quad (26)$$

$$CAPFT = \frac{\dot{Q}_{fl}}{\dot{Q}_{nom}} = D_0 + D_1 * (T_{out} - T_{out,nom}) + D_2 * (T_{w,su} - T_{w,nom}) \quad (27)$$

$$EIRFPLR = \frac{\dot{W}_{pl}}{\dot{W}_{fl}} = K_1 + (K_2 - K_1) * PLR + (1 - K_2) * PLR \quad (28)$$

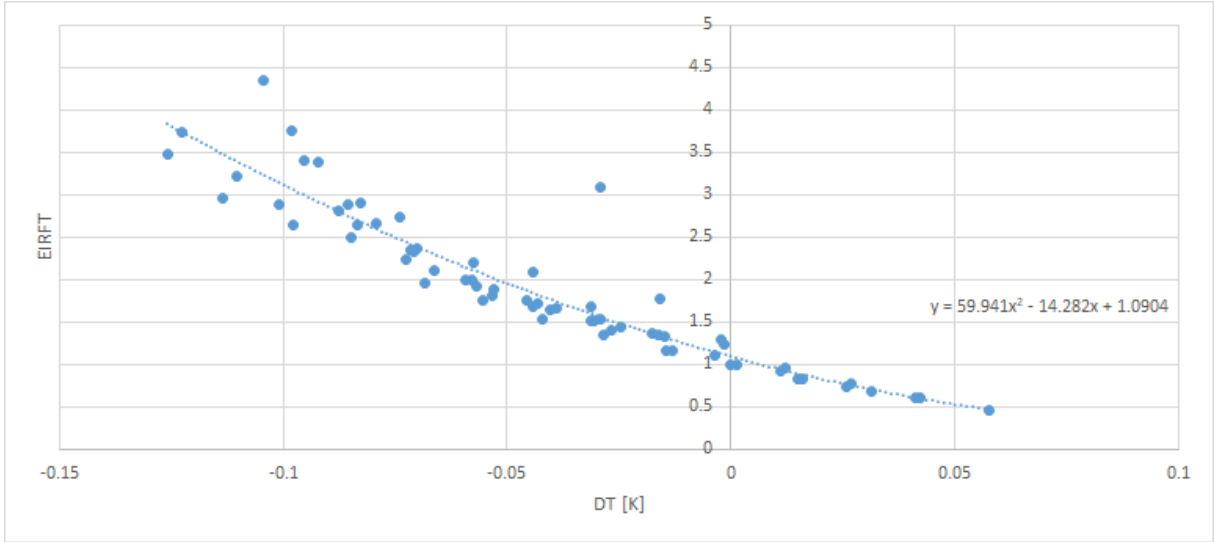


Figure 15: EIRFT curve interpolation and equation for the ERGA04 model.

$$PLR = \frac{\dot{Q}}{\dot{Q}_{fl}} \quad (29)$$

$$\frac{COP}{COP_{30\%}} = \frac{PLR_{ON/OFF}}{a \cdot PLR_{ON/OFF} + b} \quad (30)$$

$$PLR_{ON/OFF} = \frac{PLR}{0.3} \quad (31)$$

HP model:	ERGA04EV	ERGA06EV	ERGA08EV	
$COP_{nom}$	4.9	4.7	4.5	
$\dot{Q}_{nom}$ [kW]	6.4	7.7	9.4	
EIRFT	$C_0$	1.0904	1.0454	1.0507
	$C_1$	-14.2821	-12.9223	-12.1637
	$C_2$	59.9411	61.3201	42.9953
CAPFT	$D_0$	0.8633	0.8736	0.862
	$D_1$	0.0024	0.0051	0.0059
	$D_2$	-0.0085	-0.0065	-0.0038

Table 8: Calibration parameters updated for ERGA04-08 heat pumps.

It is chosen to update the heat pump model present in FlexiPac with the selected heat pumps. EIRFT and CAPFT curves are interpolated from the manufacturer data. Figure 15 shows the interpolation and equation of the EIRFT curve for the ERGA04 heat pump model. The calibration parameters are presented in Table 8. Since there is no part load data available,  $K_1$  and  $K_2$  can not be computed. The parameters of the original heat pump modelled in FlexiPac (a 8 kW Daikin Altherma) are  $K_1 = 0.154723$  and  $K_2 = 0.318399$ .

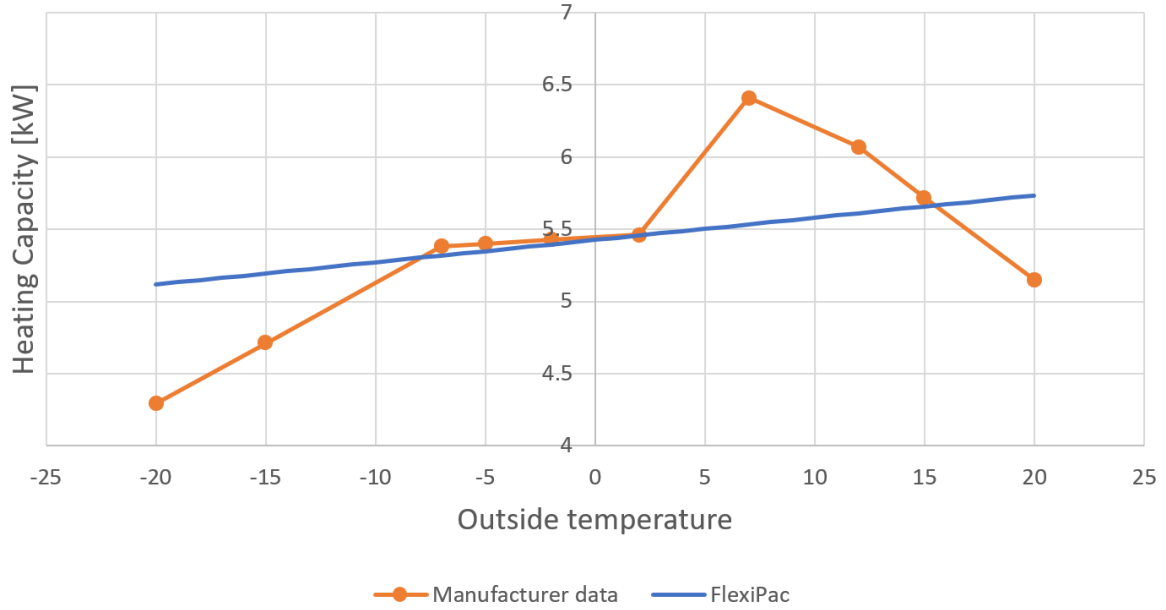


Figure 16: Simulation of the heating capacity at  $T_{w,su} = 35^\circ\text{C}$  with FlexiPac (blue) compared to the manufacturer data (orange). It is seen that FlexiPac behaviour is really different than the manufacturer data, due to the polynomial representation of the heat pump, and information on the defrost cycles impact on the performance is lost.

Figure 16 compares the FlexiPac simulation results with the manufacturer data for a water temperature of  $35^\circ\text{C}$  at full load. The results are quite different, with an underestimation of 16% of the heating capacity at  $7^\circ\text{C}$ , and an overestimation at the boundaries, up to 19% at  $-20^\circ\text{C}$ . This is explained by the way of modelling of FlexiPac, as the other polynomial model described in Section 1.4: since it interpolates the data to represent them via a polynomial law, an averaged curve is resulting. The overconsumption can be neglected, since the model will not heat the house for such low temperatures in the Belgian climate. The error of underestimation is problematic, since the heat pump will mostly run in this range. Moreover, the information regarding the effect of the defrost cycles on the heat pump performance is lost. These types of model can be really interesting to interpolate unknown points. However, since Daikin provides all the information of the performance of the heat pump, it is decided to choose a different way of modelling.

As it is done in HeaSyPac and mentioned by Patteeuw and Helsen (2014), a linear double interpolation of the manufacturer data is performed to model the heat pump at full load. The data used to define the model is the same: the electrical consumption and thermal power provided for the different outdoor conditions and supply water temperature conditions. The model takes as input the outdoor temperature  $T_{out}$  and the supply water temperature  $T_{w,su}$ , and returns the full load thermal power  $\dot{Q}_{fl}$  and full load electrical consumption  $\dot{W}_{fl}$ .

The general linear interpolation equation is given by equation 61. This equation is used three times in order to perform a double interpolation, with the two inputs data ( $T_{out}$  and  $T_{w,su}$ ). To illustrate this method and express the related equations, a simple case on a two by two data table is explained in appendix A.4. The results of the model at full load

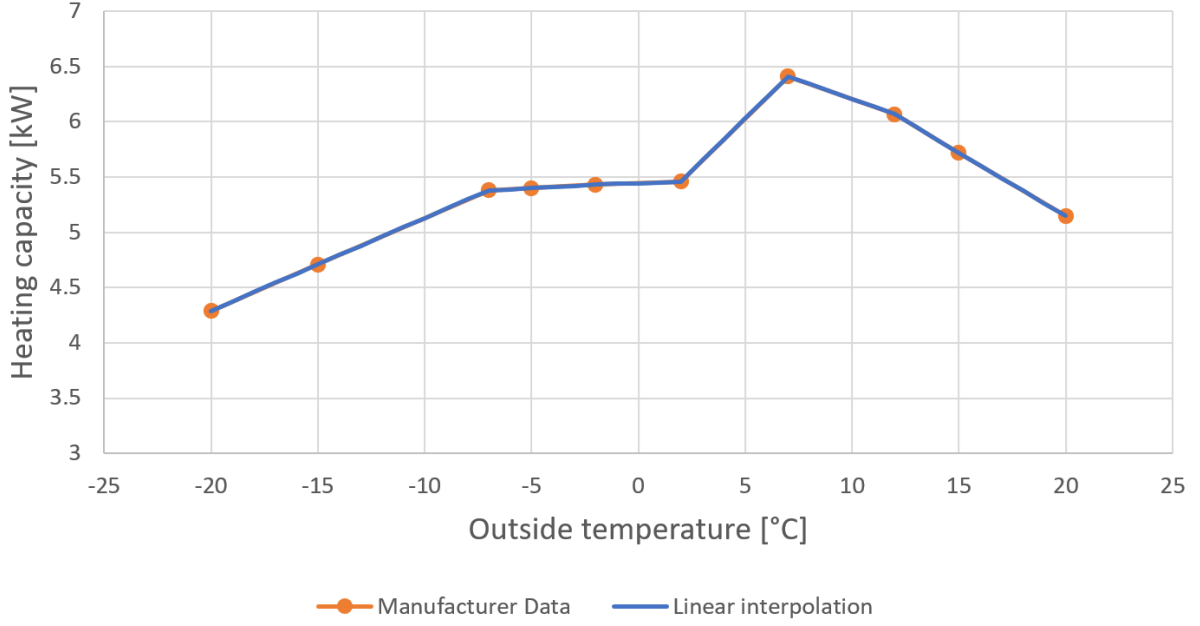


Figure 17: Simulation of the heating capacity of ERGA04 at  $T_{w,su} = 35^\circ\text{C}$  with the linear interpolation (blue) compared to the manufacturer data (orange).

is presented in Figure 17 for the ERGA04 with a water temperature of  $35^\circ\text{C}$ . The COP is computed from the general equation (equation 1).

$$y = y_1 + (y_2 - y_1) * \frac{x - x_1}{x_2 - x_1} \quad (32)$$

A part load model can also be added, in the same way as developed in the FlexiPac tool (equation 29 and 28). However, without any part load data, the following assumption is made: from 30 to 100% of the load, the heat pump runs with the same performance as the full load (constant COP). Under 30%, the performance is modelled using the assumption in FlexiPac and the coefficient of (Rivière, 2004). The back up resistance will be used when the power required is larger than the full load power of the heat pump, or when the part load is very low and the COP is lower than 1. These assumptions are discussed in Section 4.3. Considering the water supply temperature, it is shown in Section 2.4 that low energy buildings often require water at a supply temperature range of 25 to  $30^\circ\text{C}$ . However the manufacturer data provides values only from 30 to  $60^\circ\text{C}$ . Therefore, without any clue on the range below  $30^\circ\text{C}$ , it is assumed that the performances for this range are the same as for  $30^\circ\text{C}$ . This assumption is a conservative assumption, since the performance are better with the decrease of the water temperature. However, only a series of test in real condition or in a climatic chamber could provide information in the  $20^\circ\text{C}$  to  $30^\circ\text{C}$   $T_{w,su}$  range. This is illustrated in Figure 18, where the COP is computed according to the water temperature, with an outdoor temperature fixed to  $7^\circ\text{C}$  for the ERGA04 at full load.

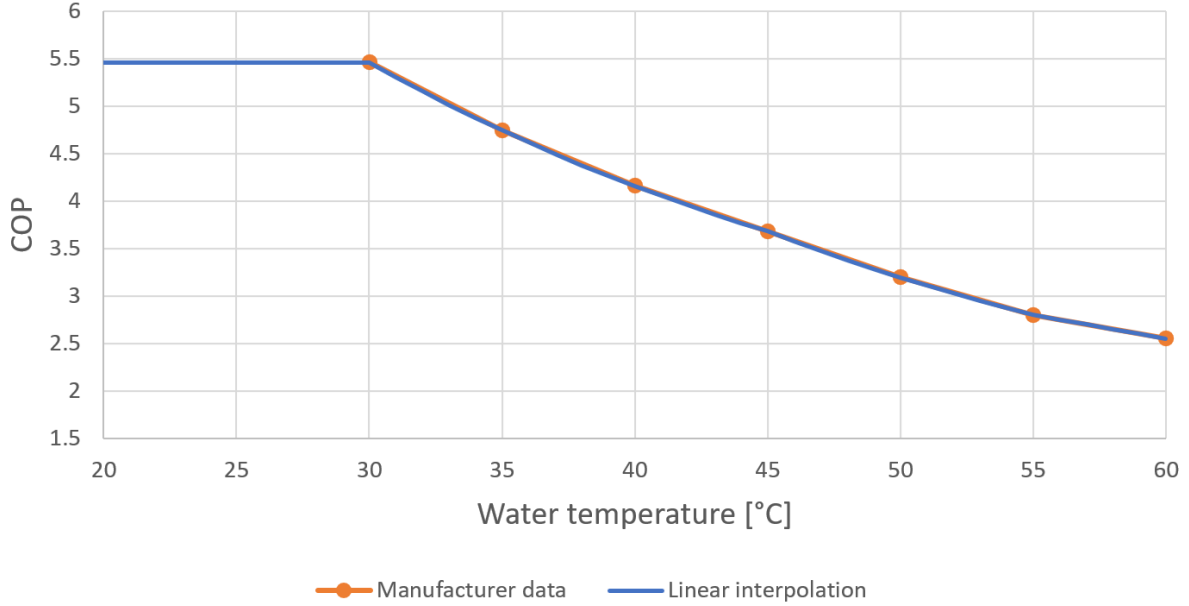


Figure 18: Simulation of the COP of ERGA04 at  $T_{out} = 7^\circ\text{C}$  with the linear interpolation (blue) compared to the manufacturer data (orange).

## 2.4 Interface between heat pump and building models

In this section, the static building model and the heat pump model are coupled, by modelling a radiative underfloor heating. Then the choice of the heat pump between the different sizes is explained. Finally, the water law to control the water supply temperature is computed.

### 2.4.1 Floor heating model

The floor heating model is the last block to link the heat demand of the house and the heat pump thermal power. The heat flux between the floor and the zone is defined in equation 33 from ISO 11855-2 with  $\dot{Q}_{fh}$  the heating power emitted by the floor,  $A_{floor}$  the total floor surface,  $T_{surf}$  the surface temperature of the floor and  $T_z$  the zone temperature. In the static model,  $T_z$  is fixed to  $20^\circ\text{C}$ . A simple model of floor heating is provided by Georges (2017) with two assumptions:

- The floor surface temperature is assumed to be the average of the supply and the return water temperature (equation 34)
- The Delta of temperature between the supply and return temperature is constant of 10K (equation 35)

Dongellini et al. (2020) assume that the floor heating is designed to have nominal  $\Delta T$  of 5 K, as well as Daikin Europe N.V. (2020), and this value is chosen. A last resistance  $R_{fh}$  is added to represent the cement screed and covering material composing the floor upper part, with example of standard values found in ISO 11855-2:2012 and illustrated in Figure 19. This example expresses the screed and covering material thickness and conductivity. The final model is expressed by the set of equation 33, 36 - 39, where:

- $T_{w,su}$  is the supply water temperature, the temperature of the water coming from the heat pump

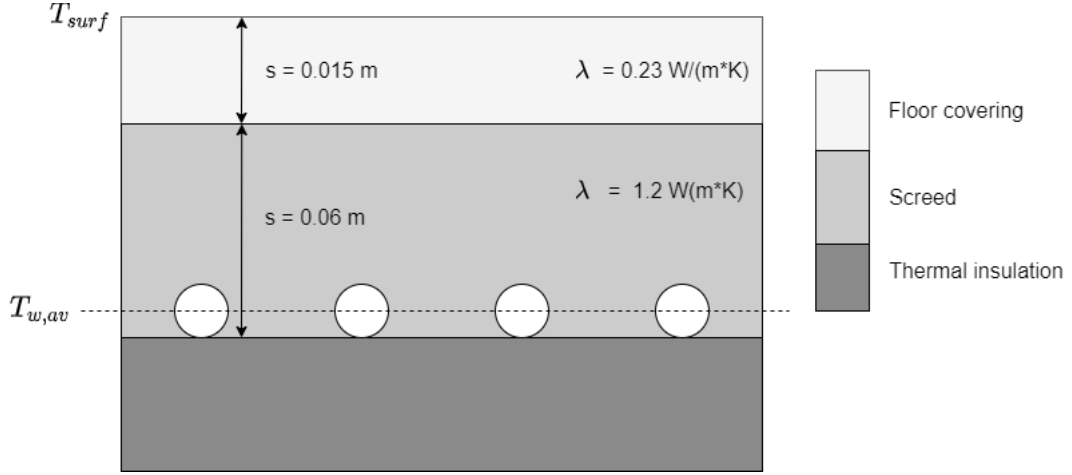


Figure 19: Floor heating example configuration from standard ISO 11855-2:2012.

- $T_{w,ex}$  is water temperature leaving the floor, returning to the heat pump
- $T_{w,av}$  is the average temperature at the pipe level, assumed to be the mean of the supply and exit water temperature

$$\dot{Q} = 8.92 * A_{\text{floor}} * (T_{\text{surf}} - T_z)^{1.1} \quad (33)$$

$$T_{\text{surf}} = \frac{T_{w,su} + T_{w,ex}}{2} \quad (34)$$

$$\Delta T = T_{w,su} - T_{w,ex} = 10K \quad (35)$$

$$T_{w,av} = \frac{T_{w,su} + T_{w,ex}}{2} \quad (36)$$

$$\Delta T = T_{w,su} - T_{w,ex} = 5K \quad (37)$$

$$\dot{Q}_{fh} = \frac{1}{R_{fh}} * A_{\text{floor}} * (T_{w,av} - T_{\text{surf}}) \quad (38)$$

$$R_{fh} = \frac{S_{cov}}{\lambda_{cov}} + \frac{S_{Screed}}{\lambda_{screed}} \quad (39)$$

The thermal comfort is a crucial point to take care of. Standard ISO 11855-1:2012 defines the maximum temperature of the floor at  $29^\circ\text{C}$ . This value is the standard of the floor heating manufacturers (Causone, Corgnati, Fabrizio, and Filippi (2009) ; Danfoss (2009)). A temperature of  $35^\circ\text{C}$  is allowed on the border of the room. However, the temperature is monitored in the model to not increase above  $T_{surf} = 29^\circ\text{C}$ .

The floor losses were computed in the static model according to the TABULA methodology, using the difference between the internal and external temperatures, a floor U-value and a soil adjustment factor (see Section 2.1). Considering the floor heating model, the losses are from the average water temperature to the ground. Since any information about

an existing underfloor heating or not in the building chosen, a new model of the ground insulation of the house is proposed according to values found in the literature. Johra and Heiselberg (2018) defined a ground structure of 40 cm expanded polystyrene insulation (EPS) ( $\lambda = 0.03$  [W/(m\*K)]), with a constant ground temperature set to 9°C, presented in Figure 20.

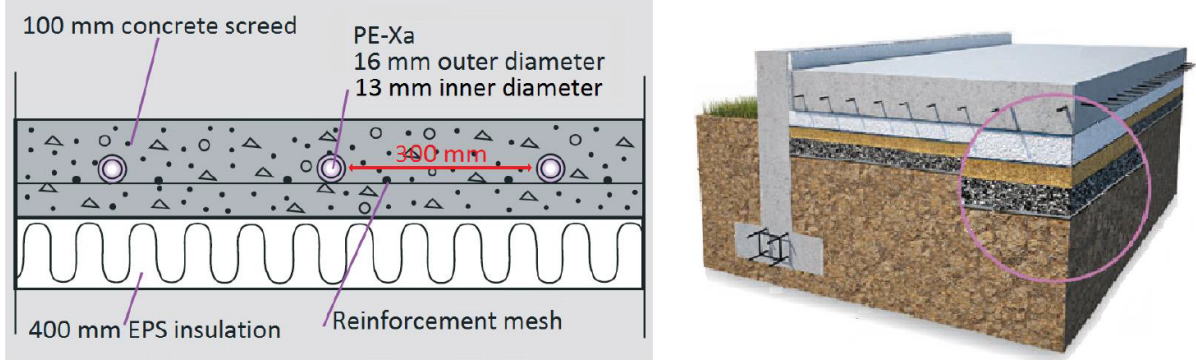


Figure 20: Ground insulation configuration with 40 cm of EPS insulation (Johra & Heiselberg, 2018).

This characteristic adds a resistance  $R_{ground}$  between the screed and the ground (equations 40 and 41). The results of this update are computed and compared to the original static model (Table 9). A 11% drop appears for CS1. This is not significant, and the drop represents 0.4 % of the total consumption. and the configuration is validated. For the nZEB, since a lower power is required, the temperature of the supply water is decreased (explained in Section 2.4). Therefore, much lower losses appear, with a drop of 52% compared to the static model. However, this drop represents 2.9% of the building heating needs. More accurate parameters can be found by decreasing the insulation thickness in Table 10. A more accurate value is 30 cm of EPS insulation for the nZEB. To keep the model flexible, a standard value of 40 cm is chosen for both buildings, to relate to the literature. The impact of this value is discussed in Section 4.4.

$$R_{ground} = \frac{0.4}{0.03} \quad (40)$$

$$\dot{Q}_{ground} = \frac{1}{R_{ground}} * A_{floor} * (T_{w,av} - T_{ground}) \quad (41)$$

	CS1		CS2	
	Static model	Update	Static model	Update
Floor consumption [kWh/(m <sup>2</sup> *year)]	4.05	3.62	4.09	2.7
Ratio	-11%		-52%	

Table 9: Comparison of the ground losses between the static model and the update for CS1 and CS2.



	Static model	Update	Ratio
Floor consumption (30 cm insulation) [kWh/(m <sup>2</sup> *year)]	4.09	3.57	- 14%
Floor consumption (20 cm insulation) [kWh/(m <sup>2</sup> *year)]	4.09	5.35	+31%

Table 10: Comparison of the ground losses for 20 and 30 cm of EPS insulation for case CS2.

### 2.4.2 Sizing of the heat pump

The next step is to run the model for the building chosen in order to size the heat pump correctly. Each heat pump is run for both buildings and the best heat pump for each will be chosen according to the highest SCOP. As explained in Section 1.3, the SCOP is the ratio between the total heat provided during the heating season and the total electricity consumed for the heating (equation 3). This SCOP is strongly related to the sizing of the heat pump:

- If the heat pump is undersized, the back up resistance is more used during the coldest days and the SCOP decreases
- If the heat pump is oversized, it will work at a low part load ratio at the beginning and the end of the heating season, decreasing also the SCOP

The size of the heat pump has also a large impact on its price and smaller heat pumps are usually favoured in order to decrease the investment costs. Therefore, choosing a heat pump with a larger capacity should be considered only if the SCOP is largely improved. A first simple analysis can be conducted by simulating the heating need of the building and the heat pump's full load capacity for different outside temperatures to analyse the bivalent points, as explained by Dongellini et al. (2020). These simulations are computed with the ground losses update and are provided for CS1 in Figure 21 and Figure 22 for CS2. For CS2, the first approximation leads directly to the choice of the 4 kW heat pump since it will already cover all the needs until -8°C. Concerning CS1 the estimation is leading to the 8 kW heat pump. However a more accurate method is to simulate over the whole heating season to obtain the SCOP. This method takes also in account the solar gains that have been neglected. To understand the impact of the use of the back up resistance, a  $SCOP_{net}$  is introduced. It expresses the ratio between the thermal power provided by the heat pump and its electrical consumption, without the thermal and electrical contribution of the back up resistance, when the SCOP takes into account the contribution of the backup resistance. The results are provided in Table 11. It confirms the choice of the ERGA04 for CS2. The results suggest the choice of ERGA08 for CS1. A more in depth economic analysis could provide the optimum choice.

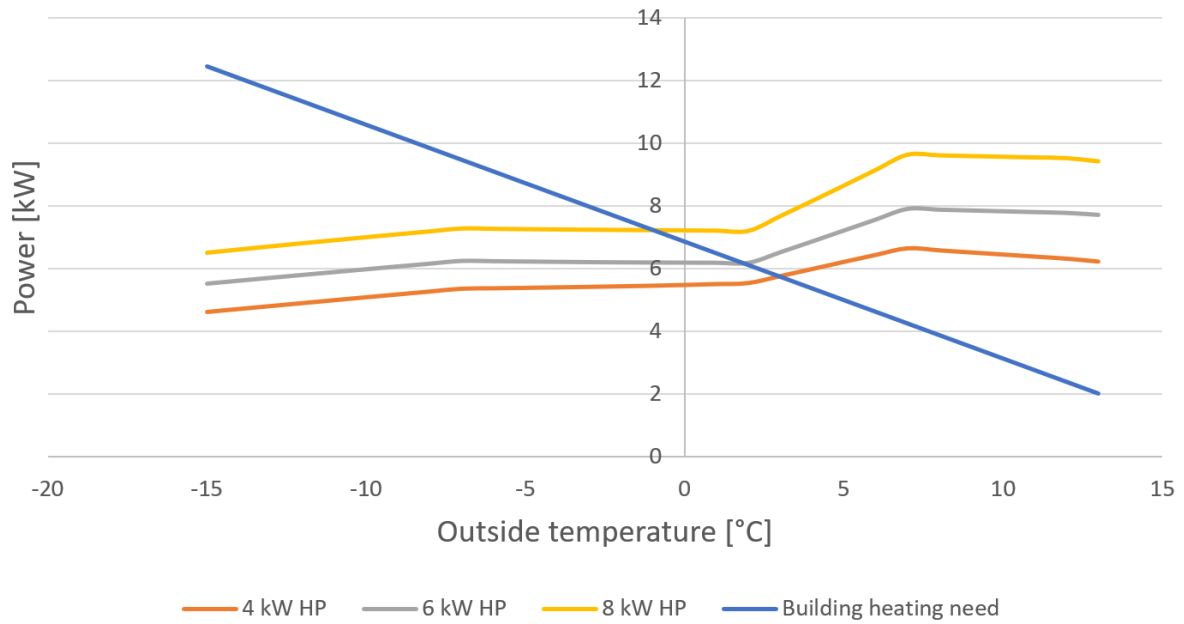


Figure 21: Bivalent points of the three different heat pumps and CS1 heating needs. The most suitable heat pump model from this first approximation is the 8kW heat pump.

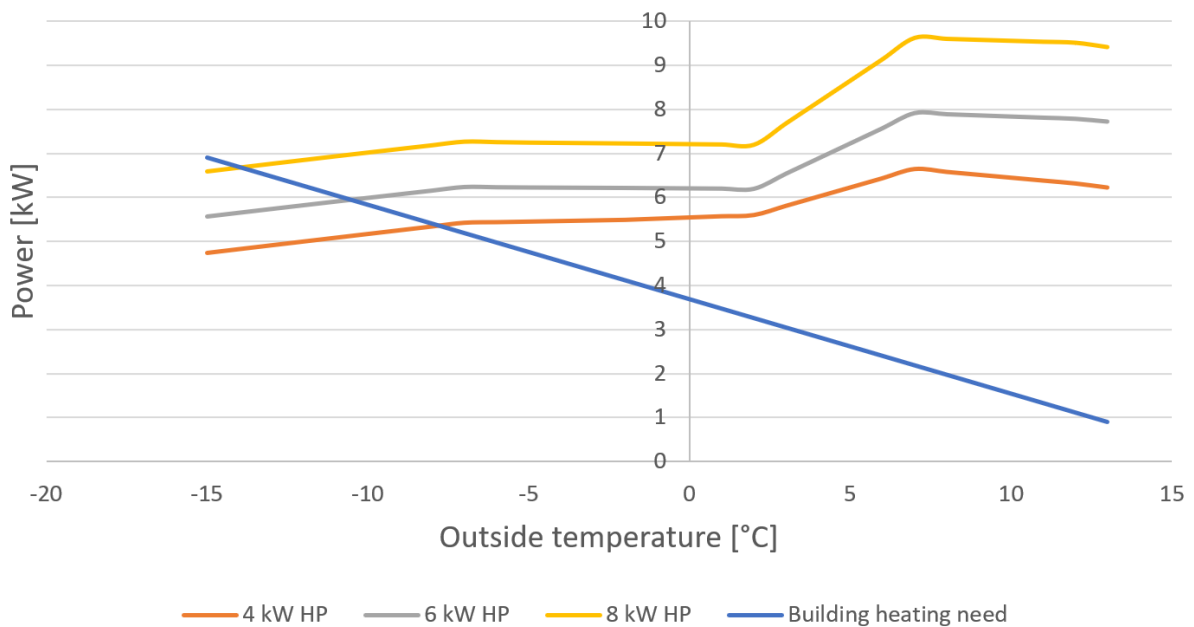


Figure 22: Bivalent points of the three different heat pumps and CS2 heating needs. It is seen from this first approximation that the 4kW heat pump is largely sufficient to provide the full amount of heat.

Heat pump model		4 kW	6 kW	8 kW
CS1	$\dot{Q}_{HP}$ [kWh]	22 038	22 038	22 038
	$\dot{W}_{HP}$ [kWh]	5 785	5 463	5 406
	SCOP <sub>net</sub>	4.7135	4.5052	4.2149
	<b>SCOP</b>	<b>3.8098</b>	<b>4.0339</b>	<b>4.0768</b>
CS2	$\dot{Q}_{HP}$ [kWh]	11 001	11 001	11 001
	$\dot{W}_{HP}$ [kWh]	2 335	2 401	2 545
	SCOP <sub>net</sub>	4.7137	4.5827	4.3229
	<b>SCOP</b>	<b>4.7114</b>	<b>4.5827</b>	<b>4.3229</b>

Table 11: Results of the simulations of each heat pumps for CS1 and CS2. It is seen that the 8kW model is suitable for CS1 and the 4kW heat pump model for CS2.

The results of the electrical consumption during the heating season of this simulation are compared to a provided sizing study of Daikin, referred as *Daikin CS*. This study concerns a low energy residential building with an annual thermal heating need of 9683 kWh. This consumption can be related to CS2 that has an annual need of 11001 kWh. Daikin determined with a simulation that the ERGA06EV suits for this case study, with a backup resistance of 6 kW. In the static model, the ERGA04EV has been chosen. This can be explained by the fact that not only heating is considered by Daikin but also the DHW need (Table 12). These values are in the same range than the one computed with the static model. In both cases, the heating need is completely covered by the heat pump without the need of the backup resistance. The range of the supply water temperature is determined between 25°C and 35°C by Daikin, and is similar as the range found in the static model and this is explained in the next part of this section. A few graphs are provided and compared.

Simulation	Static model	Daikin	Difference
Heat pump model	4 kW	6 kW	/
$\dot{Q}_{HP}$ [kWh]	11 001	9 683	14%
$\dot{W}_{HP}$ [kWh]	2401	2 192	10%
<b>SCOP</b>	<b>4.5714</b>	<b>4.42</b>	3.4%

Table 12: Comparison of the heating needs over the whole heating season and performance between CS2 (4 kW) and Daikin CS with  $\dot{Q}$  the thermal power provided and  $\dot{W}$  the electrical power consumed. The two cases analysed are in the same consumption range. Moreover the SCOPs of the heat pumps are similar, validating the model configuration of the envelope and ground modelling as well as the heat pump interpolation model used.

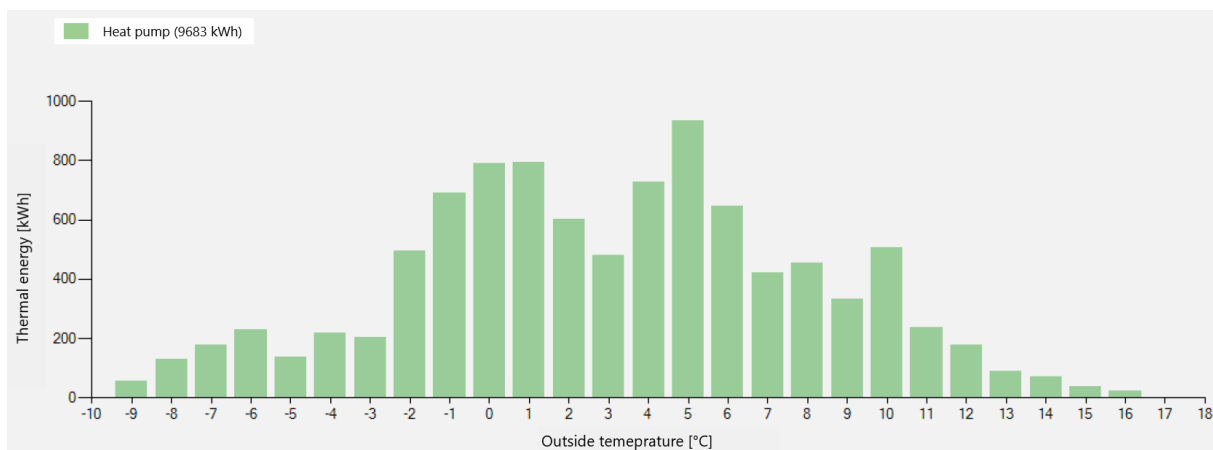


Figure 23: Thermal power distribution according to the outside condition for Daikin CS.

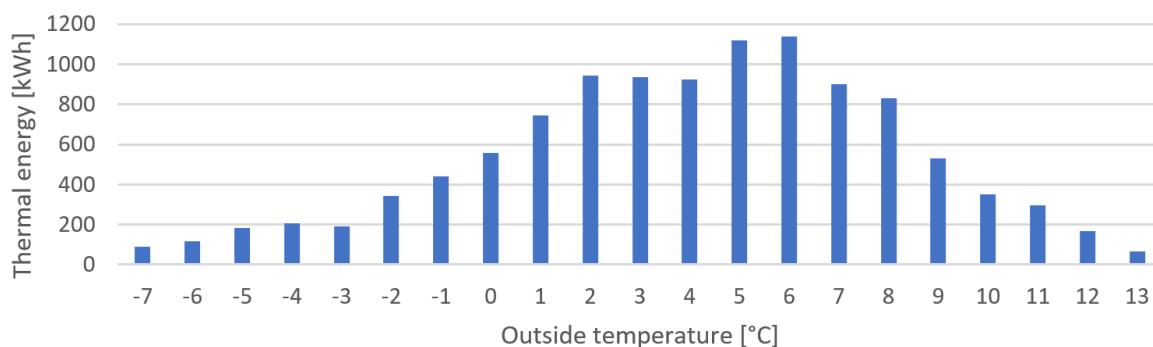


Figure 24: Thermal power distribution according to the outside condition for CS2 (4 kW).

Figures 23 and 24 show the thermal power distribution according to the outside temperature. It is seen that more heat is provided at lower temperature for Daikin CS comparing to CS2, with a peak at 800 kWh around 0°C and over 200 kWh around -6°C. It explains the lower COP of Daikin CS and this situation depends on the weather data, that are different for both computations. However, it is shown in the Daikin case study that the heat provided in the range from 14 to 16 °C is really low. The assumption in the static model to neglect the heating over 13°C due to the thermal capacity of the building is confirmed.

Finally, Figure 25 shows the monthly electrical consumption for both case studies. The summer period defined in the static model is corresponding well to the evolution of the consumption of Daikin CS. However, a larger consumption is seen in May, and a lower in January. The last one is mostly due to the different weather data and explains the larger needs of heating a low  $T_{out}$  of Daikin CS.

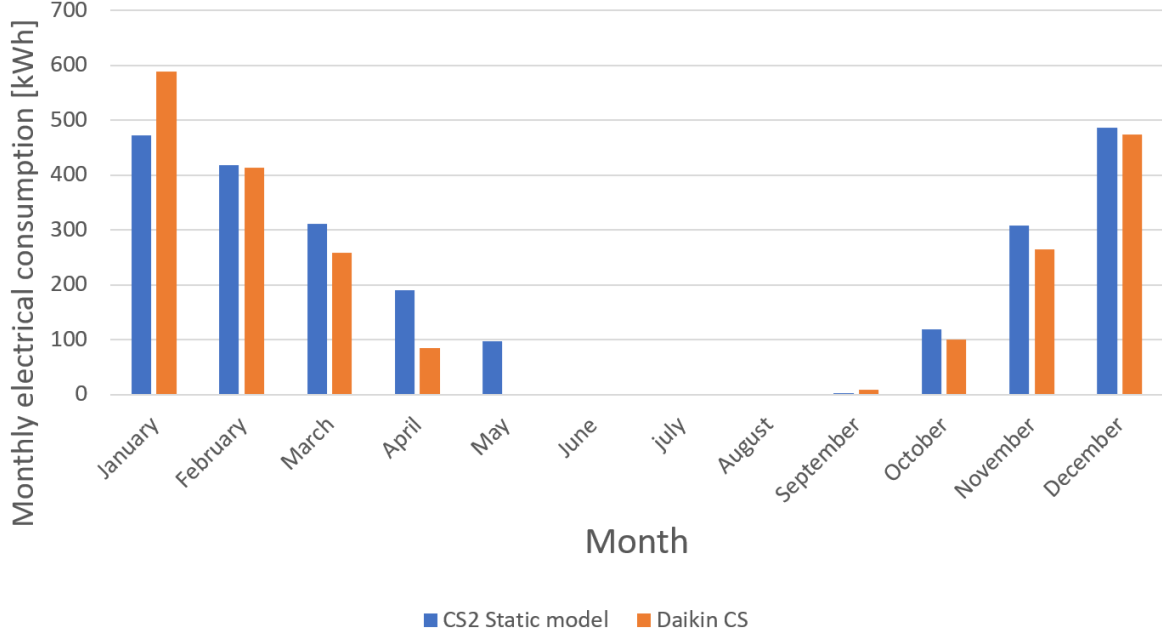


Figure 25: Comparison of the monthly electrical consumption between CS2 (6 kW) and Daikin CS.

### 2.4.3 Water law

In order to perform dynamic simulations of the building, the heat pump has to be controlled in order to provide the right amount of heating needed. A usual way to control heat pumps is to set the supply temperature according to the outside temperature (Georges, 2017), since the heat flux provided from the heat pump to the house directly depends on the supply water temperature (equations 38 and 36). In practice, this *water law* is tuned according to the building by the installer. In the scope of this work, a similar approach as Verhelst et al. (2012) is used: the water law is set using the static model. This law is independent of the heat pump model, and depends only on the outside temperature, the inside set temperature, and the envelope characteristics of the house. This law is computed by simulating the outside temperature from  $-10$  to  $13$  °C (since the model stops heating at  $13$ °C) and interpolating the supply water temperature resulting. The internal temperature is set to  $20$ °C. Solar radiation is not taken into account in this simulation: the aim is to obtain a water law that drives the power of the heat pump precisely, and depending only on the inside and outside temperature. If the solar irradiation are taken into account, it will shift the water law to a colder curve, and not enough energy will be provided to the building during the night. On the opposite, if there are solar gains, the gain will be in excess, a condition will stop the heat pump the next hour if the setpoint temperature is exceeded. This water law is critical for the dynamic simulations: during these simulations, the inside temperature can be set higher or lower than  $20$ °C, in order to store/release the thermal energy. Therefore, the water law is computed for  $T_{set}$  from  $16$  to  $24$ °C. Figure 26 represents the water law for CS1 at  $T_{set} = 20$ °C. The water law is linearly interpolated resulting in equations of the form of equation 42. The values found for all the  $T_{set}$  of CS1 and CS2 are provided in Table 13.

$$T_{w,su} = m * T_{out} + p \quad (42)$$

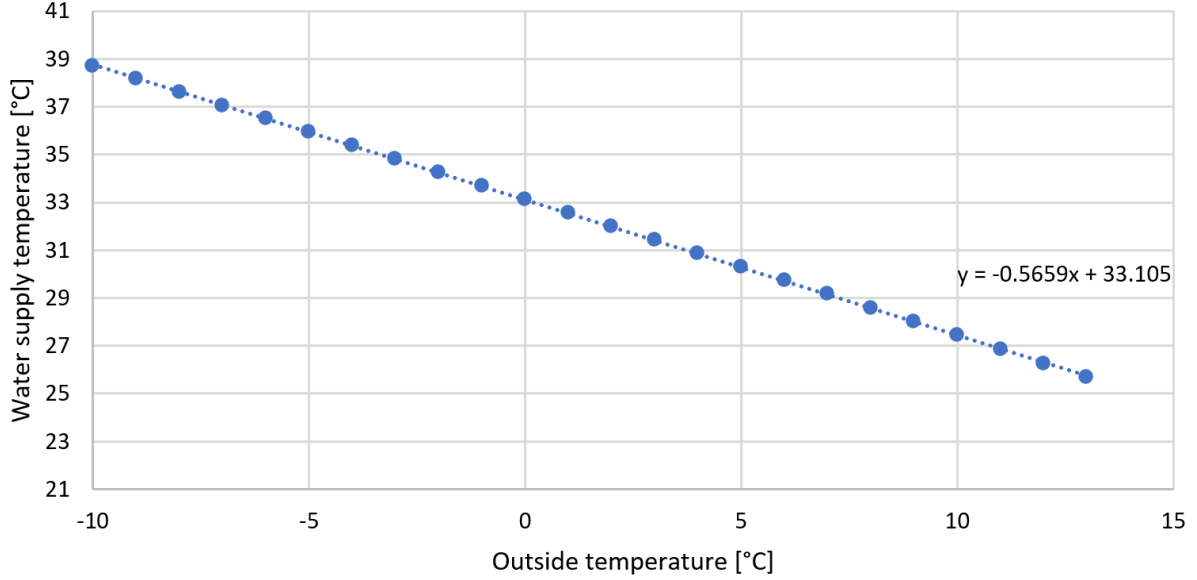


Figure 26: Water law for CS1 at  $T_{set} = 20^{\circ}\text{C}$ .

Building		CS1		CS2	
Coefficients of the water law		m	p	m	p
Zone setpoint temperature [°C]	16	-0.5737	26.832	-0.33822	22.93239
	17	-0.5713	28.403	-0.33764	24.26735
	18	-0.5693	29.972	-0.33613	25.60373
	19	-0.5675	31.54	-0.33485	26.93858
	20	-0.5659	33.105	-0.33372	28.27215
	21	-0.5644	34.669	-0.33271	29.60465
	22	-0.5631	36.232	-0.33178	30.93618
	23	-0.5618	37.793	-0.33093	32.26683
	24	-0.5606	39.353	-0.33014	33.59667

Table 13: Coefficient of the water law at different setpoint temperatures for CS1 and CS2.

By plotting the different m and p values, it is easy to understand that they can also be interpolated : m with a quadratic law (Figure 27), and p with a linear law (Figure 28). This method leads to a single equation of the water law for each building, in the form of equation 43, depending directly on the inside and outside temperature, without implementing different cases in the code of the dynamic model. The final water law for CS1 is provided by equation 44 and equation 45 for CS2.

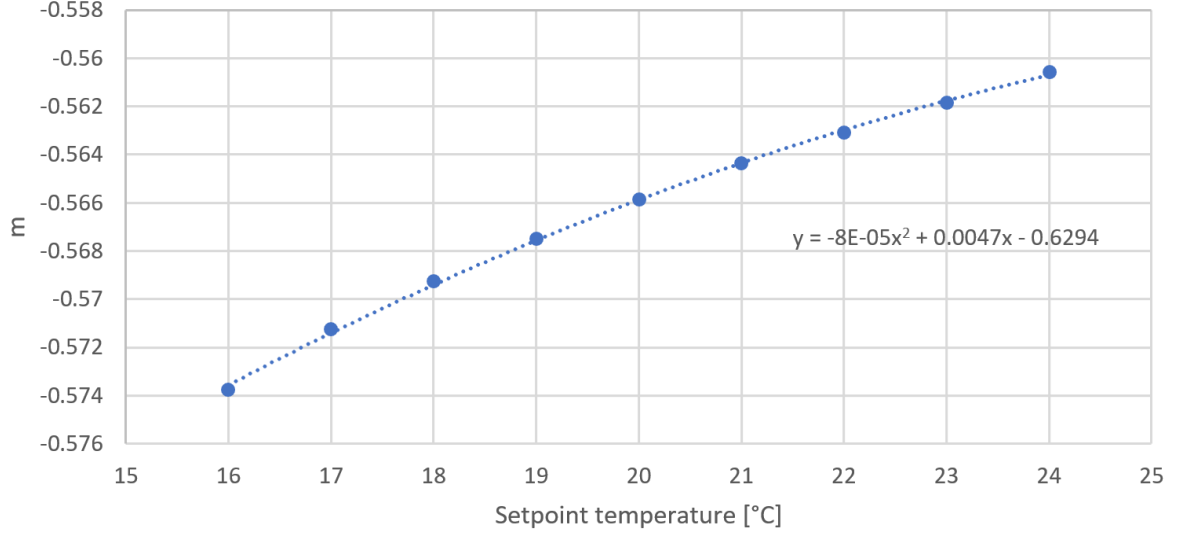


Figure 27: Quadratic interpolation of m coefficients of CS1.

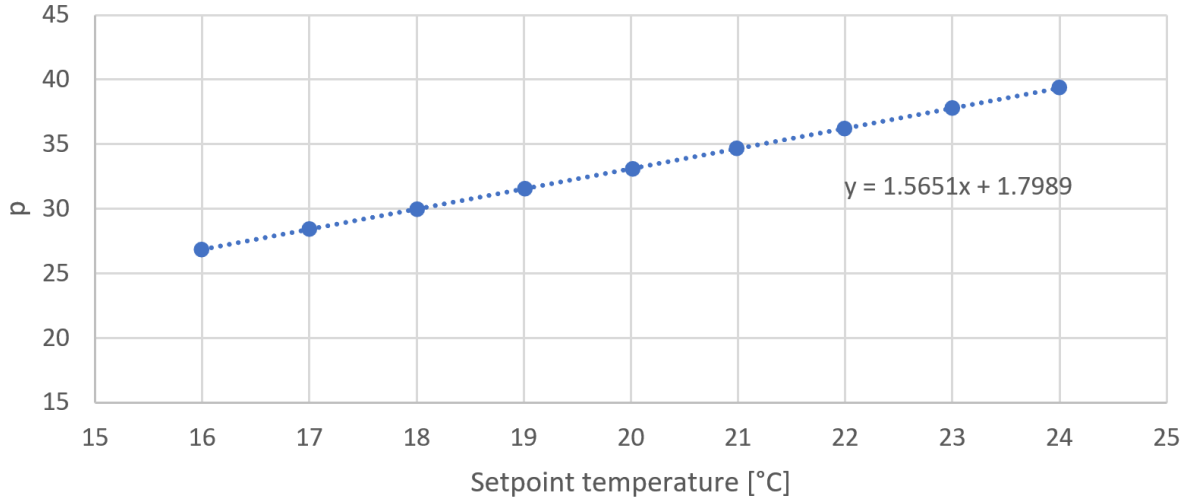


Figure 28: Linear interpolation of p coefficient of CS1.

$$T_{w,su} = (\alpha_1 * T_{set}^2 + \alpha_2 * T_{set} + \alpha_3) * T_{out} + \beta_1 * T_{set} + \beta_2 \quad (43)$$

$$T_{w,su} = (-8 * 10^{-5} * T_{set}^2 + 0.0047 * T_{set} - 0.6294) * T_{out} + 1.5651 * T_{set} + 1.7989 \quad (44)$$

$$T_{w,su} = (-3 * 10^{-5} * T_{set}^2 + 0.0023 * T_{set} - 0.3669) * T_{out} + 1.3331 * T_{set} + 1.6066 \quad (45)$$

## 2.5 Dynamic model

In this section, the dynamic model developed in order to perform the simulations of the flexibility is explained. This model is based on assumptions and methodology explained for the static building model in Section 2.2, the heat pump model investigated in Section 2.3 and the interface between both explained in Section 2.4. Then the dynamic model results are compared to the static one in terms of heat demand and power consumption to validate it.

### 2.5.1 Dynamic model definition

The dynamic model is the continuous evolution of the static model and its assumptions defined in the previous sections. Different types of approaches are found in the literature as explained in Section 1.4.2. According to Georges (2017), Yang et al. (2007), Verhelst et al. (2012) and others, a single-zone model is already able to capture the dynamic of the building.

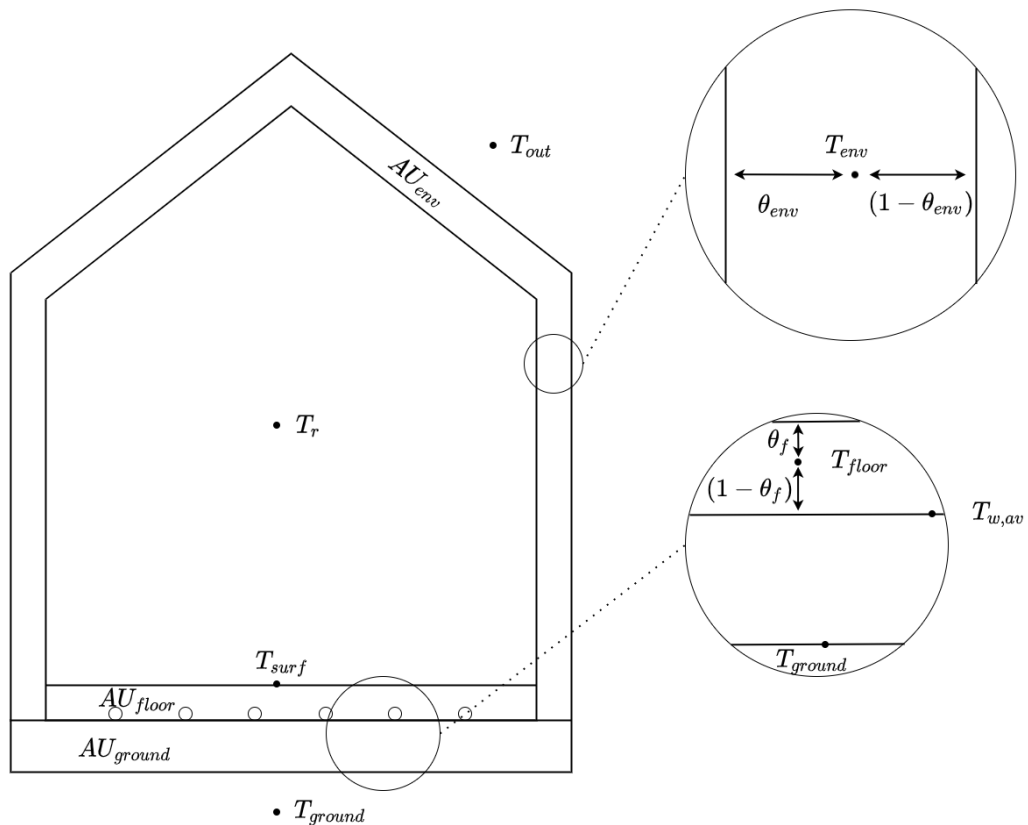


Figure 29: Schematic representation of the building modelled.

The electrical RC analogy method with lumped capacities is used. Figure 29 presents the final configuration of the house. It consists of the house's envelope (external walls, roof, windows and door), described in Section 2.1, the ground insulation and the floor



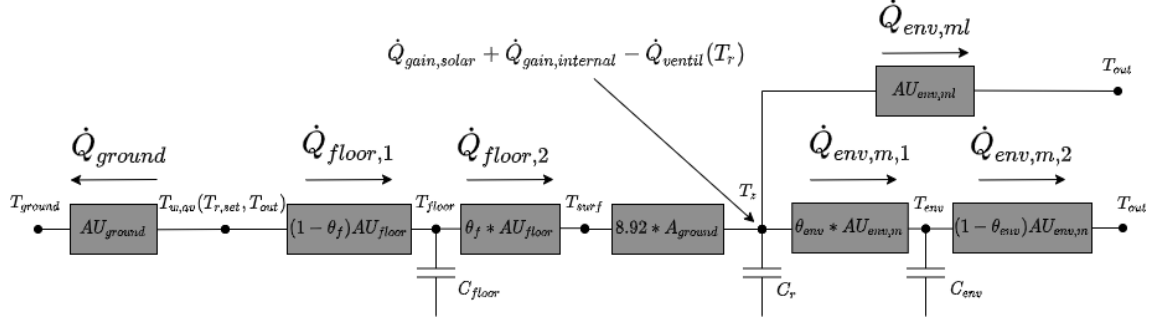


Figure 30: Equivalent resistance circuit of the dynamic building model.

heating, described in Section 2.4. It is chosen to model the walls and the ground by a 2R1C equivalent, as described by Masy (2008). The adjustment parameters of the walls, defined according to Masy (2008) for concrete blocs insulated and brick walls, are  $\phi_{env} = 0.7$  and  $\theta_{env} = 0.1$ . Considering the floor, only the capacity of screed is modelled.  $\phi_f$  is set to 1 since no insulation material are present and the accessibility  $\theta_f$  is assumed to be 0.5: the capacity of the ground is in the middle of the screed. As found in standard ISO13790, it is chosen to decouple from the envelope losses the *massive elements* that possess a capacity, such as the walls or the roof, and the *mass-less elements* that do not act in the building TES (windows and door).

Figure 30 presents the equivalent RC circuit of the dynamic model. The system is composed of 3 states variables:

- $T_{floor}$ , the virtual temperature of the floor where the floor's capacity is connected;
- $T_z$ , the zone's temperature that is assumed homogeneous in the whole zone considered as in the static model;
- $T_{env}$ , the virtual temperature of the envelope where the envelope's capacity is connected.

Seven main heat fluxes compose the model:

- $\dot{Q}_{HP}$  is the power provided by the heat pump (equation 47)
- $\dot{Q}_{ground}$  is the power lost in the ground, defined in section 2.4 (equation 50)
- $\dot{Q}_{floor,1}$  is the power supplying the floor (equation 51)
- $\dot{Q}_{floor,2}$  is the power emitted by the floor heating (equation 52)
- $\dot{Q}_{env,ml}$  is the power lost from the mass-less elements of the envelope to the outside environment (equation 54)
- $\dot{Q}_{env,m,1}$  is the power lost from the zone to the massive elements of the envelope (equation 55)
- $\dot{Q}_{env,m,2}$  is the power lost from the envelope's massive elements to the outside environment (equation 56)

The final set of equations of the model is defined by equations 46 to 59. The solar gains, internal gains and ventilation losses (respectively  $\dot{Q}_{gain,solar}$ ,  $\dot{Q}_{gain,internal}$  and  $\dot{Q}_{ventil}$ ) are defined in Section 2.2.

$$T_{w,su} = (\alpha_1 * T_{set}^2 + \alpha_2 * T_{set} + \alpha_3) * T_{out} + \beta_1 * T_{set} + \beta_2 \quad (46)$$

$$\dot{Q}_{HP} = \dot{Q}_{ground} + \dot{Q}_{floor,1} \quad (47)$$

$$\dot{W}_{HP} = HP(\dot{Q}_{HP}, T_{out}, T_{w,su}) \quad (48)$$

$$T_{w,av} = T_{w,su} - \frac{\Delta T}{2} \quad (49)$$

$$\dot{Q}_{ground} = \frac{1}{R_{ground}} * A_{floor} * (T_{w,av} - T_{ground}) \quad (50)$$

$$\dot{Q}_{floor,1} = (1 - \theta_f) * AU_{floor} * (T_{w,av} - T_{floor}) \quad (51)$$

$$\dot{Q}_{floor,2} = \theta_f * AU_{floor} * (T_{floor} - T_{surf}) \quad (52)$$

$$\dot{Q}_{floor,2} = 8.92 * A_{floor} * (T_{surf} - T_z)^{1.1} \quad (53)$$

$$\dot{Q}_{env,ml} = AU_{env,ml} * (T_z - T_{out}) \quad (54)$$

$$\dot{Q}_{env,m,1} = \theta_{env} * AU_{env,m} * (T_z - T_{env}) \quad (55)$$

$$\dot{Q}_{env,m,2} = (1 - \theta_{env}) * AU_{env,m} * (T_{env} - T_{out}) \quad (56)$$

$$C_{floor} * \frac{dT_{floor}}{dt} = \dot{Q}_{floor,1} - \dot{Q}_{floor,2} \quad (57)$$

$$C_z * \frac{dT_z}{dt} = \dot{Q}_{floor,2} + \dot{Q}_{gain,solar} + \dot{Q}_{gain,internal} - \dot{Q}_{ventil} - \dot{Q}_{env,ml} - \dot{Q}_{env,m,1} \quad (58)$$

$$C_{env} * \frac{dT_{env}}{dt} = \dot{Q}_{env,1} - \dot{Q}_{env,2} \quad (59)$$

An hourly time step is considered, since the building is heated with underfloor heating that has a response time in the order of one to three hours (Danfoss, 2009). This assumption also secures the single zone assumption: since the buildings chosen are relatively well insulated, an hourly computation can assume the diffusion of heat between the rooms of the house. A quicker time step would also lead to consider transitive effects and a necessary more complex model of the heat pump, since the start and stop of the heat pump is limited during an hour to avoid damages, and this limit is specific to each model of heat

pump. On the other hand, a slower time-step will not catch all the dynamic of the system.

Capacity	$C_{floor}$	$C_z$	$C_{env}$
[J/K]	1.519e7	0.5386e7	4.1256e7
[Wh/K]	4220.8	1496	11460

Table 14: Values of the capacity used for the dynamic model

At each step, the 3 states variables are updated by performing a heat balance according to equation 9, respectively in equations 57, 58 and 59. Since the time-step is chosen as an hour, the system is discretised and  $dt$  equals to 3600 seconds. The capacities  $C_{floor}$ ,  $C_z$  and  $C_{env}$  are presented in Table 14 and computed according to the following references:

- The ground’s capacity composed by the cement screed and the covering material is computed assuming only the cement screed volume, with the density and heat capacity of concrete provided by Johra and Heiselberg (2018).
- The zone’s capacity is computed using the heat capacity of air ( $C_{p,air} = 1006$  [KJ/(kg\*K)]), its density ( $\rho_{air} = 1.2041$  [kg/m<sup>3</sup>]), the protected volume of the house considered (741 [m<sup>3</sup>] for CS1 and CS2 (Cuyppers et al., 2014)). This value is multiplied by a factor 6 according to Masy (2008) to take into account the stratification of the air temperature inside the zone. As explained, the internal walls or furniture are not taken into account. Therefore, this capacity is considered as the minimal zone capacity, and the impact of an increase in the zone capacity is analysed in Chapter 3.
- The envelope’s capacity is more difficult to set and has to be discussed. According to TABULA, the capacity of the CS1/CS2 house is 45 Wh/(m<sup>2</sup>\*K). Since no information on the floor configuration is provided by the tool, it is assumed that this capacity does not take into account the floor capacity. Typical values are also found in the literature. Standard ISO 13760 defined 5 thermal inertia classes, according to the type of construction material. They are referred as very light, light, medium, heavy and very heavy and are presented in Table 15. Le Dréau and Heiselberg (2016) defined for a *light capacity 80’s house* a capacity of 44 Wh/(m<sup>2</sup>\*K), and 53 Wh/(m<sup>2</sup>\*K) for a *medium capacity passive house*. Johra (2018) classified 3 thermal inertia classes with each three different sub-variations (Table 16). Masy (2008) defined some values of the capacities of the heavy elements composing the envelope, the walls and the roof (Table 17). It is chosen to consider a value of 50 Wh/(m<sup>2</sup>\*K). However, different cases regarding a higher or lower inertia building are investigated in Chapter 3.

Building structure	Envelope capacity			
	J/K*m <sup>2</sup>	Wh/K*m <sup>2</sup>	J/K	Wh/K
Very light	80000	22.2	1.8336e7	5088.24
Light	110000	30.5	2.5212e7	6990.6
medium	165000	45.83	3.7818e7	10504
heavy	260000	72.2	5.9592e7	16548
Very heavy	370000	102.7	8.4804e7	23538

Table 15: Values of building capacities of different building structure types according to standard ISO 13760.

Building structure	Envelope capacity
	Wh/K*m <sup>2</sup>
Light	30 - 40 - 45
Medium	50 - 60 -70
Heavy	90 - 100 -110

Table 16: Values of building capacities of different building structure types according to Johra (2018)

Element of the envelope	Capacity [Wh/K*m <sup>2</sup> ]	
	External walls	Roof
Value per unit of element surface	80.6	21.5
Total per unit of reference area	74.7	

Table 17: Values of the capacities of roof and walls according to Masy (2008)

Equations 52 and 53 form together a non linear system with  $\dot{Q}_{floor,2}$  and  $T_{surf}$  as unknowns. This is resolved using *Fsolve* function in Python. This function uses Newton-Raphson optimisation algorithm to provide the solution. For time step  $i$ , the convergence is ensured by providing as guess values for  $T_{surf}$  the zone temperature at time step  $i$ , and for  $\dot{Q}_{floor,2}$  its value at the previous time step. However, when the heating stops and restarts,  $\dot{Q}_{floor,2}[i-1]$  is negative and the system does not converge. Therefore a condition is defined by investigation in order to make the model converge: if  $\dot{Q}_{floor,2}[i-1] < 30$ , the initial value  $\dot{Q}_{floor,2}[0]$  is chosen as guess value.

However, equation 53 is valid only if  $\dot{Q}_{floor,2}$  is positive. When there are a lot of solar gains, the zone temperature can increase, and be superior to the floor temperature, leading to a heat transfer from the zone to the floor. In this case, equation 53 (representing the heat transfer of underfloor heating as explained in Section 2.4) is replaced by equation 60 representing the heat transfer of a floor cooling (heat from the zone to the floor) according to standard ISO 11855:2012.

$$\dot{Q}_{floor,2,<0} = 7 * A_{floor} * (T_{surf} - T_z) \quad (60)$$

Different conditions are implemented to the dynamic model. First of all, as the model focuses on heating only, the behaviour of the building during the summer is not computed. During this period, the gains are superior to the losses and the temperature will continuously increase until the end of the summer. This *summer period* is the same as the one defined in Section 2.2. Then a condition on the heat pump operation is applied: if the temperature of the zone at step  $i$  is lower than the set point temperature, the heat pump provides the heat following the water law; on the opposite, if  $T_z > T_{set}$ , the heat pump is shut down for the step  $i+1$  and the condition is computed again for the next steps until  $T_z < T_{set}$ . Finally, a condition is applied if the heating power required from the heat law to the heat pump is over the heat pump's full load capacity. Three possibilities raise: either the back up resistance is used, or not, referred as resistance *ON* and *OFF*, or the backup resistance is used as less as possible : resistance *MIN*. In the first case, if the surplus heat to provide is lower than the maximal capacity of the back up resistance, it provides the exact amount of the heat demand. If the heat demand is over the resistance maximum power (6 kW as defined in Section 2.3),  $T_{w,av}$  is computed in order to define  $\dot{Q}_{HP}$  equal to the sum of the full load power at that temperature level and the backup resistance maximum power. In the second case,  $T_{w,av}$  is directly computed in order to define  $\dot{Q}_{HP}$  equal to the full load power at that temperature level. In the third case, the resistance is turned on if the outside temperature is lower than the bivalent temperature, defined at  $-1^\circ\text{C}$  for CS1 and  $-8^\circ\text{C}$  for CS2, and the backup resistance is turned off if the outside temperature is superior to the bivalent point.

### 2.5.2 Dynamic model validation

Simulations are performed in order to compare the results to the static model. As done in the static model, the inside temperature is set to  $20^\circ\text{C}$ . The initial conditions on the states are set to  $T_{floor} = 22^\circ\text{C}$ ,  $T_z = 20^\circ\text{C}$  and  $T_{env} = 16^\circ\text{C}$ . The results computed are presented in Table 18. These simulations are performed for CS1 and CS2 with, without and with the minimum of the auxiliary resistance.

CS	R	Flux	$\dot{Q}_{demand}$	$\dot{Q}_{HP}$ [kWh]	R	W	SCOP	$\dot{Q}_{ground}$	$\dot{Q}_{loss,ventil.}$	$\dot{Q}_{gain,solar}$ [kWh]	$\dot{Q}_{gain,internal}$	$\dot{Q}_{loss,env}$
		Unit										
OFF	Static	22038	21805	232.3	5405.8	4.0768	885.76	10289	2462.7	3594.1	16920	
	Dynamic	19555	19555	0	4681.3	<b>4.177</b>	936.8	10783.8	3890.1	3960.6	15579	
	Difference	<b>-12.7%</b>	-	-	-15.48%	2.4%	<b>5.45%</b>	<b>4.59%</b>	<b>36.69%</b>	<b>9.25%</b>	-8.61%	
ON	Static	22038	21805	232.3	5405.8	4.0768	885.76	10289	2462.7	3594.1	16920	
	Dynamic	19739.6	17299.6	2440	6654.7	<b>2.966</b>	944.69	10858.1	3890.1	3960.6	15687	
	Difference	<b>-11.6%</b>	-	-	18.77%	-37.45%	<b>6.24%</b>	<b>5.24%</b>	<b>36.69%</b>	<b>9.25%</b>	-7.86%	
MIN	Static	22038	21805	232.3	5405.8	4.0768	885.76	10289	2462.7	3594.1	16920	
	Dynamic	20023	19225	768	5377.8	<b>3.72</b>	955.7	10957	3890.1	3960.6	15830	
	Difference	<b>-9.14%</b>	-	-	-8.75%	-37.45%	<b>7.9%</b>	<b>6.49%</b>	<b>36.69%</b>	<b>9.25%</b>	-6.44%	
OFF	Static	11001	10999	1.406	2334.9	4.7114	690.43	1300.6	1723.5	3594.1	14328	
	Dynamic	8675	8675	0	1878.6	<b>4.6178</b>	784.43	1399.2	3241.7	3960.6	13555	
	Difference	<b>-26.81%</b>	-	-	-24.29%	-2.03%	<b>11.98%</b>	<b>7.05%</b>	<b>46.83%</b>	<b>9.25%</b>	-5.7%	
ON	Static	11001	10999	1.406	2334.9	4.7114	690.43	1300.6	1723.5	3594.1	14328	
	Dynamic	8683.9	7969.9	714	2410.1	<b>3.603</b>	784.9	1400	3241.7	3960.6	13562.4	
	Difference	<b>-26.68%</b>	-	-	3.12%	-30.76%	<b>12.04%</b>	<b>7.1%</b>	<b>46.83%</b>	<b>9.25%</b>	-5.65%	

Table 18: Comparison of the static and dynamic computation power results over the heating season for CS1 and CS2 with, without and with a minimum use of the backup resistance  $R$  in dynamic. The massive and mass-less elements contribution of the envelope are summed in the envelope losses  $\dot{Q}_{loss,env}$ . For CS2, minimum use of the heat pump lead to no use of the heat pump (R OFF).

The results show that the dynamic model has lower heating needs in all cases compared to the static model. In terms of gains and losses, the main difference is on the solar gain. This is due to the fact that in the static model, during the neglected hours ( $T_{out} > 13^{\circ}\text{C}$ ), the solar gains are not computed, as well as the solar irradiation when it is in excess to the losses, since in the static model the zone temperature is fixed. In the dynamic model all the radiations during the heating period are considered, and the excess gain leads to an increase of the zone temperature (Figure 32 and 33). For the same reason the internal gains are larger in the dynamic model. A simple computation is done as example for CS1 with a minimal use of the backup resistance. The dynamic simulation shows an increase in the solar gains of 1427.4 kWh and 366.5 kWh of internal gains. If these two gains are reduced to the value in the static model, the heating need difference is reduced to -1%. However, it is chosen to keep the values as they are: in reality, all the solar gains is absorbed by the building. Only the internal gains will be overestimated, but the assessment of flexibility will be done comparing two dynamic simulations. Finally, the ground losses are slightly higher in the dynamic simulation. The explanation is that the floor capacity stays at higher temperature in the dynamic model than the zone temperature of the static model. Therefore, the losses through the ground are higher.

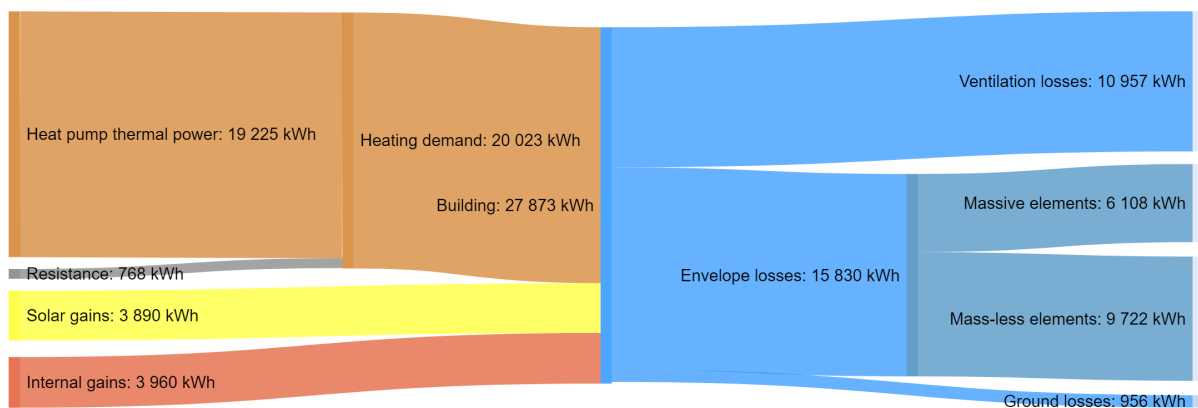


Figure 31: Sankey diagram representing the gains and the losses of the building's zone over the heating season for CS1 with a minimum use of the backup resistance.

Figure 31 presents a Sankey diagram in order to understand better the weight of the different components of the heat balance. This is performed for CS1 with a minimum use of the backup resistance. It is seen that the major heat comes from the heat pump; the solar and internal gains are similar; the main losses are the envelope losses and the losses from the door and windows (mass-less elements) are superior than the losses from the walls and roof (massive elements). Finally the ventilation losses are strong, but are reduced by 80% in CS2 thanks to the heat recovery ventilation.

Figure 32 shows also that for CS1 without the back up resistance, the heat pump does not provide enough power when the outside temperature is very low (less than  $19^{\circ}\text{C}$  between hours 160 and 230, and between hours 1300 and 1500). This case is also seen for CS1 with the backup resistance, and for CS2. This is not due to a lack of capacity in these cases, but to the way the heat pump is controlled: as explained, the simple control of the heat pump is to turn it of during an hour if the zone's setpoint is exceeded. The time reaction of the floor heating lead therefore to situation where the zone temperature is below the

zone's setpoint, but will be only heated the next hour, and the temperature will strongly decrease. Different ways to control the heat pump are discussed in Section 4.7. However, this simple control is assumed sufficient to assess the flexibility potential over the whole heating season. Finally, it is also seen that the building is impacted by overheating, and this is discussed in Section 4.8. However, this overheating takes place at the end of the mid season where the heating is not needed anymore, and therefore this will not have any impact on the flexibility potential assessment.

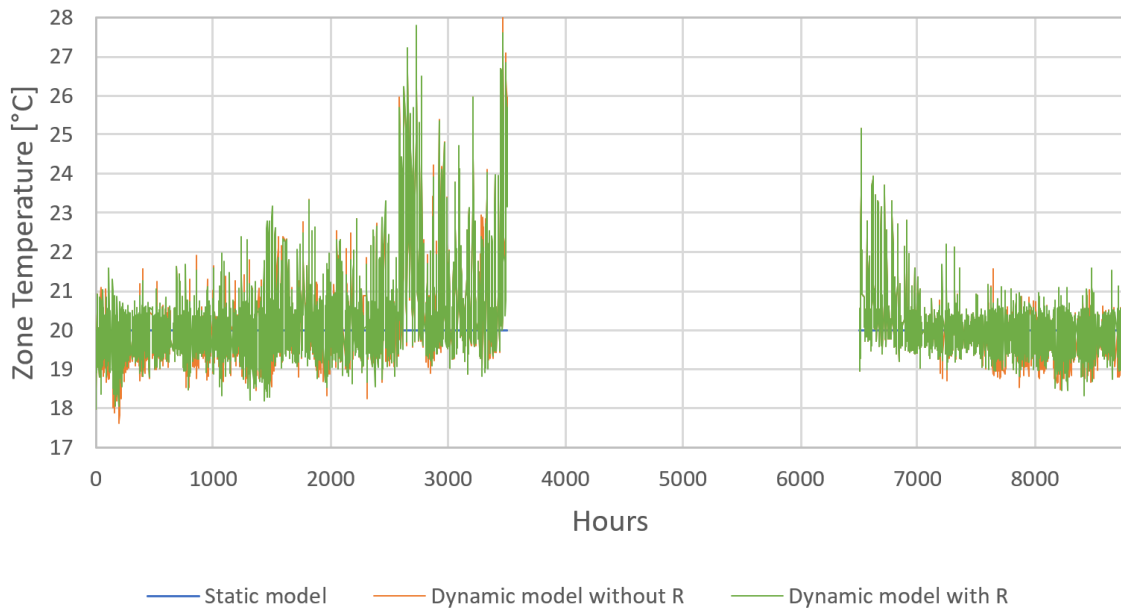


Figure 32: Comparison between the dynamic and static temperature evolution over the heating season for CS1.

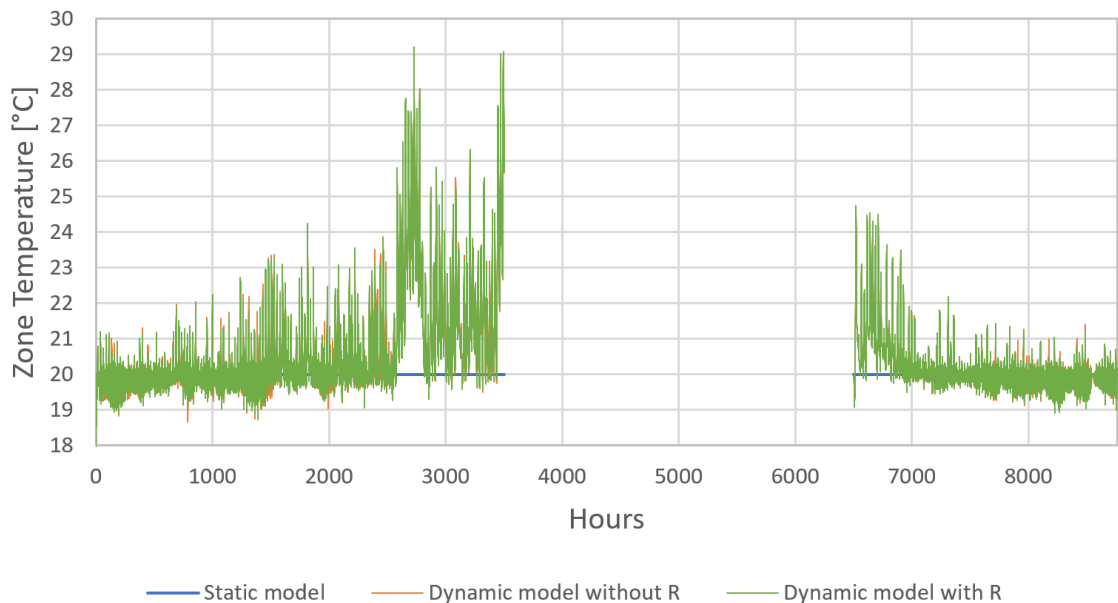


Figure 33: Comparison between the dynamic and static temperature evolution over the heating season for CS2.



To conclude, a choice is made on the configuration of the case studies that are simulated to assess the flexibility (see Chapter 3). The back up resistance has a really strong and negative impact on the SCOP. It is chosen to use as minimum as possible the resistance. Therefore, the resistance is used only when the heat pump is working below the bivalent temperature, defined as  $-1^{\circ}\text{C}$  for CS1 and  $-8^{\circ}\text{C}$  for CS2.

### 3 Results

In this section, case studies used to investigate the flexibility potential are defined and the results are presented. They are referred to *flexibility studies* (FS). The first one (FS A) is to analyse the time response when the setpoint is changed and the outside temperature is fixed. This allows to understand the dynamic of the house’s TES and the eventual rebound effects or overshoots. The second FS (FS B) analyses the potential increase of self-consumption for a house equipped with photovoltaic (PV) solar panels. This capability will be computed either in terms of amounts of power that can be self-consumed and costs saving. The third and last FS (FS C) analyses the potential to shift the consumption from peak to off peak hours, in a dynamic pricing of electricity context.

It is important to firstly define the different setpoint temperatures that will be used. Table 19 presents some setpoints defined in the literature. It is decided to consider a neutral setpoint temperature of 20.5°C in the house, that can be increased up to 22.5°C or decreased down to 18.5°C to assess the flexibility potential. These values and the impact of lower setpoints on the flexibility assessment are discussed in Section 4.5.

Reference	Neutral setpoint	Storage setpoint	Discharge setpoint
(Masy et al., 2015)	21°C	+1°C	-1°C
(Verhelst et al., 2012)	20°C	+2°C	-2°C
(Dongellini et al., 2020)	20.5°C	+2°C	-2°C
(Le Dréau & Heiselberg, 2016)	22°C	+2°C	-2°C
(Zhang, Good, & Mancarella, 2019)	19°C	+2°C	-2°C

Table 19: Setpoint temperatures found in literature for DSM in houses equipped with underfloor heating.

### 3.1 FS A: Time response of setpoint temperatures changes

The first results of the flexibility potential is the analysis of the temporal response when the zone setpoint is modified. The simulation is performed without any solar gains and with a constant outdoor temperature. Three outdoor temperatures are considered ( $-5^{\circ}\text{C}$ ,  $5^{\circ}\text{C}$  and  $10^{\circ}\text{C}$ ) in order to understand and quantify the dependency on the climatic conditions.

	Setpoint temperature [ $^{\circ}\text{C}$ ]	From	22.5	20.5	22.5	18.5	20.5	18.5
		To	20.5	18.5	18.5	20.5	22.5	22.5
		Outside temperature	Discharge time			Storage time		
CS1	$-5^{\circ}\text{C}$		<b>2h</b>	3h	5h	<b>6h</b>	<b>6h</b>	<b>11h</b>
	$5^{\circ}\text{C}$		5h	4h	9h	<b>8h</b>	<b>6h</b>	<b>14h</b>
	$10^{\circ}\text{C}$		<b>8h</b>	7h	18h	3h	3h	8h
CS2	$-5^{\circ}\text{C}$		5h	6h	10h	<b>24h</b>	<b>33h</b>	<b>51h</b>
	$5^{\circ}\text{C}$		9h	9h	20h	6h	6h	13h
	$10^{\circ}\text{C}$		13h	22h	<b>42h</b>	3h	4h	8h

Table 20: Results of the time response simulation of CS1’s and CS2’s TES for 3 zone’s setpoint temperatures changes to store and corresponding discharge setpoints for different outside conditions. Bold values are mentioned in the text.

Table 20 shows the results from which different conclusions can be draw. Firstly, the outside temperature has a strong impact (e.g. 2h of non heating for CS1 with setpoint varied from 22.5 to 20.5 and  $T_{out} = -5^{\circ}\text{C}$  versus 8h at  $T_{out} = 10^{\circ}\text{C}$ ). Shifting to the lowest setpoint (from 20.5 to 18.5 instead of 22.5 to 20.5) is the more advantageous solution to spend a long periods of time without having to heat the building. Secondly it shows that less time is needed to store from a low to a high setpoint at  $-5$  that at  $5^{\circ}\text{C}$ . This is due to the use of the backup resistance (see Figure 35) when the outside temperature is below the bivalent temperature ( $-1^{\circ}\text{C}$  for CS1). Finally, the discharge time can be from 2h for CS1 worst case up to 42h for CS2 best case. However, a strong rebound is seen when the setpoint has to return to the neutral point. This is strongly seen for CS2 when the outside temperature is low ( $-5^{\circ}\text{C}$ ) and the backup resistance is not used. In reality, the solar gains will also have a strong impact on the charge and discharge time during the hours of sunshine.

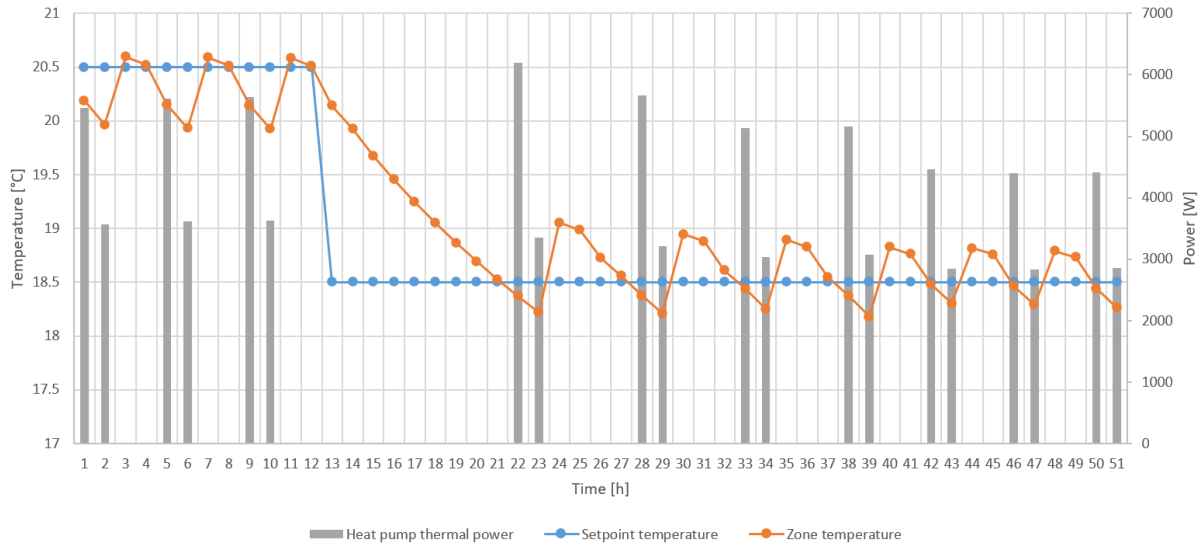


Figure 34: Discharge time (time of non heating) for CS2 with a setpoint temperature changed from 20.5 to 18.5 when  $T_{out} = 5^{\circ}\text{C}$ . Nine hours without heating the zone can be reached.

Figure 34 shows the discharge time of CS2 when  $T_{out} = 5^{\circ}\text{C}$  with a setpoint changed from  $20.5^{\circ}\text{C}$  to  $18.5^{\circ}\text{C}$ . Before the setpoint shift, the zone’s temperature is oscillating around the setpoint (from  $19.9^{\circ}\text{C}$  to  $20.6^{\circ}\text{C}$ ). This is due to the hysteresis control of the heat pump as explained in Section 2.5. A small undershoot is seen when the low setpoint is reached and the heat pump switches on. This is the consequence of the floor heating’s inertia, taking two hours to be heated and to heat the zone again. However this can also be managed by using a better way to control the heat pump, discussed in Section 4.7. These oscillations and overshoots are stronger when the outside temperature is decreased to  $-5^{\circ}\text{C}$  and the lower insulation building is simulated as shown in Figure 35.

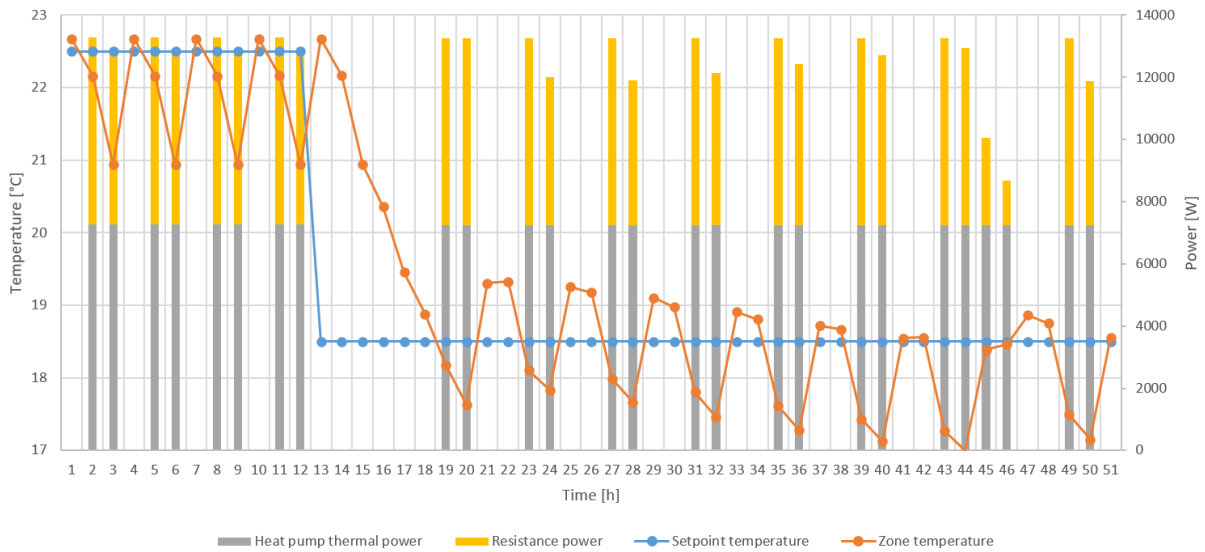


Figure 35: Discharge time for CS1 with a setpoint temperature changed from 20.5 to 18.5 when  $T_{out} = -5^{\circ}\text{C}$ . Five hours without heating the zone can be reached. Since the outside temperature is below the bivalent temperature of  $-1^{\circ}\text{C}$ , the backup resistance is used to provide the needed power.

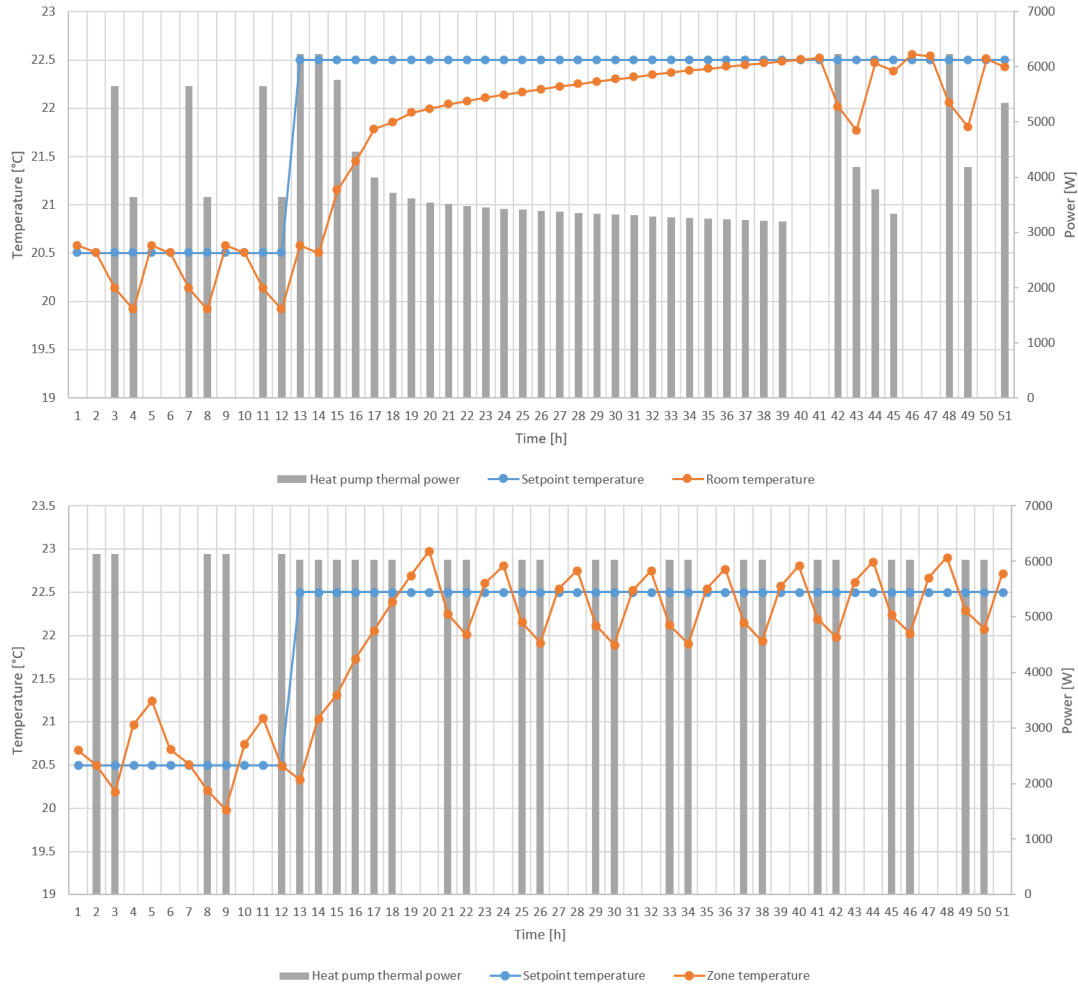


Figure 36: Comparison between two control strategies of the heat pump when the setpoint is increased. On the top, the water law provides the necessary amount of power to maintain the house and it leads to a logarithmic convergence to the setpoint. On the bottom, the heat pump is forced to deliver the full load capacity and the convergence is faster.

Finally, Figure 36 shows two different heat pump control strategies when the setpoint is increased. On the top, the water law is set according to the zone's setpoint temperature. This leads to a full load demand the first hours of the new setpoint. However, as the floor temperature increases, the water law is configured to ask to the pump the power to maintain the setpoint temperature and not a larger power to attain the new setpoint. This lead to a logarithmic convergence to the new setpoint. In order to converge faster to the new setpoint, a full load is asked to the heat pump, increasing by 5°C the water law result. This new control strategy is used to assess the results of Table 20, and is implemented in FS B and FS C as follows: when the setpoint is changed to the highest setpoint (22.5°C), the water law is increased by 5°C to ensure a full load demand during these hours and enable the storage strategy. This can be seen in practice as the forced ON mode of the Smart Grid Ready strategy, explained in Section 1.3. However it is seen that this strategy leads to an overshoot, but still limited.

### 3.2 FS B: Improving self-consumption of PV with TES

The second flexibility study focuses on the impact of the TES storage on the self-consumption of PV electricity production in Belgium. The aim is to perform load shifting by setting a higher setpoint during the hours of sunshine, and to analyse by how much the self-consumption can be increased, the impact on the total electricity consumption from the grid, and the money that can be saved using this strategy. In order to perform the simulations, information about the PV production, the electricity consumption of residential house and the costs of the electricity are used for Belgium:

- The PVGIS <sup>7</sup> tool from the European Commission. This tool provides the hourly electricity generation data according to the year, the location, and the configuration of the PV installation. It is chosen to model an installation in Uccle, for the year 2016. The peak power is defined according to the consumption of each CS. The orientation is fixed to the south with an inclination of 45°. The tool also provides the hourly data for the year at the selected location, as well as the direct irradiation ( $G_d$ ), diffuse irradiation ( $G_d$ ) and the solar elevation angle ( $\alpha$ ). The solar data input of the model is the global surface horizontal irradiation  $G_{global}$ , and is computed according to:  $G_{global} = G_{d,vertical} + G_{b,vertical} * \sin(\alpha)$ .
- The synthetic load profile data of electricity consumption from Synergrid <sup>8</sup> for 2016. This provides the probability distribution of the electricity consumption for a residential dwelling of the corresponding year.
- From Engie internal data, the yearly consumption of a 4 person house is 4469 kWh in Flanders and 4729 in Wallonia. An average value of 4500 kWh/year is considered.
- According to VREG (2021), the consumer's electricity cost for this range of consumption is 0.25 €/kWh.
- A representative injection tariff was found in Engie's *Easy 3* electricity supply contract. The reward of electrical injection in the grid is 0.04078 €/kWh. It is assumed for the simulations that the price of the self consumed electricity is 0 €/kWh, considering that the PV installation investment took place in the past.

The scenario without any heat pump management is referred to the *business as usual* (BAU) scenario, and the one with a load shifting strategy is referred to the *smart* scenario. The BAU scenario is computed with the weather data of 2016 and a setpoint temperature of 20.5°C. The BAU results for CS1 and CS2 are presented in Table 21. The sizing of the solar panels installation is done according to the total yearly electrical consumption needed to cover it. This leads to a 10 kW-peak installation for CS1 and 6 kWp for CS2.

<sup>7</sup>PVGIS: PhotoVoltaic Geographical Information System, available at [https://re.jrc.ec.europa.eu/pvg\\_tools/fr/#PVP](https://re.jrc.ec.europa.eu/pvg_tools/fr/#PVP)

<sup>8</sup>Available at <http://www.synergrid.be/index.cfm?PageID=16896#>

Scenario	$\dot{Q}_{HP}$	$\dot{W}_{HP}$	SCOP	Electrical consumption	PV peak power	PV generation
Unit	[kWh/year]		-	kWh/year	kWp	kWh/year
CS1 BAU	23565	5824	3.7	10324	6	11091
CS2 BAU	9784	2079	4.7	6579	10	6655

Table 21: CS1 BAU scenarios (without any flexibility strategy), computed in order to size the PV installation.

Then the schedule of load shifting is decided according to the PV production data. This is done during the winter period, when the heating needs are the biggest and the solar production lower compared to mid season. Figure 37 presents the average daily PV electricity production over January and February. It is found that the usual production begins at 9AM, increases from 11AM, peak production at 1PM and has a significant drop from 3PM to 4PM. Therefore, the setpoint is set to 22.5°C from 11AM to 3PM, to cover the peak production, and kept to 20.5°C out of this schedule.

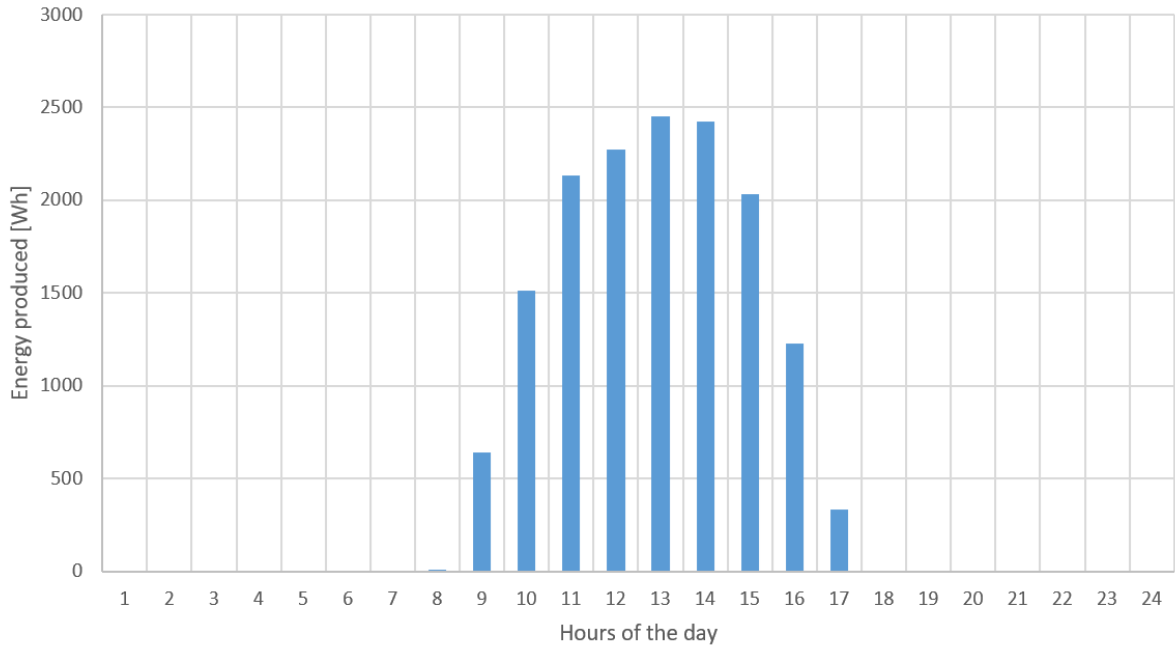


Figure 37: Average daily electricity production for CS1 over January and February.

Scenario	$\dot{Q}_{HP}$	$\dot{W}_{HP}$	SCOP	Net cons.	Net gen.	Self-cons.	HP use WI FH	Elec. paid	Elec. sold	Total cost
Unit	[kWh/year]		-	[kWh/year]			%	€		
CS1 BAU	23565	5824	3.7	8063	8830	2261	7.8	2015	360	1655
CS1 Smart	21468	6677	3.35	8290	8204	2886	30.5	2073	335	1738
Difference [%]	<b>-8.9</b>	<b>+14.6</b>	<b>-9.5</b>	<b>+2.8</b>	<b>-7.1</b>	<b>+27.6</b>	<b>+290</b>	<b>+2.9</b>	<b>-6.9</b>	<b>+5</b>
CS2 BAU	9784	2079	4.7	4746	4822	1833	6.8	1187	197	990
CS2 Smart	10365	2308	4.49	4616	4463	2192	41	1154	182	972
Difference [%]	<b>+5.9</b>	<b>+11</b>	<b>-4.5</b>	<b>-2.7</b>	<b>-7.4</b>	<b>+19.6</b>	<b>+503</b>	<b>-2.9</b>	<b>-7.6</b>	<b>-1.8</b>

Table 22: Results and comparison of FS B for CS1 and CS2 in BAU and Smart scenarios. The net consumption is defined as the electricity consumed from the grid, the net generation is the electricity sent to the grid and the self-consumption is the electricity generated and directly consumed. HP use WI FH states for the ratio of the heat pump power used within the flexibility hours (FH), from 11AM to 15PM.

Table 22 shows the results of the simulations. CS1 is firstly analysed. It can be seen that the Smart scenario leads to a strong heat pump electrical overconsumption of 14.6% and a decrease in the SCOP from 3.7 to 3.35. This is mainly due to the increase in the losses when the setpoint is higher, and is intrinsically linked to the lower insulation level of CS1. This leads to an increase of 5% in the yearly bill. However, the effect on the period of heating is effective, with the heat pump consumption shifted from 7.8% of time within the Smart schedule to 30.5% compared to the BAU scenario and a self-consumption increased of 27.6%. The results of CS2 are more encouraging. The electrical consumption of the heat pump is increased by 11%, but the electrical consumption from the grid slightly decreases, and the self-consumption increases by 19.6%. The heat pump runs 41% of the time during the flexibility hours. Finally, the result in terms of savings is really negligible, with a bill reduced by 1.8%.

Scenario	$\dot{Q}_{HP}$	$\dot{W}_{HP}$	SCOP	Net cons.	Net gen.	Self-cons.	HP use WI FH	Elec. paid	Elec. sold	Total cost
Unit	[kWh/year]		-	[kWh/year]			%	€		
CS1 BAU	23565	5824	3.7	8063	8830	2261	7.8	2015	360	1655
CS1 Smart wo R FH	21492	6407	3.49	8025	8208	2883	27.2	2006	335	1671
Difference [%]	<b>-8.8</b>	<b>+10</b>	<b>-5.7</b>	<b>-0.5</b>	<b>-7</b>	<b>+21.6</b>	<b>+249</b>	<b>-0.5</b>	<b>-6.9</b>	<b>+1</b>

Table 23: Scenario for CS1 with flexibility hours of the schedule only when the outside temperature is over the bivalent temperature in order to not use the backup resistance for the flexibility and reduce the electrical overconsumption.

In order to reduce the overconsumption of the CS1 and make the implementation of a smart scenario interesting, a scenario of flexibility hours only when the outside temperature is higher than the bivalent temperature is simulated to use the backup resistance less. The results are shown in Table 23. The SCOP is slightly improved compared to the



previous Smart scenario from 3.35 to 3.49 . The self consumption is similar. However the final bill is still not advantageous for the final consumer, the increase is limited to 1%. Other scenarios are simulated: a setpoint increased of only 1°C, a reduced schedule from 12AM to 2PM but none of these scenarios improve the results for CS1 or CS2.

Finally, the impact of the capacity's values is evaluated. Firstly the envelope's capacity has been defined to 50 kWh/(m<sup>2</sup>\*K). The cases where a heavier building structure of 80 kWh/(m<sup>2</sup>\*K) are simulated (value described in Section 2.5.1), referred to *BAU*<sub>80</sub> and *Smart*<sub>80</sub> scenarios. The inside zone's capacity has been defined as the capacity of the air inside the building (see Section 2.5.1). In reality, inside walls and furniture are participating in the TES. Therefore a doubled zone's capacity is also simulated, and is referred to *BAU*<sub>2xCz</sub> and *Smart*<sub>2xCz</sub>.

Scenario	$\dot{Q}_{HP}$	$\dot{W}_{HP}$	SCOP	Net cons.	Net gen.	Self-cons.	HP use WI FH	Elec. paid	Elec. sold	Total cost
Unit	[kWh/year]		-	[kWh/year]			%	€		
CS1 <i>BAU</i> <sub>2xCz</sub>	20770	5810	3.7	8113	8895	2197	6.5	2028	363	1665
CS1 <i>Smart</i> <sub>2xCz</sub> wo R FH	21716	6450	3.49	7915	8056	3035	30.1	1979	328.5	1650.5
Difference [%]	<b>+4.6</b>	<b>+11</b>	<b>-5.7</b>	<b>-2.4</b>	<b>-9.4</b>	<b>+38.1</b>	<b>+363</b>	<b>-2.4</b>	<b>-9.5</b>	<b>-0.87</b>
CS2 <i>BAU</i> <sub>2xCz</sub>	9762	2083	4.69	4756	4828	1827	5.6	1189	196.9	992.1
CS2 <i>Smart</i> <sub>2xCz</sub>	10463	2329	4.49	4533	4359	2295	46.3	1133	178	955
Difference [%]	<b>+7.2</b>	<b>+11.8</b>	<b>-4.3</b>	<b>-4.9</b>	<b>-9.7</b>	<b>+25.6</b>	<b>+727</b>	<b>-4.7</b>	<b>-9.6</b>	<b>-3.7</b>

Table 24: Results of the doubled zone's capacity scenario. The self-consumption strategy is finally positive for CS1 and is improved for CS2, but the impact on the costs is still insignificant.

When the envelope's capacity is modified from 50 to 80 kWh, in the case of a heavier building structure, the impact is marginal. The results are presented in appendix B.1. The impact of the zone's capacity is more interesting. The results of the *BAU*<sub>2xCz</sub> and *Smart*<sub>2xCz</sub> scenarios are presented in Table 24. The self-consumption is increased in both scenarios as well as the fraction of the heat pump use during the flexibility hours. The total costs of CS1 are finally reduced, and the decrease of CS2 costs is stronger. However, this impact is still not really significant.

To conclude, shifting the load in order to increase the self consumption seems not really interesting. However, this simulation have been done according to a rule base control that is the same for all the days of the heating period. A smarter control with a heat pump consumption following more accurately the PV production, or a reduced flexibility period of two or three hours just before the end of the sunshine could lead to better results.

### 3.3 FS C: Shifting consumption from peak to off peak hours

The last flexibility study is focused on the load shifting impact in a context of dynamic pricing. A European Directive from 2019 stated that all energy suppliers with more than 200 000 customers must propose a dynamic tariff offer (Council of European Energy Regulators, 2020). In Flanders, the VREG (Flemish regulator) decided to implement such strategies for the grid electricity costs starting from 2022. Moreover, as explained in Section 1.1, these capacity tariffs aim to be implemented in the next years in European Union. Therefore, it is interesting to analyse the potential to shift the heat pump consumption during peak hours. For this FS, the flexibility potential assessment will be done by computing the amount of consumption shifted. The impact on the costs is not implemented since not enough information about the dynamic pricing is available at the moment.

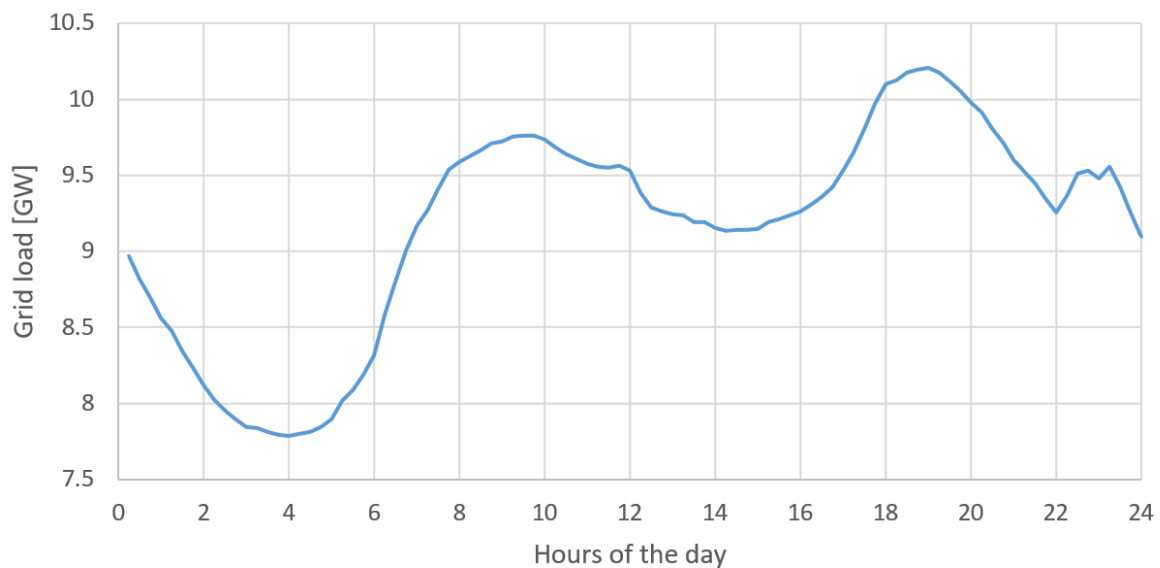


Figure 38: Average daily grid load over the heating season of the year 2016 from Elia. It is seen that the peak consumption is situated between 8AM to 11AM in the morning and 6PM to 8PM in the evening.

In order to perform the simulations, the electricity grid load has to be analysed. The year modelled is 2016. The Belgian grid load data is taken from Elia for the corresponding year. The average daily load is computed over the days composing the heating season and is presented in Figure 38. Two consumption peaks are seen during the day: in the morning from 7AM to 1PM with a maximum between 8AM and 12AM, and in the evening from 5PM to 9PM with a maximum between 6PM to 8PM. Different smart scenarios of load shifting (LS) are analysed and compared to the BAU scenario: the LS of the evening peak; the LS of the morning peak; the combination of both morning and evening peak shifting. To optimise the LS strategies, some parameters are varied:

- The time period of electricity shift
- The potential need of an energy storage period before the shift and its time
- The setpoint temperatures.

A first case is the evening LS from 6 to 8PM. The results are presented in Table 25. Without any previous charging strategy and a setpoint temperature decreased to 18.5 during the Flexibility (discharging) hours, a shift of 100% of the evening peak load is assessed for CS1 and CS2. A small overconsumption of 2.5% occurs for CS1, and a decrease in the consumption is seen for CS2.

Scenario	$\dot{Q}_{HP}$	$\dot{W}_{HP}$	SCOP	Use of HP within FH
Unit	kWh/year		-	%
CS1 BAU	20201	5823	3.47	10.6
CS1 Smart	19916	5961	3.34	0
Difference [%]	<b>-1.4</b>	<b>+2.4</b>	<b>-3.7</b>	<b>-100</b>
CS2 BAU	9579	2043	4.69	10.4
CS2 Smart	9509	20379	4.67	0
Difference [%]	<b>-0.7</b>	<b>-0.3</b>	<b>-0.5</b>	<b>-100</b>

Table 25: Load shifting strategy during the evening (from 6PM to 8PM) by setting the zone's temperature to 18.5°C. 100% of the load is shifted.

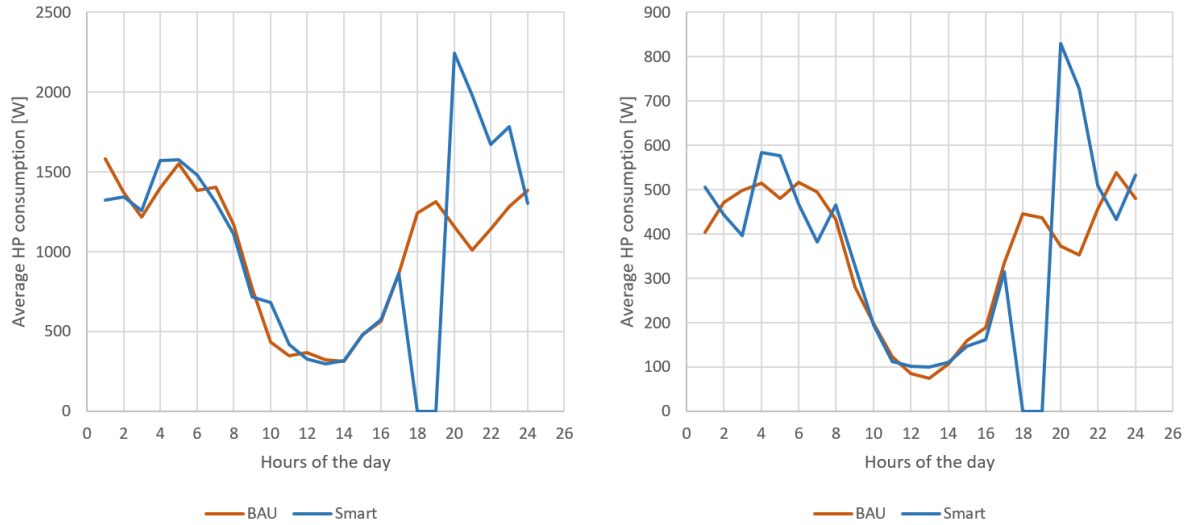


Figure 39: Average heat pump consumption within the day over the heating season. The LS is seen, and the consumption is shifted to the hours of the end of the evening, with a rebound time of 4 hours for CS1 and 2 hours for CS2.

Figure 39 shows the average heat pump consumption within the day over the heating season. The LS is seen from 6 to 8PM. It also shows that the load is shifted to the hours later in the evening. The increase of CS1 consumption is explained by the fact that it needs time to recover the heat lost, and the consumption is delayed late in the evening/beginning of the night when the SCOP is lower. The average rebound time is 4 hours. For CS2, the high insulation keeps more the heat and the SCOP is not impacted since the average rebound is only 2 hours.

Finally, a typical cold winter day is analysed, the 8<sup>th</sup> of January, with outside temperature from 0 to 5°C. Figure 40 shows the evolution of the zone’s temperature and the heat pump consumption during the day. The temperature peak in the afternoon is due to the solar gains. The load shifting is seen during the evening. However, as discussed in Section 4.7, the control of the heat pump can be upgraded to get a smoother zone’s temperature evolution.

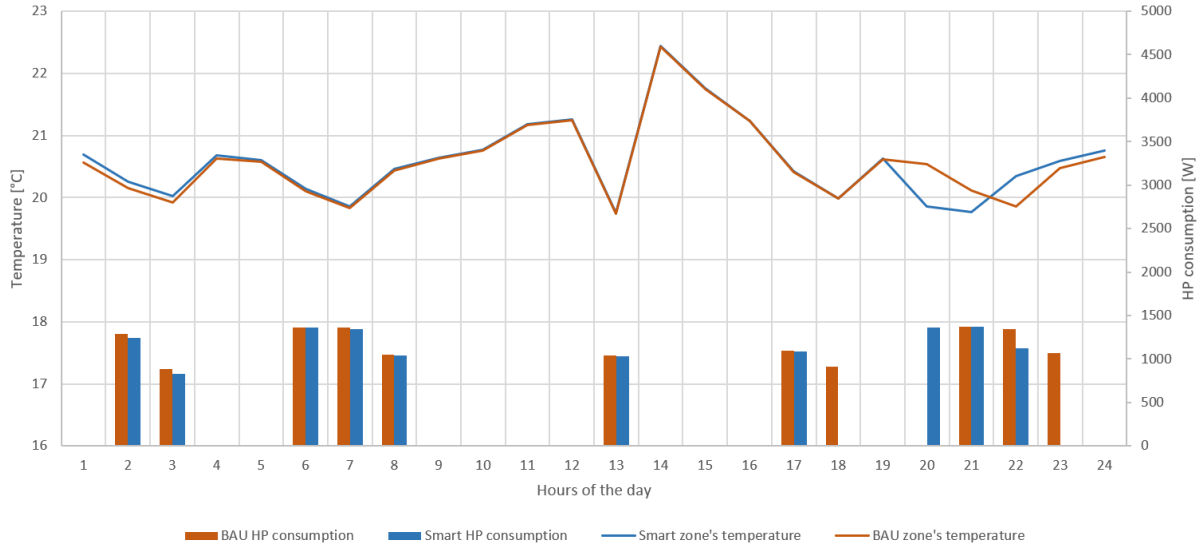


Figure 40: Zone’s temperature evolution and heat pump consumption of a typical cold day (8<sup>th</sup> of January)for CS2 with LS from 6 to 8PM.

A second case to analyse is the LS for a longer period in the evening, from 5PM to 9PM. The results are presented in Table 26. It is seen that for CS2, 99.2% of the load is shifted with only 0.15% of the heat pump working time within the flexibility hours. For CS1, still 3.9% of the total heat pump consumption is done within the flexibility hours. However, this remains marginal, and it is found that 3 hours of preheating are needed to bring the use under 1% but leads to an overconsumption of 9.7%. Due to the lower insulation level of CS1, it is seen that a long period leads to low zone’s temperature (18°C in Figure 41).

Scenario	$\dot{Q}_{HP}$	$\dot{W}_{HP}$	SCOP	Use of HP within FH
Unit	kWh/year		-	%
CS1 BAU	20202	5823	3.47	19
CS1 Smart	19566	5869	3.33	3.9
Difference [%]	<b>-3.1</b>	<b>+0.78</b>	<b>-3.9</b>	<b>-79</b>
CS2 BAU	9579	2043	4.69	10.4
CS2 Smart	9395	2027	4.64	0.15
Difference [%]	<b>-1.9</b>	<b>-0.8</b>	<b>-1.13</b>	<b>-99.2</b>

Table 26: Load shifting strategy during a longer period of time in the evening (from 5PM to 9PM) by setting the zone temperature to 18.5. 79% of the load is shifted for CS1 and almost all of the load for CS2.

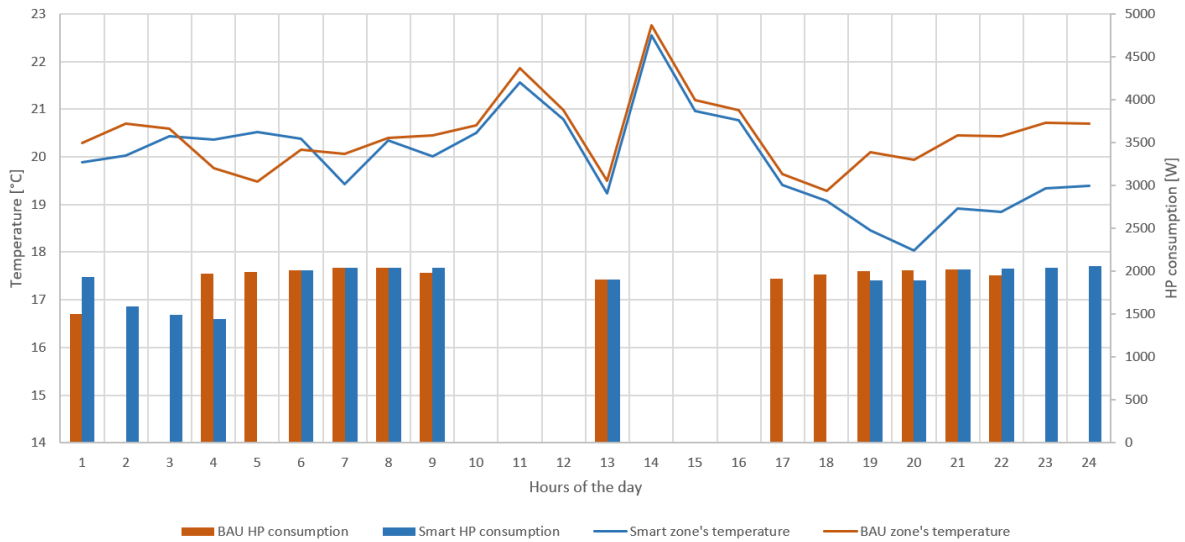


Figure 41: Zone's temperature evolution and heat pump consumption on a typical cold day (8<sup>th</sup> of January) for CS1 with LS from 5 to 9PM.

The same simulation is done in the morning between 9AM to 11AM for CS1 and 8AM to 12AM for CS2. The results are displayed in appendix B.2. It is assessed that 100% of the load is shifted for both cases, with an increase in the SCOP from 3.47 to 3.49 for CS1 and from 4.69 to 4.75 for CS2.

Scenario	$\dot{Q}_{HP}$	$\dot{W}_{HP}$	COP	Use of HP within FH
Unit	kWh/year	-	-	%
CS1 BAU	20202	5823	3.47	15.6
CS1 Smart	19866	5897	3.37	0
Difference [%]	<b>-1.7</b>	<b>+1.3</b>	<b>-2.9</b>	<b>-100</b>
CS2 BAU	9579	2043	4.68	31
CS2 Smart	9261	1974	4.69	0.2
Difference [%]	<b>-3.3</b>	<b>-3.4</b>	<b>+0.05</b>	<b>-99.3</b>

Table 27: Load shifting strategy during the whole day: from 9 to 11AM and 6 to 8PM for CS1, and from 8 to 12AM and 5 to 9PM for CS2. All the load is shifted for CS1 and almost all for CS2.

The last scenario consists in the analysis of the combined strategies. The flexibility hours are defined for CS1 between 9 to 11AM and 6 and 8PM; for CS2, between 8 to 12AM and 5 to 9PM. The results are presented in Table 27. A complete shift from the flexibility hours is assessed for CS1 and almost assessed for CS2 with a 0.2% residual use of the heat pump within the FH. A slight overconsumption is seen for CS1 and a decrease of 3.4% of the consumption is obtained for CS2.

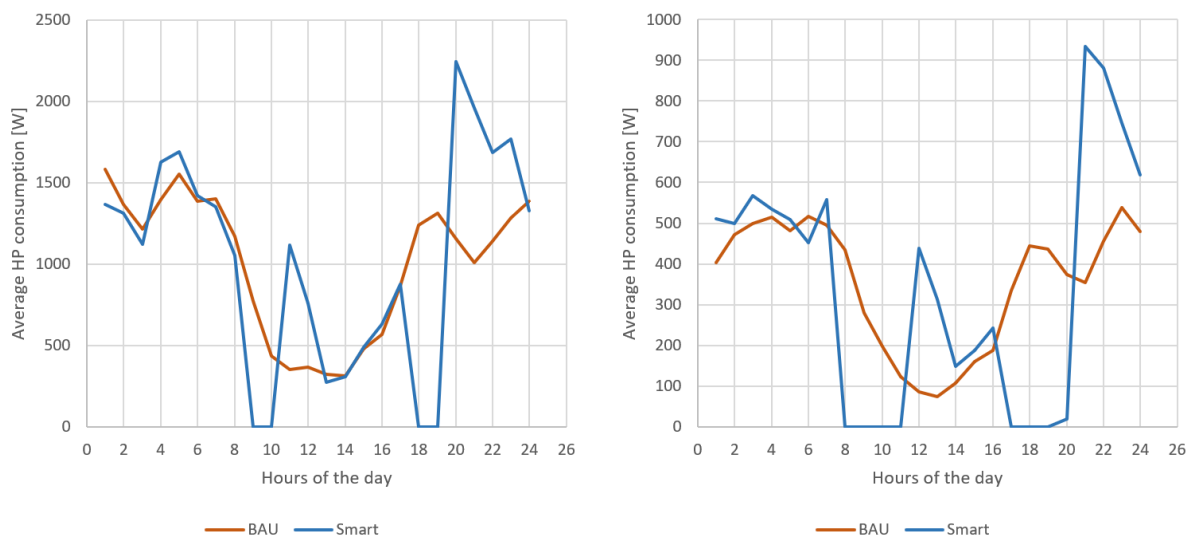


Figure 42: Average heat pump consumption within the day over the heating season. The consumption is shifted to the end of the evening, with a rebound of 4 hours for CS1 and 2 hours for CS2.

Figure 42 presents the average consumption for case 1 and case 2. The two LS are seen, with a shift in the energy consumption from the morning until the noon, and from the early evening to the end of the evening. For CS1, a longer period of 2x3h is discussed in Section 4.9. This shows that 92% of the load is shifted in that case. However, a strong temperature undershoot is seen at the end of the flexibility period when the outside temperature is low (e.g. zone temperature under 18°C for the 8<sup>th</sup> of January), and this case

is not consider as realistic all over the year. However, different flexibility time periods for different the different moments of the heating season (e.g. by separating the spring/autumn and the winter) can lead to interesting results.

In order to analyse the effect of a lower interval of the setpoint temperature on the flexibility, a last simulation is done. The low setpoint is chosen at 19.5°C. The results are presented in Table 28. For CS1, due to the short period of flexibility within the day (2x2h), all the load is still shifted. For CS2, a strong impact is seen. The long LS period of 2x4h leads to a temperature under 19.5°C. Therefore, the load within the flexibility hours decreases only from 31% for the BAU scenario to 6.7%, when a setpoint of 18.5 lead to almost a 100% of LS.

Scenario	$\dot{Q}_{HP}$	$\dot{W}_{HP}$	COP	Use of HP within FH
Unit	kWh/year		-	%
CS1 Smart 18.5	19866	5897	3.37	0
CS1 Smart 19.5	20218	5905	3.42	0
Difference [%]	<b>+1.8</b>	<b>+0.14</b>	<b>+1.5</b>	<b>0</b>
CS2 Smart 18.5	9261	1974	4.69	0.2
CS2 Smart 19.5	9586	2042	4.69	6.7
Difference [%]	<b>+3.5</b>	<b>+3.4</b>	<b>0</b>	<b>+3250</b>

Table 28: Comparison of the LS within the whole day with setpoint temperatures of 18.5 and 19.5°C. All the load is still shifted for CS1 due to the short period of shift (2h), but a strong impact is seen on CS2 with a load only shifted to 6% of the heat pump used within the FH.

To conclude, the flexibility potential of load shifting is definitely interesting for both configurations. The insulation level of the building has a strong impact, as well as the setpoint temperature of the flexibility hours. Finally, a rule based control has been used, but in a dynamic pricing context, different strategies can be applied. Johra (2018) defined a more automatic strategy by setting a high and low price of the electricity, and shifting the demand from high to low price period. The spot market prices could be used in this case. This could lead to enhanced results and money savings.

## 4 Discussion

This section is dedicated to the discussion of some assumptions made in this work. The assumptions are explained, justified, criticised and suggestions of improvements are given.

### 4.1 Single zone model

In this work, it has been chosen to use a single zone model. This assumption has three main advantages:

- the model is simple and easily computable;
- no detailed information on the inside configuration is needed (and this is not provided in TABULA);
- other buildings can be modelled easily by just replacing the area and U-values of the envelope components.

This assumption has been justified as follows: since the buildings modelled are equipped with floor heating and heat pumps, buildings with a relatively good insulation are chosen. In these buildings, there are no huge temperature differences between the rooms, since the heat has time to diffuse. Moreover it is chosen to simulate on an hourly basis, giving the time to the heat to diffuse. Finally it is not needed to know the temperature in each room.

However, a multi zones modelling has other advantages and can model the building more precisely. The diffusion between the zones can be investigated. Different temperature setpoints can be defined according to the zones, with higher setpoint in the bathroom and lower one in the lobby for instance. Finally, the heating gains can also be distributed in the room according to the probabilistic distribution of occupancy.

### 4.2 Building choice

As explained in the single zone justification, buildings with a relatively good insulation level have been chosen. This choice is confirmed by the simulation results: CS1 has the lower insulation level and the flexibility potential is already largely impacted and reduced.

However, CS1 case is still interesting. As mentioned by Johra (2018), buildings that are less insulated can't assess the same period of non-heating than well-insulated building, but since they consume more, they can have a really strong impact in terms of load shifting. For example, CS1 in FS C has a total flexibility period of 4 hours during the day against 8 hours for CS2. Nevertheless, 908 kWh are shifted from the short LS period for CS1 and only 633 kWh for the large LS period of CS2.

Other buildings with lower insulation levels and a larger consumption than CS1 can be modelled to invest their load shifting potential. The underfloor heating condition of a temperature surface below 29°C always has to be respected. If not, or if the buildings investigated are not heated with this technology, other configurations can be analysed. A new heat pump flux can be added to the zone temperature node in order to model A/A heat pumps or A/W HP with conventional radiators (in this case a convection coefficient



has to be introduced). The floor heating part can be suppressed and the floor U-value of TABULA can be used (see Figure 43).

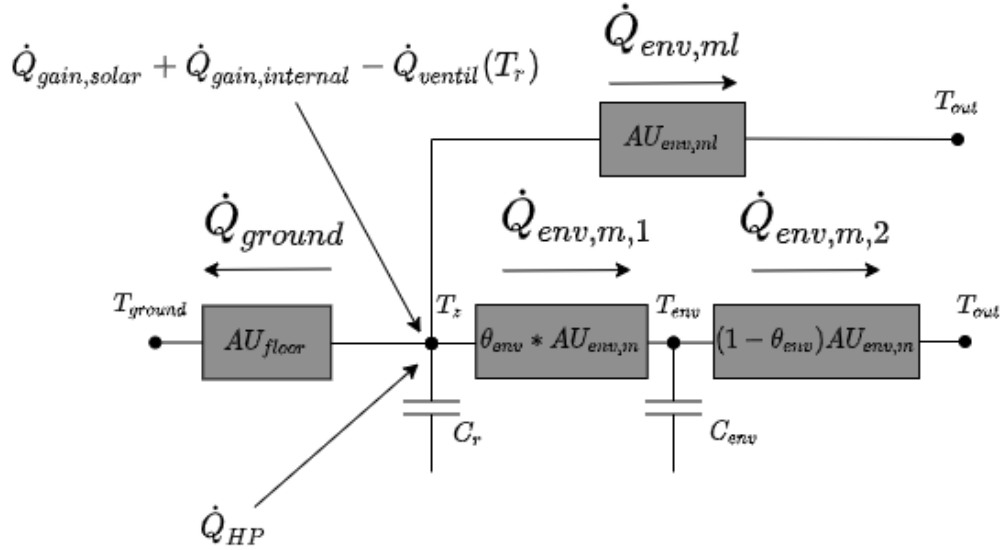


Figure 43: Suggestion of an equivalent RC circuit in order to model A/A heat pumps or A/W HPs with conventional radiators (in this last case a convection coefficient has to be introduced).

### 4.3 Heat pump model at part load

In this work, any part load performance modification has been modelled (between 30 and 100% of the load) since the part load data of the selected heat pumps is not available. However the implementation of the part load dependence of the double interpolation heat pump model using manufacturer data is described in Section 2.3. Masy et al. (2015), Georges (2017) and Garsoux (2015) used the FlexiPac heat pump model. For this model the part load of A/W heat pumps has been modelled. A typical evolution of the performance at partial load is provided by Gendebien, Georges, and Lemort (2014) in Figure 44. It is seen that at partial load, the performance of the variable speed heat pump increases. This is mainly due to the over sizing of the heat exchangers.

By assuming a performance of the heat pump constant at part load, the results of the heat pump electrical consumption can be overestimated. A part load model of the heat pump can lead to better SCOP and lower electrical consumption of the heat pump over the heating season. However, due to the type of control of the heat pump, it is seen in Chapter 3 that the heat pump is mainly used at full load within the hours of use. Therefore a precise partial load modelling would not have a large impact on the conclusion of this work. If a better control of the heat pump is implemented (discussed in Section 4.7), the heat pump will work more at part load, and a modelling of the part load could be interesting in order to represent the consumption over the heating season better. Finally, under 30% of the load, the heat pump has been modelled as in FlexiPac, using a and b coefficient from (Rivière, 2004) as explained in Section 2.3 with a large decrease of the COP as seen in Figure 44.

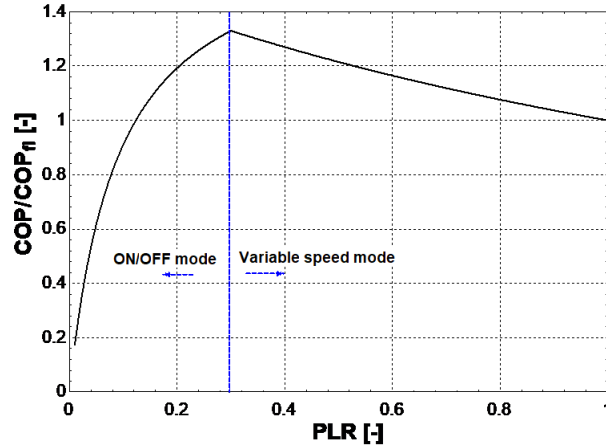


Figure 44: Example of performance at partial load according to the FlexiPac model (Gendebien, Georges, & Lemort, 2014).

#### 4.4 Ground insulation of CS2

It has been decided to keep the floor heating model uniform between CS1 and CS2. According to Johra (2018), a ground EPS insulation of 40 cm has been selected. It has been showed that a 30 cm insulation is more realistic according to the TABULA computation results. Therefore this is analysed. FS C is performed with a 30 cm EPS insulation and is compared to the 40 cm case in Table 29. The results shows that the impact of the assumption is marginal with an overconsumption of 2.3 to 2.4% and a use of the heat pump within the FH increased from 0.23 to 0.29%.

Scenario	Q_dot_HP	W_DOT_HP	COP	Use of HP within FH
Unit	kWh/year		-	%
BAU 40 cm	9579	2043	4.68	31
BAU 30 cm	9821	2090	4.69	31.5
Difference [%]	<b>+2.5</b>	<b>+2.3</b>	<b>+0.2</b>	<b>+1.4</b>
Smart 40 cm	9261	1974	4.69	0.23
Smart 30 cm	9505	2022	4.7	0.29
Difference [%]	<b>+2.6</b>	<b>+2.4</b>	<b>+0.2</b>	<b>+32</b>

Table 29: Comparison of CS2 BAU and FS C smart scenario within the day to analyse the impact of the ground insulation. The results show that the impact is very limited with an increase of the heat pump within the flexibility hours from 0.23 to 0.29%.

#### 4.5 Comfort

Le Dréau and Heiselberg (2016) state that according to standard ISO 7730, a temperature span of 4°C around the neutral setpoint temperature corresponds to a percentage of dissatisfaction of 10%. They also point that according to standard , the transient variation of the indoor temperature should be always kept under the thermal comfort limit of 2.1

K/h. This last condition has been verified for all the scenarios presented in FS B and FS C. For CS1 BAU scenario, this condition is not respected 54 times over the heating season composed of 5784 hours. In the smart scenario, the transgression is only increased to 60. However, the condition on the floor temperature under 29°C is always respected. The effect of the temperature setpoint as been shown in Section 3.3. A strong decrease of the flexibility potential appears. However, the setpoint of 18.5 have been found in the literature and according to (Johra, 2018), underfloor heating permits a lower setpoint temperature due to the large amount of heat that is emit by radiation and not by convection.

## 4.6 Impact of the capacities

The capacities values have been chosen according to values found in the literature. The dependency of the flexibility according to these values have been investigated in Section 3.2. It has been highlighted that the zone's capacity has a bigger impact than the envelope capacity. Heavy buildings lead to a better energy flexibility potential. In order to choose more precise values, real buildings have to be investigated and their capacities computed. Finally, the level of insulation have a stronger impact for the flexibility potential than the capacity values.

## 4.7 Heat pump control

The type of control used for the heat pump is to heat the zone for on hour if the temperature is below the setpoint, and stop it for on hour if the temperature is above the setpoint. It has been showed in Section 2.5 and in Chapter 3 that this type of control leads to oscillation in the zone's temperature. Some possible improvement of the heat pump control are listed:

- As the water law is built to deliver the right amount of heat for the zone setpoint temperature at the corresponding outside temperature, a small hysteresis (e.g. setting a setpoint increased by 0.25°C) can lead to prevent the shutdown of the heat pump if the setpoint is slightly exceeded, due to some solar gains for example.
- A smaller time-step can also help the control of the heat pump and limit the shutdown time. However, with a smaller time-step transient phenomena or limit of the shutting ON/OFF of the heat pump have to be investigated.
- The best solution could be to implement a proportional integrative (PI) control of the heat pump. In this way, the heat pump will not shut down completely, but the capacity will be decrease progressively. This can be done on the  $T_{w,av}$  in order to modulate the power of the heat pump. This solution is used in the literature (Yang et al., 2007), (Johra, 2018) or (Dongellini et al., 2020). This type of control has to be carefully tuned. If the response is too low, the solar radiations and the low capacity modulation will lead to strong overheating of the zone.

## 4.8 Overheating

Section 2.5 has shown that the buildings are subject to overheating at mid season when the solar gains are significant. Lomas and Porritt (2017) state that this is a growing problem across Europe and especially for buildings where the winter insulation to keep the heat has been the principal focus of thermal design. However, in reality the overheating is reduced by opening the windows. Also, the heat recovery has been defined as having a by-pass but this was not implemented. Two suggestions are proposed to improve the model and decreased the overheating:

- To implement the opening of the windows when the setpoint temperature is exceeded;
- To implement the by-pass of the heat recovery ventilation in order to not recover the heat after exceeding the setpoint temperature.

Masy et al. (2015) propose to perform these solutions when the setpoint temperature is exceeded by 2°C and the outdoor is higher than 16°C.

## 4.9 FS C: flexibility period of 2x3h for CS1

A 3x2h flexibility period have been also analysed, with FH from 8AM to 11AM and 6PM to 9PM. The results are shown in Table 30. This leads to a reduction of 92% of the load during the flexibility hours. However, strong undershoots of temperature appear in winter. This is illustrated for a typical day in Figure45. Therefore, this case is considered not realistic to implement for the whole heating season. Different flexibility time periods for the different moments of the heating season (e.g. by separating the spring/autumn and the winter) can lead to more interesting results in order to perform 2h and 3h periods during the heating season.

Scenario	$\dot{Q}_{HP}$	$\dot{W}_{HP}$	SCOP	Use of HP within FH
Unit	kWh/year		-	%
CS1 BAU	20202	5823	3.47	25
CS1 3h	19747	5898	3.35	1.95
Difference [%]	<b>-2.3</b>	<b>+1.3</b>	<b>-3.5</b>	<b>-92</b>

Table 30: Load shifting strategy during a longer period of time for CS1 by setting the zone temperature to 18.5°C from 8AM to 11AM and 6PM to 9PM. 79% of the load is shifted for CS1 and almost all of the load for CS2.

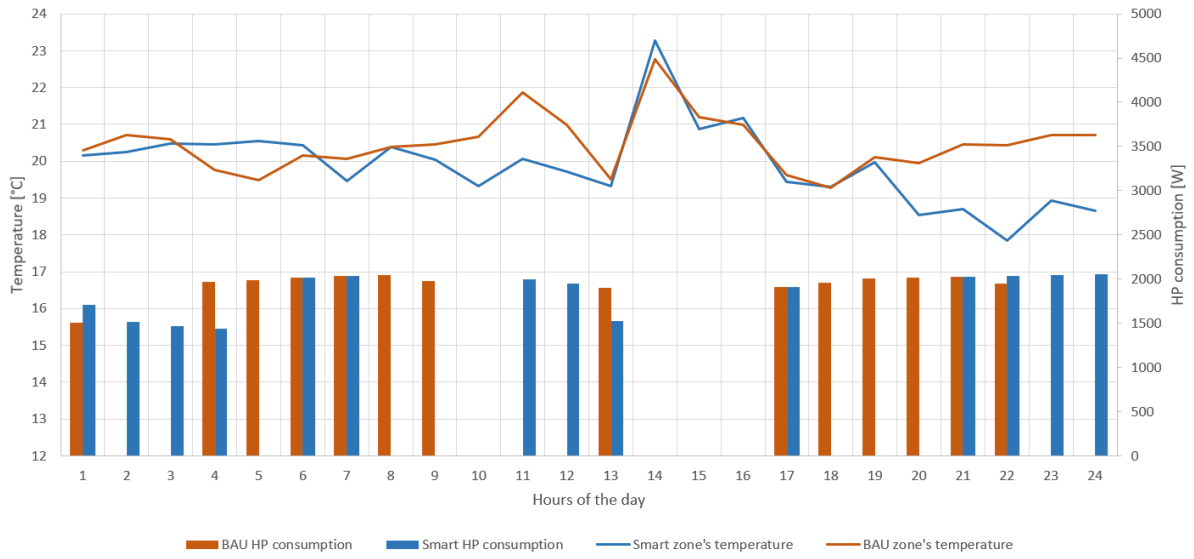


Figure 45: Zone's temperature evolution and heat pump consumption on a typical cold day (8<sup>th</sup> of January) for CS1 with LS from 8AM to 11AM and 6PM to 9PM.

## 5 Conclusion

In this work, the flexibility potential of residential houses equipped by air to water low temperature heat pumps and underfloor heating has been investigated. A large literature review has been done on the heat pump and building models, as well as the conclusions of the flexibility potential found in past researches. The main source for the building characteristics and data have been found in the TABULA tool, a European project with 8 years of research and more than 20 countries involved. The Belgian data of this project have been investigated by VITO, the Flemish Institute of Technology. From the literature review, it has been highlighted that well insulated buildings are the best candidates to shift the heat demand. The configuration chosen with low temperature heat pump and floor heating enable an enhanced thermal energy storage of the building and a high performance of the heat pump. This configuration is found in recent and insulated buildings. Therefore, the building selected was a representative Belgian building characterising a detached house built with 2012 standards. Two insulation levels have been selected: the existing state, with a heat demand of  $89 \text{ kWh}/(\text{m}^2 \cdot \text{y})$ , and an advanced refurbishment state where insulation was increased and a heat recovery ventilation was installed, leading to a yearly heating needs of  $43 \text{ kWh}/(\text{m}^2 \cdot \text{y})$ . The insulation level is respectively K30 and K25. A first static model has been computed in order to validate the results according to the TABULA tool results. A heat pump model has been derived from the manufacturer data by performing a double interpolation of the outdoor temperature and the heat pump exit water temperature. They have been coupled by adding a floor heating model inspired of methods found in the literature. Finally, a single zone dynamic model have been developed by introducing 3 capacities for modelling the floor, zone and envelope thermal inertia.

To assess the flexibility potential, three flexibility studies (FS) have been performed. Rule based controls have been implemented by changing the setpoint temperature in order to shift the heating demand. According to the literature, the neutral setpoint has been fixed to  $20.5^\circ\text{C}$  and could be increased or decreased by  $2^\circ\text{C}$ . The first FS investigated the temporal response of the buildings when the setpoint is changed, and the outdoor temperature is fixed. It has been found for the low insulation case that at  $-5^\circ\text{C}$ , a minimum of 2h of non heating is possible, and up to 18h at  $10^\circ\text{C}$ . For the high insulation case, a minimum of 5h at  $-5^\circ\text{C}$  and a maximum 42h at  $10^\circ\text{C}$  has been shown. This is in the range of the values found in the literature. The second FS investigated the interest of load shifting in order to increase the self-consumption of photovoltaic production. A rule based control with a higher setpoint temperature in the zone between 11AM and 3PM have been set. This has shown that the load shifting of the heat demand in order to increase the self-consumption leads to higher operating costs for the low insulation case, and small benefits for the high insulation case. This flexibility study does not seem advantageous. However, an other control of the heat pump with a load following more accurately the PV production or a reduced flexibility period of two or three hours just before the end of the sunshine could lead to better results. The final FS investigated the shift of the consumption from peak to off-peak hours. This case is really interesting in a context of dynamic pricing. It has been shown for the low insulation case that a shift of the whole heating needs is assessed with a two hours period, and a almost complete shift of the high insulation case with 4 hours period. The heating needs are shifted after the flexibility period with an average rebound period of 4 hours for both cases.

---

Potential improvements of the model have also been presented. A major enhancement is related to the heat pump control. Introducing a PI control can lead to a better representation of the intra-day heat pump behaviour, compared to the simple hysteresis ON/OFF control implemented. However, this simple control have been assumed sufficient to assess the flexibility potential over the whole heating season.

To conclude, the flexibility potential is strongly dependent on the thermal needs of the building and can be discussed according to the desired effect: to shift a large amount of energy for a small period of time or to have long periods of non heating. For very well insulated buildings, the heating needs can be shifted for several hours, but the amount of energy shifted is limited. Lower insulated building have smaller shifting periods, larger overconsumption but a larger amount of power can be shifted. However, a high heating demand is observed after the flexibility period to recover from it. Finally, it has been highlighted that the insulation level is more important than the thermal capacity of the building.


## 6 Appendix

### A Methodology

#### A.1 TABULA calculation sheets

This section provide as example the calculation sheet of the SFH after 2012 in existing state. The calculation sheets are found in the TABULA tool. Figure 46, 47 and 48 represent the pages 2,3 and 4 and values of interest for the model are highlighted in red.





**Energy Balance Calculation**

Standard Reference Calculation - based on: EN ISO 13790 / seasonal method

**Building Performance**

building: BE.N.SFH.06.Gen.ReEx.001.001      reference area  $A_{C,ref}$  (conditioned floor area) 229.2 m<sup>2</sup>

climate: BE.N (BE)

---

construction element	original U-value $U_{original,i}$ W/(m <sup>2</sup> *K)	measure type	nominal insulation thickness $d_{insulation,i}$ mm	effective thermal conductivity $\lambda_{insulation,i}$ W/(m*K)	area fraction $f_{measure,i}$	actual U-value $U_{actual,i}$ W/(m <sup>2</sup> *K)	area (basis: external dimensions) $A_{env,i}$ m <sup>2</sup>	adjustment factor soil $b_{tr,i}$	$H_{tr,i}$ W/K	annual heat flow related to $A_{C,Ref}$ kWh/(m <sup>2</sup> a)
roof 1	0.210			0.000	100%	0.21	107.4	1.00	22.6	6.1
roof 2	0.210			0.000	100%	0.198	44.895	1.00	8.9	2.4
wall 1	0.230			0.000	100%	0.23	173.2	1.00	39.8	10.8
wall 2	0.230			0.000	100%	0.22	28.0	1.00	6.0	1.6
wall 3										
floor 1	0.220			0.000	100%	0.22	48.0	0.50	5.3	1.4
floor 2	0.220			0.000	100%	0.21	83.9	0.50	8.7	2.3
window 1	1.700				100%	1.70	62.9	1.00	107.0	29.0
window 2										
door 1	1.700				100%	1.70	9.5	1.00	16.1	4.4
thermal bridging: surcharge on the U-values						$\Delta U_{tb}$	$\sum A_{env,i}$		$H_{tr,tb}$	
						0.10	557.9	1.00	55.8	15.1

**Heat transfer coefficient by transmission  $H_{tr}$**

envelope area: 0.48      reference area: 1.18       $\frac{W}{m^2K}$  sum: 270      73.3

---

Heat transfer coefficient by ventilation $H_{ve}$	volume-specific heat capacity air $c_{p,air}$ Wh/(m <sup>3</sup> *K)	air change rate by use $n_{air,use}$ 1/h	air change rate by infiltration $n_{air,infiltration}$ 1/h	reference area $A_{C,Ref}$ m <sup>2</sup>	room height (standard value) $h_{room}$ m	$H_{ve}$ W/K	annual heat flow related to $A_{C,Ref}$ kWh/(m <sup>2</sup> a)
	0.34	0.40	0.40	229.2	2.50	156	42.3

**Total heat transfer  $Q_{ht}$**

accumulated differences between internal and external temperature:  $(20.0 - 6.2) \times 210 = 2898$  Kd/a

$H_{tr}$  (W/K) +  $H_{ve}$  (W/K) = 270 + 156 = 426

temperature reduction factor:  $F_{red} (h_r = VWh/(m^2K)) = 0.89$

$Q_{ht} = 426 \times 0.89 \times 2898 \times 0.024 = 26484$  kWh/a      115.6

---

Window orientation	external shading $F_{sh}$	reduction factors frame area fraction $F_F$	non-perpendicular $F_V$	solar energy transmittance $g_{gl,n}$	window area $A_{window,i}$ m <sup>2</sup>	solar global radiation $I_{sol,i}$ kWh/(m <sup>2</sup> a)	$Q_{sol}$ kWh/a	
1. horizontal	0.80	0.30	0.90	0.60		336	0.0	
2. east	0.60	0.30	0.90	0.60	14.7	202	2.9	
3. south	0.60	0.30	0.90	0.60	20.2	340	6.8	
4. west	0.60	0.30	0.90	0.60	11.8	202	2.4	
5. north	0.60	0.30	0.90	0.60	16.2	110	1.8	
sum							<span style="border: 1px solid black; padding: 2px;">3175</span>	13.9

**Solar heat load during heating season  $Q_{sol}$**

---

Internal heat sources $Q_{int}$	internal heat sources $\phi_i$ W/m <sup>2</sup>	heating days $d_{hs}$ d/a	reference area $A_{C,ref}$ m <sup>2</sup>	$Q_{int}$ kWh/a
	0.024	3.00	210	3465

**Internal heat sources  $Q_{int}$**

internal heat capacity per m<sup>2</sup>  $A_{C,ref}$   $c_m$ : 45 Wh/(m<sup>2</sup>\*K)

time constant of the building  $\tau = \frac{c_m \times A_{C,ref}}{H_{tr} + H_{ve}} = 24$

parameter  $a_{H,0} = a_{H,0} + \frac{1}{\tau} = 1.61$

heat balance ratio for the heating mode  $\eta_{h,gn} = \frac{Q_{sol} + Q_{int}}{Q_{ht}} = 0.251$

gain utilisation factor for heating  $\eta_{h,gn} = \frac{1 - \gamma^{aH}}{1 - \gamma^{aH+1}} = 0.92$

---

**Energy need for heating  $Q_{H,nd}$**

$Q_{ht} - \eta_{h,gn} \times (Q_{sol} + Q_{int}) = 20397$  kWh/a      89.0

Figure 46: Calculation sheet of SFH after 2012 in existing state, from TABULA tool (page 2)

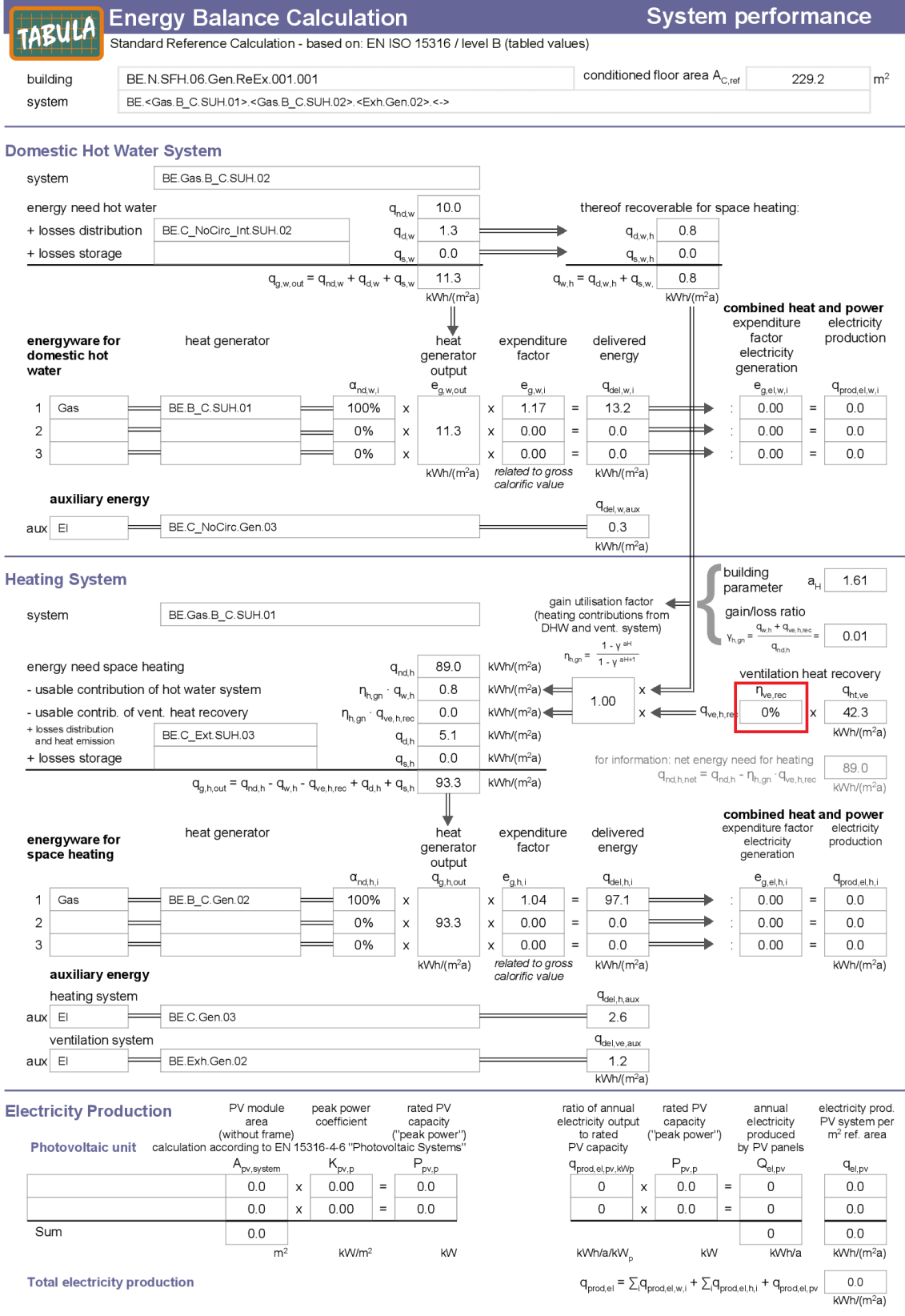



Figure 47: Calculation sheet of SFH after 2012 in existing state, from TABULA tool (page 3)



**Energy Balance Calculation**

Standard Reference Calculation - based on: EN ISO 15316 / level B (tabled values)

**Energy Carriers**

building	BE.N.SFH.06.Gen.ReEx.001.001	conditioned floor area $A_{C,ref}$	229.2	m <sup>2</sup>
system	BE.<Gas_B_C.SUH.01>.<Gas_B_C.SUH.02>.<Exh.Gen.02>.<->			

---

**Assessment of Energywares**  
version of energy carrier specification

**Assessment by Energy Carrier (Standard Calculation)**

**Heating (+ Ventilation) System**

	delivered energy $q_{del,i}$	total primary energy $f_{p,total,i}$	$q_{p,total,i} = \frac{q_{del,i}}{f_{p,total,i}}$	non-renewable primary energy $f_{p,nonren,i}$	$q_{p,nonren,i} = \frac{q_{del,i}}{f_{p,nonren,i}}$	carbon dioxide emissions $f_{CO2,i}$	$m_{CO2,i} = q_{del,i} \cdot f_{CO2,i}$	$p_i$ (energyware price)	$c_i = q_{del,i} \cdot p_i$
Gas	97.1	1.05	101.9	1.05	101.9	277	26.9	8.0	7.77
	0.0	0.00	0.0	0.00	0.0	0	0.0	0.0	0.00
auxiliary electricity	3.8	2.50	9.6	2.30	8.8	617	2.4	24.0	0.92
CHP electr. production**	0.0	0.00	0.0	0.00	0.0	0	0.0	0.0	0.00

**Domestic Hot Water System**

Gas	13.2	1.05	13.9	1.05	13.9	277	3.7	8.0	1.06
	0.0	0.00	0.0	0.00	0.0	0	0.0	0.0	0.00
auxiliary electricity	0.3	2.50	0.00	2.30	0.7	617	0.2	24.0	0.07
CHP electr. production**	0.0	0.00	0.0	0.00	0.0	0	0.0	0.0	0.00

**Photovoltaic System**

PV electr. production** (eff. values*)	0.0	0.00	0.0	0.00	0.0	0	0.0	0.0	0.00
--	-----	------	-----	------	-----	---	-----	-----	------

\*) effective assessment factors, see below  
\*\*) electricity production = negative values

**Electricity Generation - Direct Coverage of Electricity Demand**

version of coverage, depending on supply / load ratio

systems considered:

PV  
 CHP

supply/load ratio  $\frac{q_{prod,el}}{\sum q_{del,el,i} + \sum q_{del,aux,i}} = \frac{0.0}{4.1} = 0.00$

max. coverage (according to pre-determined coverage table)  $\rightarrow 0\%$

max. covered on-site demand  $\rightarrow 0.0$  kWh/(m<sup>2</sup>a)

coverage of on-site demand of electricity**	0.0	0.00	0.0	0.0	0.0	0	0.0	0.0	0.00
el. exported to the grid**	-0.0	0.00	-0.0	0.0	-0	0	-0.0	0.0	-0.00
total / resulting assessment factors**	0.0	0.00	0.0	0.00	0.0	0	0.0	0.0	0.00

\*\*) electricity production = negative values

**Summary and Expenditure Factors**

	$q_{n,d}$ heat need	$\sum q_{del}$	$e_{p,total} = \frac{q_{p,total}}{q_{del}}$	$q_{p,total} = \sum q_{p,total,i}$	$e_{p,nonren} = \frac{q_{p,nonren}}{q_{del}}$	$q_{p,nonren} = \sum q_{p,nonren,i}$	$f_{CO2,heat} = \frac{m_{CO2,heat}}{q_{del}}$	$m_{CO2,i} = \sum m_{CO2,i}$	$P_{heat} = \frac{c}{q_{del}}$	$c = \sum c_i$
heating (+ ventilation) system	89.0	100.9	1.25	111.5	1.24	110.8	329	29.3	9.8	8.69
domestic hot water system	10.0	13.5	1.46	14.6	1.46	14.6	385	3.8	11.3	1.13
<b>total</b>	<b>99.0</b>	<b>114.4</b>	<b>1.27</b>	<b>126.2</b>	<b>1.27</b>	<b>125.3</b>	<b>334</b>	<b>33.1</b>	<b>9.9</b>	<b>9.82</b>
PV electricity bonus		0.0		0.0		0.0		0.0		0.00
<b>total, considering PV bonus</b>		<b>114.4</b>		<b>126.2</b>		<b>125.3</b>		<b>33.1</b>		<b>9.82</b>

**Typical Values of the Measured Consumption - Empirical Calibration**

code	EU.M.01						current value	110.3
application field	average adaptation							
determination method	average values from countries where information is available							
accuracy level	C = estimated (e.g. on the basis of few example buildings)							
	empirical relation							
	0	100	200	300	400	500		
adaptation factor	1.10	0.95	0.80	0.65	0.55	0.47	2	0.93

**Summary (including subcategories)**

			Standard Calculation			Typical Measured Consumption		
	related to		heating	dhw	sum	heating	dhw	sum
Gas	related to	$q_{del,\Sigma gas}$	97.1	13.2	<b>110.3</b>	90.7	12.3	<b>103.0</b>
Oil	gross	$q_{del,\Sigma oil}$	0.0	0.0	<b>0.0</b>	0.0	0.0	<b>0.0</b>
Coal	calorific	$q_{del,\Sigma coal}$	0.0	0.0	<b>0.0</b>	0.0	0.0	<b>0.0</b>
Bio	value	$q_{del,\Sigma bio}$	0.0	0.0	<b>0.0</b>	0.0	0.0	<b>0.0</b>
El		$q_{del,\Sigma el}$	0.0	0.0	<b>0.0</b>	0.0	0.0	<b>0.0</b>
DH		$q_{del,\Sigma dh}$	0.0	0.0	<b>0.0</b>	0.0	0.0	<b>0.0</b>
Other		$q_{des,\Sigma other}$	0.0	0.0	<b>0.0</b>	0.0	0.0	<b>0.0</b>
Auxiliary Electricity		$q_{des,\Sigma aux}$	3.8	0.3	<b>4.1</b>	3.6	0.3	<b>3.9</b>
CHP net electricity production		$q_{exp,\Sigma chp}$	0.0	-0.0	<b>0.0</b>	0.0	-0.0	<b>0.0</b>
PV net electricity production		$q_{exp,\Sigma el,pv}$			<b>0.0</b>			<b>0.0</b>

Figure 48: Calculation sheet of SFH after 2012 in existing state, from TABULA tool (page 4)

## A.2 Static model results for CS2

This Section provides the results of the comparison between TABULA and the static model for CS2.

Parameter	Unit	TABULA	Model	Difference
Number of heating hours	-	5040	5225	3.6 % (7.7 days)
Average external temperature	°C	6.2	5.81	6.71 %
Roof 1	$\frac{\text{kWh}}{\text{m}^2 \cdot \text{year}}$	3	3.19	5.9 %
Roof 2		1.2	1.29	6.9 %
Wall 1		10.9	11.60	6.0 %
Wall 2		1.6	1.79	10.6 %
Floor 1		1.4	1.537	8.9 %
Floor 2		2.4	2.57	6.6 %
Windows		25.8	27.48	6.1 %
Door		3.9	4.15	6.0 %
Thermal bridging		12.2	12.99	6.1 %
Ventilation losses		26.6	28.37	6.2 %
Ventilation gain		21.28	22.69	6.2 %
Internal gain		15.1	14.43	4.6 %
Solar gain		11.5	9.83	17 %
Heating losses		67.2	72.29	7.0 %
Gross heating gain		26.6	25.51	4.2 %
Net heating gain		24.5	23.44	4.5 %
Neglected gain		2.1	2.07	1.4
Heating need	43.22	48.85	11.5 %	

Table 31: Results and comparison of the yearly simulation between TABULA and the static model for case 2.

## A.3 Heat pump manufacturer data

This Section provides the manufacturer data of the 3 selected heat pumps: ERGA04EV, ERGA06EV and ERGA08EV.

$T_{out}$ °C	Leaving Water Condensor Temperature $T_w$ (°C)													
	30		35		40		45		50		55		60	
	HC	PI	HC	PI	HC	PI	HC	PI	HC	PI	HC	PI	HC	PI
-20	4.38	2.43	4.29	2.45	4.21	2.47	4.13	2.48	3.99	2.82	0	0	0	0
-15	4.78	2.14	4.71	2.24	4.64	2.35	4.58	2.45	4.25	2.78	3.94	2.98	0	0
-7	5.43	1.66	5.38	1.91	5.34	2.16	5.3	2.4	4.65	2.72	4	3.04	0	0
-5	5.45	1.59	5.4	1.81	5.35	2.04	5.3	2.27	4.73	2.56	4.16	2.86	3.48	3.07
-2	5.49	1.48	5.43	1.68	5.36	1.87	5.3	2.07	4.85	2.33	4.4	2.59	4.02	2.77
2	5.6	1.4	5.46	1.49	5.38	1.64	5.3	1.8	5.01	2.02	4.73	2.23	4.41	2.36
7	6.65	1.11	6.41	1.3	6.25	1.48	6.08	1.65	5.91	1.84	5.73	2.03	5.58	2.21
12	6.32	0.86	6.07	1.01	5.76	1.15	5.46	1.29	5.23	1.48	4.99	1.67	4.92	1.8
15	6.04	0.73	5.72	0.86	5.4	1	5.08	1.13	4.62	1.28	4.17	1.42	3.65	1.55
20	5.49	0.5	5.15	0.63	4.8	0.75	4.45	0.87	3.62	0.94	2.8	1.01	1.82	1.14

Table 32: Manufacturer data of ERGA04EV.

$T_{out}$ °C	Leaving Water Condensor Temperature $T_w$ (°C)													
	30		35		40		45		50		55		60	
	HC	PI	HC	PI	HC	PI	HC	PI	HC	PI	HC	PI	HC	PI
-20	5.19	2.65	5.13	2.82	5.08	3	5.02	3.17	5	3.44	0	0	0	0
-15	5.59	2.38	5.56	2.6	5.53	2.83	5.5	3.05	5.22	3.35	4.91	3.54	0	0
-7	6.24	1.95	6.25	2.25	6.25	2.56	6.26	2.86	5.58	3.21	4.91	3.54	0	0
-5	6.23	1.86	6.23	2.14	6.23	2.42	6.22	2.71	5.65	3.03	5.07	3.34	4.24	3.62
-2	6.22	1.72	6.2	1.97	6.19	2.22	6.17	2.48	5.74	2.75	5.32	3.03	4.86	3.28
2	6.2	1.53	6.17	1.74	6.13	1.95	6.1	2.17	5.87	2.39	5.65	2.61	5.44	2.82
7	7.92	1.45	7.74	1.63	7.57	1.82	7.4	2.01	7.22	2.26	7.03	2.51	6.84	2.68
12	7.79	1.06	7.52	1.27	7.26	1.47	6.99	1.68	6.76	1.92	6.54	2.16	6.48	2.36
15	7.6	0.95	7.25	1.13	6.89	1.3	6.54	1.48	6.17	1.7	5.81	1.92	5.44	2.08
20	7.29	0.77	6.79	0.89	6.29	1.02	5.78	1.14	5.19	1.33	4.6	1.51	3.93	1.62

Table 33: Manufacturer data of ERGA06EV.

$T_{out}$ °C	Leaving Water Condensor Temperature $T_w$ (°C)													
	30		35		40		45		50		55		60	
	HC	PI	HC	PI	HC	PI	HC	PI	HC	PI	HC	PI	HC	PI
-20	6.22	3.21	6.14	3.43	6.06	3.66	5.98	3.89	5.89	4.11	0	0	0	0
-15	6.62	2.88	6.58	3.16	6.53	3.44	6.48	3.72	6.33	4.02	6.33	4.27	0	0
-7	7.27	2.37	7.28	2.73	7.29	3.08	7.3	3.44	7.02	3.86	6.74	4.28	0	0
-5	7.25	2.26	7.26	2.6	7.28	2.94	7.29	3.28	7.03	3.66	6.77	4.05	0	0
-2	7.23	2.11	7.24	2.41	7.26	2.72	7.27	3.02	7.05	3.37	6.83	3.72	6.58	4.01
2	7.2	1.9	7.22	2.16	7.23	2.42	7.25	2.68	7.07	2.97	6.9	3.27	6.72	3.52
7	9.63	1.84	9.37	2.08	9.12	2.31	8.86	2.55	8.74	3	8.61	3.45	8.38	3.64
12	9.52	1.49	9.21	1.71	8.91	1.93	8.6	2.14	8.42	2.42	8.25	2.71	8.06	2.91
15	9.22	1.3	8.82	1.5	8.42	1.7	8.02	1.9	7.79	2.16	7.55	2.42	7.4	2.6
20	8.71	0.97	8.16	1.14	7.6	1.32	7.04	1.49	6.72	1.71	6.4	1.93	6.29	2.09

Table 34: Manufacturer data of ERGA0E8V.

	$T_{w,su}(y)$	$T_{w,su}(y + 1)$
$T_{out}(x)$	$T(x,y)$	$T(x,y+1)$
$T_{out}(x + 1)$	$T(x+1,y)$	$T(x+1,y+1)$

Table 35: Example of a two by two data table to interpolate.

	$T_{w,su}(y)$	$T_{w,su}$	$T_{w,su}(y + 1)$
$T_{out}(x)$	$T(x,y)$	A	$T(x,y+1)$
$T_{out}$		C	
$T_{out}(x + 1)$	$T(x+1,y)$	B	$T(x+1,y+1)$

Table 36: Example of interpolation of  $\dot{Q}_{fl}$  or  $\dot{W}_{fl}$  from a two by two data table.

## A.4 Double linear interpolation method of the manufacturer data to model the heat pump

The general linear interpolation equation is given by equation 61. This equation is used three times in order to perform a double interpolation, with the two inputs data ( $T_{out}$  and  $T_{w,su}$ ). To illustrate this method and express the related equations, a simple case on a two by two data table is explained (Table 35). The x values represent the outside temperature values from the manufacture data, y values the water temperature, and T the heat pump full load electrical consumption or the full load thermal power produced. When  $T_{out}$  is situated between  $T_{out}(x)$  and  $T_{out}(x + 1)$ , and  $T_{w,su}$  between  $T_{w,su}(x)$  and  $T_{w,su}(x + 1)$  (Table 36), the interpolation of A, B and C are computed (respectively equation 62, 63 and 64) with C the corresponding values of  $\dot{Q}_{fl}$  or  $\dot{W}_{fl}$ . The results of the model at full load is presented in Figure 17 for the ERGA04 with a water temperature of 35°C. The COP is computed from the general equation (equation 1).

$$y = y_1 + (y_2 - y_1) * \frac{x - x_1}{x_2 - x_1} \quad (61)$$

$$A = T(x, y) + [T(x, y + 1) - T(x, y)] * \frac{T_{w,su} - T_{w,su}(y)}{T_{w,su}(y + 1) - T_{w,su}(y)} \quad (62)$$

$$B = T(x + 1, y) + [T(x + 1, y + 1) - T(x + 1, y)] * \frac{T_{w,su} - T_{w,su}(y)}{T_{w,su}(y + 1) - T_{w,su}(y)} \quad (63)$$

$$C = A + (B - A) * \frac{T_{out} - T_{out}(x)}{T_{out}(x + 1) - T_{out}(x)} \quad (64)$$

## B Results

### B.1 Results of 80 kWh envelope capacity

This section presents the results of the FSB simulation with an envelope capacity of 80 kWh.

Scenario	$\dot{Q}_{HP}$	$\dot{W}_{HP}$	COP	Net cons.	Net gen.	Self-cons.	HP use WI FH	Elec. paid	Elec. sold	Total cost
Unit	[kWh/year]		-	[kWh/year]			%	€		
CS1 BAU <sub>80</sub>	20687	5826	3.7	8075	8840	2251	7.9	2019	361	1658
CS1 Smart <sub>80</sub>	21474	6646	3.37	8255	8200	2891	30.1	2064	334	1730
Difference [%]	<b>+3.8</b>	<b>+14.1</b>	<b>-8.9</b>	<b>+2.2</b>	<b>-7.2</b>	<b>+28.4</b>	<b>+281</b>	<b>+2.2</b>	<b>-7.5</b>	<b>+4.3</b>
CS2 BAU <sub>80</sub>	9797	2075	4.7	4744	4824	1831	6.6	1186	197	989
CS2 Smart <sub>80</sub>	10374	2303	4.5	44623	4474	2181	40.5	1156	183	973
Difference [%]	<b>+5.9</b>	<b>+11</b>	<b>-4.3</b>	<b>-2.6</b>	<b>-7.3</b>	<b>+19.1</b>	<b>+514</b>	<b>-2.5</b>	<b>-7</b>	<b>-1.6</b>

Table 37: Results of the 80 kWh envelope zone’s capacity scenario. The impact on the costs is not significant.

## B.2 Morning flexibility

This section provides the results of FSB for the morning LS, with a period from 9AM to 11AM for CS1 and 8AM to 12AM for CS2.

Scenario	Q_dot_HP	W_DOT_HP	COP	Use of HP within FH
Unit	kWh/year		-	%
CS1 BAU	20202	5823	3.47	5
CS1 Smart	20147	5773	3.49	0
Difference [%]	<b>-0.27</b>	<b>-0.86</b>	<b>+0.6</b>	<b>-100</b>
CS2 BAU	9579	2043	4.69	12
CS2 Smart	9449	1990	4.75	0
Difference [%]	<b>-1.35</b>	<b>-2.59</b>	<b>+1.27</b>	<b>-100</b>

Table 38: Load shifting strategy for the morning period.

## References

- Allacker, K. (2010). *Sustainable building: The development of an evaluation method*.
- Arteconi, A., Hewitt, N. J., & Polonara, F. (2013). Domestic demand-side management (dsm): Role of heat pumps and thermal energy storage (tes) systems. *Applied thermal engineering*, 51(1-2), 155–165.
- Ballarini, I., Corgnati, S. P., & Corrado, V. (2014). Use of reference buildings to assess the energy saving potentials of the residential building stock: The experience of tabula project. *Energy policy*, 68, 273–284.
- Braun, J. E., & Chaturvedi, N. (2002). An inverse gray-box model for transient building load prediction. *HVAC&R Research*, 8(1), 73–99.
- BRG Building Solutions. (2018). The european heating product markets.
- Causone, F., Corgnati, S., Fabrizio, E., & Filippi, M. (2009). Radiant system-technical guideline. *Uponsor*.
- Climat.be. (2019). Émissions par secteur. <https://climat.be/en-belgique/climat-et-emissions/emissions-des-gaz-a-effet-de-serre/emissions-par-secteur>. (Access: 31/05/2021)
- Council of European Energy Regulators. (2020). Recommendations on dynamic price implementation.
- Crunelle, C., & Demeyer, F. (2014). Air-water electrical heat pumps for residential application : Technology position paper. *Engie Laborelec*.
- Cuypers, D., Holm, M. V., Vandeveld, B., & de Vyver, I. V. (2016). Renovatie-analyse van een bouwblok in 19de eeuwse gordel in sint-amandsberg, gent. *VITO*.
- Cuypers, D., Vandeveld, B., Van Holm, M., & Verbeke, S. (2014). *Belgische woningtypologie nationale brochure over de tabula woningtypologie*.
- Cyx, W., Renders, N., Van Holm, M., & Verbeke, S. (2011). Iee tabula-typology approach for building stock energy assessment. *VITO, Mol, Belgium*.
- Daikin Europe N.V. (2020). *Daikin altherma low temperature split : Technical data book erga04-08ev*.
- Danfoss. (2009). Planning underfloor heat.
- De Coninck, R., & Helsen, L. (2013). Bottom-up quantification of the flexibility potential of buildings. In *Building simulation 2013: 13th international conference of the international building performance simulation association* (pp. 3250–3257).
- Diefenbach, N., Loga, T., Corrado, V., Corgnati, S., I., B., Despretz, H., ... Kragh, J. (2012). *Use of energy certificate databases as data source for national building typologies - thematic report n° 1*.
- Diefenbach, N., Loga, T., Dascalaki, E., Costas, B., Zavrl, M., Rakušček, A., ... Kragh, J. (2012). *Typology approach for building stock energy assessment application of building typologies for modelling the energy balance of the residential building stock-tabula - thematic report n° 2*.
- Dongellini, M., Valdiserri, P., Naldi, C., & Morini, G. L. (2020). The role of emitters, heat pump size, and building massive envelope elements on the seasonal energy performance of heat pump-based heating systems. *Energies*, 13(19), 5098.
- Dott, R., Afjei, T., Genkinger, A., Dalibard, A., Carbonell, D., Consul, R., ... others (2013). Models of sub-components and validation for the iea shc task 44/hpp annex 38 part c: heat pump models. *International Energy Agency, A technical report of subtask C Deliverable C, 2*.



- EHPA. (2019). Heat pump sales overview. *European Heat Pump Association*. [http://www.stats.ehpa.org/hp\\_sales/story\\_sales/](http://www.stats.ehpa.org/hp_sales/story_sales/). (Access: 12/05/2021)
- EHPA. (2021). What's a heat pump? *European Heat Pump Association*. <https://www.ehpa.org/technology>. (Access: 29/04/2021)
- EnergiePlus. (2007). Climats-types en belgique. <https://energieplus-lesite.be/theories/climat8/climats-types-en-belgique/>. (Access: 02/03/2021)
- Episcopo Project Team. (2015). *Evaluation of the tabula database : Comparison of typical buildings and heat supply systems from 20 european countries*.
- European Commission. (2020). 2030 climate energy framework. [https://ec.europa.eu/clima/policies/strategies/2030\\_en#tab-0-0](https://ec.europa.eu/clima/policies/strategies/2030_en#tab-0-0). (Access: 31/05/2021)
- EuroStat. (2020). Energy consumption in households. [https://ec.europa.eu/eurostat/statistics-explained/index.php?title=Energy\\_consumption\\_in\\_households#Energy\\_consumption\\_in\\_households\\_by\\_type\\_of\\_end-use](https://ec.europa.eu/eurostat/statistics-explained/index.php?title=Energy_consumption_in_households#Energy_consumption_in_households_by_type_of_end-use). (Access: 31/05/2021)
- Fischer, D., & Madani, H. (2017). On heat pumps in smart grids: A review. *Renewable and Sustainable Energy Reviews*, 70, 342–357.
- Fischer, D., Triebel, M.-A., & Selinger-Lutz, O. (2018). A concept for controlling heat pump pools using the smart grid ready interface. In *2018 IEEE PES Innovative Smart Grid Technologies Conference Europe (ISGT-Europe)* (pp. 1–6).
- FPS Public Health. (2021). Scenarios for a climate neutral belgium by 2050.
- Garsoux, P. (2015). Master's thesis: Analysis of the flexibility of belgian residential buildings equipped with heat pumps and thermal energy storages (demand side management).
- Gebäudetypologie, D. (2005). Systematik und datensätze. *Institut Wohnen und Umwelt GmbH, Darmstadt*.
- Gendebien, S., Georges, E., Bertagnolio, S., & Lemort, V. (2014). Methodology to characterize a residential building stock using a bottom-up approach: a case study applied to belgium. *International Journal of Sustainable Energy Planning and Management*, 4, 71–88.
- Gendebien, S., Georges, E., & Lemort, V. (2014). Projet flexipac: Développement d'un modèle de pompe à chaleur destiné à l'intégration dans un modèle bâtiment.
- Georges, E. (2017). *Modulation strategies of integrated hvac systems used in residential buildings for demand-side management at different scales* (Unpublished doctoral dissertation). Université de Liège, Liège, Belgique.
- Georges, E., Gendebien, S., Bertagnolio, S., Dechesne, B., & Lemort, V. (2013). Procebar : Evolution des profils de consommations énergétiques des bâtiments résidentiels en belgique, suite à l'introduction de nouvelles technologies de chauffage, climatisation et cogénération, final report. *Laboratoire de Thermodynamique*.
- GreenSpec. (2021a). Thermal mass. <https://www.greenspec.co.uk/building-design/thermal-mass/>. (Access: 23/02/2021)
- GreenSpec. (2021b). U-value for dummies. <https://www.greenspec.co.uk/building-design/u-value-introduction/>. (Access: 24/02/2021)
- Gromicko, N., & Gromicko, B. (2021). Defrost cycle of a heat pump. <https://www.nachi.org/defrost-cycle-heat-pump.htm>. (Access: 11/05/2021)
- Institut Wohnen und Umwelt GmbH. (2016). Resources of development. consecutive projects co-funded by the intelligent energy europe programme (iee). <https://episcopo.eu/iee-project/overview/>. (Access: 03/05/2021)
- Johra, H. (2018). *Integration of a magnetocaloric heat pump in energy flexible buildings*

- (Unpublished doctoral dissertation). (PhD supervisor: Prof. Per K. Heiselberg, Aalborg University)
- Johra, H., & Heiselberg, P. K. (2018). Description and validation of a matlab-simulink single family house energy model with furniture and phase change materials (update). *Department of Civil Engineering, Aalborg University*.
- Kranzl, L., & TUW, S. F. (2019). D2. 3 wp2 report—open data set for the eu28.
- Le Dréau, J., & Heiselberg, P. (2016). Energy flexibility of residential buildings using short term heat storage in the thermal mass. *Energy*, *111*, 991–1002.
- Loga, T., Diefenbach, N., Stein, B., Dascalaki, E., Balaras, C. A., Droutsas, K., ... Popovic, M. J. (2012a). *Typology approach for building stock energy assessment. main results of the tabula project. tabula final report*.
- Loga, T., Diefenbach, N., Stein, B., Dascalaki, E., Balaras, C. A., Droutsas, K., ... Popovic, M. J. (2012b). Typology approach for building stock energy assessment. main results of the tabula project. tabula final report : Appendix volume. *Institut Wohnen und Umwelt GmbH*.
- Loga, T., Stein, B., & Diefenbach, N. (2016). Tabula building typologies in 20 european countries—making energy-related features of residential building stocks comparable. *Energy and Buildings*, *132*, 4–12.
- Lomas, K. J., & Porritt, S. M. (2017). Overheating in buildings: lessons from research. *Building Research & Information*, *45*(1-2), 1-18. Retrieved from <https://doi.org/10.1080/09613218.2017.1256136> doi: 10.1080/09613218.2017.1256136
- Masy, G. (2008). Definition and validation of a simplified multi-zone dynamic building model connected to heating system and hvac unit. *PhD, Université de Liege*.
- Masy, G., Georges, E., Verhelst, C., Lemort, V., & André, P. (2015). Smart grid energy flexible buildings through the use of heat pumps and building thermal mass as energy storage in the belgian context. *Science and Technology for the Built Environment*, *21*(6), 800–811.
- Mlecnik, E., Hilderson, W., Cré, J., Desmidt, I., Uyttebroeck, H., Van den Abeele, S., ... Henz, O. (2010). Low energy housing retrofit (lehr), final report. *Belgian Science Policy*.
- Nowak, T. (2018). Heat pumps—integrating technologies to decarbonise heating and cooling. *European Copper Institute*.
- Patteeuw, D., Bruninx, K., Arteconi, A., Delarue, E., D’haeseleer, W., & Helsen, L. (2015). Integrated modeling of active demand response with electric heating systems coupled to thermal energy storage systems. *Applied Energy*, *151*, 306–319.
- Patteeuw, D., & Helsen, L. (2014). Residential buildings with heat pumps, a verified bottom-up model for demand side management studies. In *International conference on system simulation in buildings, date: 2014/12/10-2014/12/12, location: Liège, belgium*.
- Patteeuw, D., Henze, G. P., & Helsen, L. (2016). Comparison of load shifting incentives for low-energy buildings with heat pumps to attain grid flexibility benefits. *Applied energy*, *167*, 80–92.
- Rivière, P. (2004). *Performances saisonnières des groupes de production d’eau glacée* (Unpublished doctoral dissertation). École Nationale Supérieure des Mines de Paris.
- Senter Novem. (2007). Voorbeeldwoningen bestaande bouw 2007. *VROM*.
- Simonart, S. (2020). Electric air to water heat pumps: update on the technology, market, economics and connectivity. *Engie Laborelec*.
- Stein, B., Loga, T., Diefenbach, N., Atanasiu, B., Arcipowska, A., Kontonasiou, E., ...

- Zivkovic, B. (2014). *Energy performance indicator tracking schemes for the continuous optimisation of refurbishment processes in european housing stocks inclusion of new buildings in residential building typologies steps towards nzebs exemplified for different european countries.*
- Stein, B., Loga, T., Diefenbach, N., Atanasiu, B., Arcipowska, A., Kontonasiou, E., ... Zivkovic, B. (2016). *Monitor progress towards climate targets in european housing stocks : Main results of the episcope project.*
- TABULA Project Team. (2013). *Tabula calculation method – energy use for heating and domestic hot water – reference calculation and adaptation to the typical level of measured consumption.*
- Van Craenendonck, S., Lauriks, L., & Vuye, C. (2016). Energy efficient renovation of belgian houses: sensitivity analysis for thermal bridges. *Energy Procedia*, 96, 158–169.
- Vandermeulen, A., Vandeplass, L., Patteeuw, D., Sourbron, M., & Helsen, L. (2017). Flexibility offered by residential floor heating in a smart grid context: the role of heat pumps and renewable energy sources in optimization towards different objectives. In *Iea heat pump conference, date: 2017/05/15-2017/05/18, location: Rotterdam, the netherlands.*
- Van Holm, M., Verbeke, S., & Stoppie, J. (2011). *Belgische woningtypologie nationale brochure over de tabula woningtypologie.*
- Verhelst, C., Logist, F., Van Impe, J., & Helsen, L. (2012). Study of the optimal control problem formulation for modulating air-to-water heat pumps connected to a residential floor heating system. *Energy and buildings*, 45, 43–53.
- VREG. (2021). Hoeveel kost 1 kwh elektriciteit (all in, incl. btw)? prijzen voor huishoudelijke afnemers. <https://infogram.com/hoeveel-kost-1-kwh-elektriciteit-aardgas-prijzen-voor-gezinnen-all-in-incl-btw-1h9j6qj8ovd54gz>. (Access: 26/05/2021)
- Yang, Z., Pedersen, G. K., Larsen, L. F., & Thybo, H. (2007). Modeling and control of indoor climate using a heat pump based floor heating system. In *Iecon 2007-33rd annual conference of the ieee industrial electronics society* (pp. 2985–2990).
- Zhang, L., Good, N., & Mancarella, P. (2019). Building-to-grid flexibility: Modelling and assessment metrics for residential demand response from heat pump aggregations. *Applied Energy*, 233, 709–723.